Laboratory and Mechanistic Studies of Volatile Organic Carbon Oxidation Systems in the Atmosphere

by

Joshua A. Moss

B.S., Chemical Engineering, University of California, Berkeley (2015)

Submitted to the Department of Civil and Environmental Engineering
in Partial Fulfillment of the Requirements for the Degree of

Doctor of Philosophy

at the
MASSACHUSETTS INSTITUTE OF TECHNOLOGY

January, 2022

Signature of Author …… _____
Department of Civil and Environmental Engineering
January 14th, 2021

Certified by …… _____
Jesse H. Kroll
Professor of Civil and Environmental Engineering
Professor of Chemical Engineering
Director, Ralph M. Parsons Laboratory
Thesis Supervisor

Accepted by …… _____
Colette L. Heald
Germeshausen Professor of Civil and Environmental Engineering
Professor of Earth, Atmospheric, and Planetary Sciences
Chair, Graduate Program Committee

Laboratory and Mechanistic Studies of Volatile Organic Carbon Oxidation Systems in the Atmosphere

by
Joshua A. Moss

Submitted to the Department of Civil and Environmental Engineering on January 14th, 2022
in Partial Fulfillment of the Requirements for the
Degree of Doctor of Philosophy in Environmental Chemistry

Abstract:

Volatile Organic Compounds (VOCs) oxidize in the troposphere and significantly influence the formation of pollutants including ground-level ozone, CO_2, and particulate matter (PM). Ozone and PM negatively impact human health, and all three pollutants influence Earth's climate. VOCs also dominate the OH reactivity of the atmosphere which in turn influences concentrations of other important radical species including NO_x and HO_2. Chamber experiments are often conducted to measure VOC oxidation in a controlled laboratory setting, but these studies are may be complicated by vapor deposition on chamber surfaces and potential VOC decomposition in the Chemical Ionization Mass Spectrometers (CIMS) which are used to measure a broad range of oxidation products. Mechanistic simulations are also frequently performed to emulate chamber chemistry with less effort and fewer complications than may arise during a chamber experiment, but the results of these simulations are limited by uncertainties and gaps in our understanding of VOC oxidation chemistry from empirical studies. This thesis addresses uncertainties in chamber measurements and mechanisms and uses both in tandem to provide mutual benefits. Chapter 2 focuses on the development and characterization of a Total Suspended Carbon (TSC) apparatus which may be used to parametrize chamber vapor deposition. Chapter 3 centers around the development of new methodology to compare carbon closure chamber datasets and mechanistic datasets using GECKO-A as the base mechanism. Comparisons suggest a propensity for the decomposition of nitrate, peroxyacyl nitrate, alcohol, and aldehyde functional groups in the process of being detected by CIMS, so the final comparison methodology is based on carbon number and average carbon oxidation state distributions which are largely unaffected by decomposition. Chapter 4 uses the methodology from Chapter 3 to investigate how targeted edits to GECKO-A mechanism generator affect its overall agreement with chamber observations for α-pinene, isoprene, and 1,2,4-trimethylbenzene oxidation studies. This chapter highlights reaction pathways of particular importance for each VOC oxidation system and provides new methods to target pathways and specific reactions for further study. Overall, this thesis provides broadly applicable new tools to reduce uncertainty and improve chemical understanding of VOC oxidation systems.

Thesis Supervisor: Jesse H. Kroll
Title: Professor of Civil and Environmental Engineering and Chemical Engineering

Acknowledgements

First and foremost, I need to thank Jesse for being an incredible advisor. I honestly believe that I would not have made it through my Ph.D. without his stalwart support, brilliant insights, and invaluable guidance. Jesse is the most sympathetic and kind professor I have ever met, and he is an example that other PI's should follow as they look to improve their mentoring styles. I also need to thank every member of Jesse's lab for their friendship and collaboration over the past six years. Special thanks goes to former lab member Prof. Gabriel Isaacman-Van Wertz who I met all the way back in my undergraduate days at U.C. Berkeley and who served as my first direct research supervisor. The work in this thesis would not be possible without direct contributions from past Kroll lab members Dr. Abigail Koss, Dr. Christopher Lim, Dr. Kevin Nihill, Dr. Mark Goldman, Dr. Jonathan Franklin, James Rowe, and Stephen Duncan. Kevin and his wife Laura get a second shout out for being the best pub trivia partners I could ask for. Our collaborators from Prof. Frank Keutsch's group at Harvard including Dr. Martin Breitenlechner, Dr. Alex Zaytzev, Dr. Josh Shutter, and Josh Cox and our collaborators from Aerodyne Inc. including Dr. Jordan Krechmer, Dr. Manjula Canagaratna, Dr. Brian Lerner, and Dr. Douglas Worsnop for all providing instrumentation and data analysis. Last but not least, I must thank Dr. Bernard Aumont, Dr. Marie Camredon, and Dr. Richard Valorso at the Université Paris-Est Créteil for developing GECKO-A and teaching me how to use it. The sheer number of researchers who contributed to my thesis is humbling as is the energy and time they contributed. If this acknowledgement section doesn't communicate the intensely collaborative nature of the field of atmospheric chemistry, nothing will.

I also must thank my committee members, Profs. Colette Heald and Dan Cziczo, for their commitment to helping me improve upon my research and for their input during committee meetings. I also learned a tremendous amount when I took their classes at MIT which is knowledge I will take with me even as I transition out of academia. Last but not least for academic thanks, I must thank Prof. Allen Goldstein at U.C. Berkeley for not only introducing me to the field of atmospheric chemistry and giving me an opportunity to conduct research in his lab, but also for being a great family friend.

My friends and family were my incredible support system throughout my entire Ph.D., and there's no way I would have made it through without them. My husband Will has been more supportive than I could have hoped for, I love you so much. You are the greatest discovery I made during my entire time at MIT. Our dogs Olive and Fennel are always ready for cuddles and playtime to distract me when I get stressed. Last but not least, my parents and siblings have been very supportive during this stressful time in my life, and I honestly could not have asked for anything more from them.

Table of Contents

I. Introduction 6

1. Background Information and Motivation 6
2. Research Questions 14
3. References 17

II. Development and Characterization of an Instrument to Measure Total Suspended Carbon for Chamber Experiments 21

1. Introduction 21
2. Design and Methodology 24
3. Results: Calibration and Characterization 26
4. Discussion and Future Work 28
5. References 32

III. Multiparameter Quantitative Comparisons of Smog Chamber and Chemical Mechanistic Datasets 35

1. Introduction 35
2. Materials and Methods 39
3. Discussion and Further Work 57
4. References 60

IV. Comparing Chamber Data to Chemical Mechanistic Simulations Suggests Targeting Pathways for Mechanism Improvements 63

1. Introduction 63
2. Methods 68
3. Results 70
4. Conclusions and Implications 82
5. References 85

V. Conclusions, Implications, and Future Directions 88

1. Summary of Results 88
2. Future Directions and Implications 91
3. References 95

I. Introduction

1. Background Information and Motivation

99.9% of Earth's atmosphere (not including water vapor) is composed of nitrogen, oxygen, and argon, yet a fraction of the remaining 0.1% of the atmosphere contains a remarkably important class of compounds known as Volatile Organic Compounds (VOCs). There are millions of VOCs in the atmosphere, of which 90% are biogenic in origin and 10% are anthropogenic in origin (Sindelarova et al. 2014). Many of these VOCs are familiar compounds like the smell of vanilla, pine trees, and oranges. Some VOCs are toxic to human health including formaldehyde, benzene, and chloroform ("Initial List of Hazardous Air Pollutants with Modifications | US EPA"). As discussed below, all VOCs play an integral role in the Earth-Climate system and have important implications for human health as well.

VOCs can be oxidized in the atmosphere by a variety of oxidants including the OH radical and ozone (O_3) which are of particular interest to this work (e.g. Ziemann 2011; Zhang et al. 2014). VOCs are the largest contributor to the overall OH reactivity of the troposphere and therefore are largely responsible for controlling OH concentrations (Heald and Kroll 2020). OH concentrations, in turn, directly affect the concentrations of other inorganic radical species including NO_x and HO_2 which, in part, determine concentrations and rates of formation of ozone, nitrogen-containing organic species, and carbon monoxide (CO) among other species (Shrivastava et al. 2017; Seinfeld and Pandis 2006). VOC oxidation also leads to the formation of CO_2 and other greenhouse gases which have positive radiative forcing effects and lead to tropospheric warming (IPCC 2014). The highly interconnected nature of the chemical systems in the atmosphere means that if we are able to improve our understanding of VOC oxidation mechanisms, we will also improve our understanding of the formation and consumption of these other species which impact Earth's climate.

When VOCs react in the atmosphere they may become more oxygenated and have lower vapor pressures (e.g. Camredon et al. 2007; Jordan et al. 2008). These Semi Volatile OCs (SVOCs), Intermediate Volatility OCs (IVOCs), and Low Volatility OCs (LVOCs) often will partition out of the gas phase into microscopic condensed phase specks that are known as Particulate Matter (PM). Low vapor pressure gas-phase species may also form new particles via nucleation, although this process contributes less to the overall mass of organic particles than condensation onto existing particles (Debevec et al. 2018). This constantly evolving mixture of VOCs and PM is known as Secondary Organic Aerosol (SOA) which is of high interest to the atmospheric chemistry community because of its direct effects on the Earth-climate system and its negative effects on human health . SOA may be removed from the atmosphere via deposition on to surfaces, scavenging by rain droplets, and particle-phase reactions leading to evaporation/sublimation of certain species (Seinfeld and Pandis 2006). A depiction of this process can be found in Figure 1.

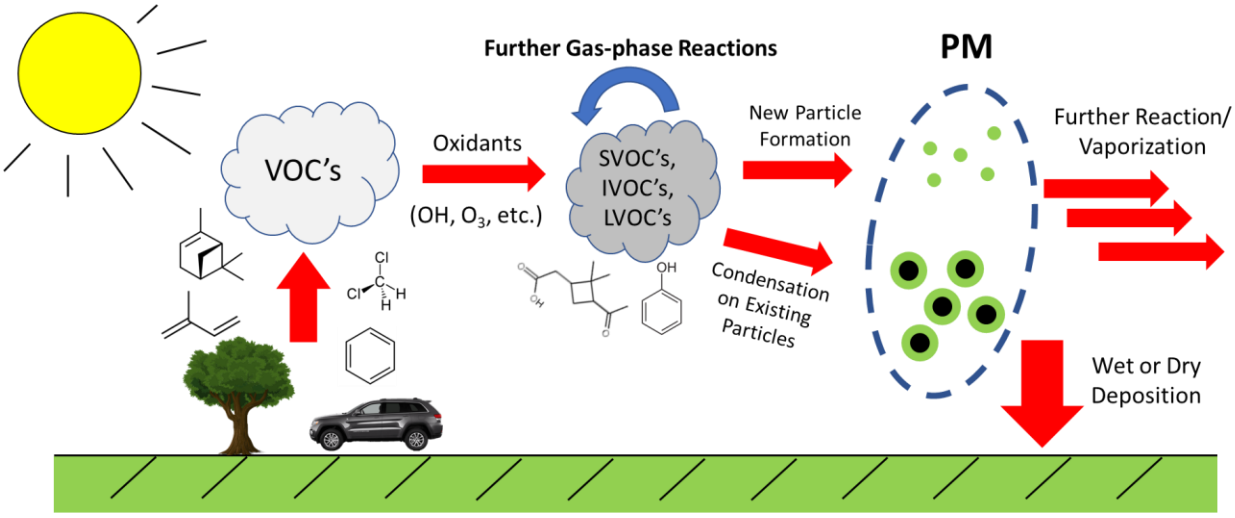

Figure 1: This diagram illustrates the basic processes underpinning SOA formation. VOCs from biogenic and anthropogenic sources (represented by a tree and car respectively) are oxidized to form lower-volatility compounds. These compounds are prone to condense onto existing particles or, less often, form new particles. These particles can then undergo further reactions and partitioning, and eventually they are either vaporized or deposited out of the atmosphere. This thesis is primarily concerned with the gas-phase oxidation of VOC's, SVOC's, etc. leading up to the formation of PM.

SOA and particulate matter in general have been linked to significant health concerns such as Chronic Obstructive Pulmonary Disease (COPD), stroke, and heart disease (III, C Arden Pope, Dockery 2006). Some previous studies have estimated that in regions of high particulate matter pollution such as

Delhi, India, aerosols may be responsible for decreasing average life expectancy by approximately six years (Ghude et al. 2016). Perhaps the clearest depiction of how increased particulate matter concentrations negatively impact human health comes from the so-called "Harvard Six Cities Study" and the corresponding follow-up study which both show a clear and dramatic linear increase in mortality rate with increased particulate loadings (Laden et al. 2006; Dockery et al. 1993). Furthermore, aerosols can have a profound influence on the Earth-climate system by both directly scattering and absorbing incoming solar radiation and by inducing cloud formation which alters the albedo of cloudy regions (IPCC 2014). Aerosol particle effects on climate are also currently the largest source of uncertainty in radiative forcing in global climate models which makes understanding SOA formation and evolution imperative for improving climate model predictive capabilities (IPCC 2014).

Many experiments studying SOA formation and evolution are conducted in environmental chambers (Kroll and Seinfeld 2008). Each chamber is unique in design and operation, but they generally consist of a large Teflon bag surrounded by UV lights (to mimic the sun's actinic flux) in a temperature-controlled environment. Organic species may then be injected into the chamber with ozone and nitrous acid (HONO) to produce OH radicals; ozone photolyzes to form O_2 and $O(^1D)$ which may then react with water vapor to produce OH radicals while HONO directly photolyze to form OH radicals (Seinfeld and Pandis 2006). Ammonium sulfate seed particles are also often added during chamber experiments onto which low-volatility species may condense. After VOCs enter the particle phase, they may continue to react and interact with the gas phase resulting in a dynamic system where species are constantly chemically transforming and partitioning between the gas and particle phases (Donahue et al. 2013). The removal processes of organic compounds from the atmosphere are highly dependent on the phase in which they exist which is why it is important to study this partitioning process (Knote, Hodzic, and Jimenez 2015; Donahue et al. 2013).

Lower volatility species may also condense onto chamber surfaces and instrument inlets which complicates our interpretation of both gas- and particle-phase data (Krechmer, Day, and Jimenez 2020). Particle-phase data may be affected because observed SOA yields are lower than they would be in the absence of vapor losses to surfaces. Additionally, SVOCs may partition out of the particle phase in an equilibrium response to gas-phase wall losses of the same SVOCs which results in lower observed SOA yields (Ye et al. 2016). Gas-phase data may be affected because the measured concentrations for lower-volatility species may be artificially low due to direct vapor losses to surfaces and inlets (Krechmer et al. 2016). Studies have been conducted to parametrize wall losses, including by observing the decay of oxidation products formed from rapid initial burst of photocatalyzed oxidation followed by dark and inert chamber conditions in the absence of seed particles (Krechmer et al. 2016). The time series decay of the species in this study were measured by I- and NO_3-CIMS, and wall loss was assumed to be the only loss mechanism. Krechmer et al. then developed an equilibrium partitioning model based on the SIMPOL-calculated vapor pressure of each species, the lifetime of each species to wall loss, and the "concentration" of the wall (C_w) which is also a function of each compound's vapor pressure (Pankow and Asher 2008). While this model represents an import step in wall loss parametrizations it is also susceptible to uncertainties which arise from estimating each compound's vapor pressure. SIMPOL is also less acuurate for species which are more functionalized which makes this method potentially problematic for estimating wall losses of late-generation compounds which are often quite functionalized (Pankow and Asher 2008; Krechmer et al. 2016). The equilibrium model in Krechmer et al. is the most explicit loss model currently available, yet uncertainties in vapor wall loss corrections will arise from uncertainties in predicted vapor pressures. A direct measure of total suspended carbon (TSC) over the course of a chamber experiment can be used to constrain these wall loss corrections and reduce uncertainty.

Regional and global chemical transport models also often rely on chamber SOA yield studies to parametrize SOA production, and model yields may be underestimated because of wall loss influences on

observed yields. One relevant study used the University of California, Davis / California Institute of Technology regional air quality model with the statistical oxidation model for SOA production (Cappa et al. 2016). The statistical oxidation model was parametrized using chamber data, both accounting for and discounting wall loss. The study found that accounting for vapor wall losses increased modeled SOA concentrations by a factor of 2-10 depending on the assumed degree of wall loss (Cappa et al. 2016). The scenarios in which vapor wall losses were assumed to be higher led to improved agreement with observations from the SOAR-2005 campaign in terms of the absolute concentrations and diurnal profiles of the [OA]/CO ratio and OA O:C and H:C ratios. Other studies, however, do not necessarily suggest that wall loss influences on SOA yield affect model agreement with observed reality. One recent study compared observations from 15 globally distributed aircraft campaigns to GEOS-Chem simulations which incorporated a simple model parametrization for SOA formation based on reported laboratory SOA yields (Pai et al. 2020). This study found little systemic underestimation of OA across a distribution of observed OA loading although the models were still only able to capture the observed variability in OA with an r^2 of 0.41. Both of the studies we just discussed suggest that more accurate measurements of SOA yields from chamber studies could yield improvements in model-measurement agreement.

TSC is a top-down metric which is another way of saying that it provides an overarching measure of the entire system. The complement to top-down measurements are bottom-up measurements, which in this case refers to speciated measurements of all of the compounds in the chamber. The organic species produced over the course of chamber experiments are often measured with a variety of mass spectrometry instruments with each instrument specializing in detecting different classes of compounds based on different characteristics including their functionalities and size (e.g. Koss et al. 2020; Isaacman-VanWertz et al. 2018). The chamber experiments described herein were conducted with a suite of Chemical Ionization Mass Spectrometers (CIMS) which were selected to comprehensively measure all organic species, yet it remains to be seen if all species were, in fact, detected and quantified properly.

Current CIMS calibration methods yield uncertainties on the order of 10%-30% for compounds which can be identified by structure, measured with the Proton Transfer Reaction MS (PTR-MS), and/or measured with the Ammonia (NH_4^+) CIMS; however, the Iodide (I^-) CIMS which generally measures larger and more heavily oxidized compounds can yield significantly larger uncertainties on the order of 2.5x (Isaacman-VanWertz et al. 2018). While more precise calibrations would certainly be useful in reducing uncertainties in chamber measurements, we can also attempt to reduce uncertainty by comparing chamber results with chemical mechanistic predictions.

Mechanisms can be used to model the dynamic chamber system, thereby providing a direct (albeit simulated) comparison to chamber measurements. Mechanisms represent the culmination of our field's understanding of the chemistry and dynamic partitioning of a variety of different VOC precursors and are often constructed from a list of known chemical reactions (Saunders et al. 2003; Jenkin, Saunders, and Pilling 1997; Camredon et al. 2007). In reality, completely exhaustive mechanisms would may comprise hundreds, thousands, or even millions of different species, many or most of which are unknown or present in such small quantities that they are essentially undetectable (Camredon et al. 2007).

Mechanistic simulations have been compared to chamber datasets in order to, for example, validate the mechanisms ability to accurately predict the time series behavior of specific compounds over the course of an experiment (e.g. Yee et al. 2012; Bates and Jacob 2019). Similarly, these studies have been used to suggest compound identities for ions measured by CIMS. These types of studies are certainly helpful in increasing the accuracy and precision of individual reaction rates in mechanisms and are also useful for disambiguating chamber data by providing reasonable structures for detected ions. However, the two aforementioned studies did not tackle the pressing challenge of assessing the completeness and accuracy of the mechanism as a whole, and the mechanisms in the studies were not able to reproduce time series behavior for each species to within experimental uncertainty.

Performing experiments to detect each product, measure their rate(s) of production and consumption, and then writing them all down in an explicit mechanism would be tedious and extremely time consuming, but computer simulations provide an attractive alternative to this difficult chamber work. Much of the work in this dissertation relies heavily on GECKO-A (Generator for Explicit Chemistry and Kinetics of the Organics in the Atmosphere), a unique computational program which uses empirical kinetic data coupled with structure-activity relationships to generate explicit oxidation mechanisms (Aumont, Szopa, and Madronich 2005). Simply put, GECKO-A takes a precursor VOC, predicts how it will react with common atmospheric species (i.e. OH, O_3, NO, etc.), generates explicit mechanisms for these predicted reactions, and then iterates through the same procedure for the VOC products it has just generated. Structure-Activity Relationships (SARs) are the main levers we can control to improve GECKO-A's ability to accurately model VOC and SOA oxidation (Aumont, Szopa, and Madronich 2005; Camredon et al. 2007). SARs are ways to estimate reaction rates by analyzing the bond(s) involved in the reaction while simultaneously accounting for the structure of the organic molecule around the bond of interest (Vereecken and Peeters 2010). There are SARs for most of the currently studied atmospherically relevant reactions, so while we may not have explicit measurements of every reaction rate, we can use SARs to provide a rate constant for reactions which we believe may occur but have yet to be studied. We will discuss these SARs in more detail in Chapter 4, but the main takeaway here is that SARs dictate the path that organic carbon will take in a mechanism. By changing the value of the parameters in any given SAR we can change the way that the SOA oxidation system will behave.

GECKO-A has been improved over time to incorporate experimental nuances that are relevant for chamber SOA studies, including gas-particle partitioning (Aumont et al. 2013). A relatively recent study incorporated wall losses into the model framework using a simple vapor-pressure-dependent function in order to assess loss effects on SOA yield (La et al. 2016). GECKO-A, however, is only as good as the

knowledge with which it is parametrized; any uncertainties and gaps in our knowledge will persist in the mechanisms GECKO-A creates.

GECKO-A has been used to simulate chamber chemistry (e.g. La et al. 2016) as well as non-chamber chemistry, for example, by simulating chemistry observed in the real atmosphere during field campaigns. One such study used the GECKO-A mechanism to simulate the formation and evolution of OA in the outflow from Mexico City as measured during the 2006 MILAGRO campaign (Lee-Taylor et al. 2011; Molina et al. 2010). Specifically, this study assessed the contributions of explicit n-alkane chemistry on SOA formation because n-alkanes were known to be emitted in significant quantities in and around Mexico City (Apel et al. 2010). This study found that the mechanism was able to replicate the diurnal profiles of OA and key species including ozone, NOx, and OH, although the absolute concentrations for ozone and NOx were not perfectly matched. The mechanism results over multiple days of oxidation also suggested higher-than-reported OA concentrations compared to aircraft observations; the authors suggest that changes to GECKO-A's alkoxy radical SARs to increase decomposition rates relative to isomerization rates could reduce the OA discrepancy, but no laboratory studies at that time suggested that editing those SARs would be justified. Resolving these discrepancies is a critical task for our field in order to reduce uncertainty in chemical transport models which rely on mechanisms to provide accurate predictions of, among other parameters, ozone formation and pollution transport (Ahmadov et al. 2015; Park et al. 2021).

To date, no study has compared speciated chamber measurements to mechanism outputs on a holistic level. One reason that this research had not been performed (until now) is that speciated chamber data measuring all organic species is highly uncommon. Our lab, however, has been performing experiments and generating such datasets (hereafter referred to as TotalC datasets) which afford us the relatively unique position of being able to perform the first of these kinds of comparisons. However, there are no clear or preexisting ways to perform these comparisons. New approaches must be developed to

compare chamber and mechanistic datasets in their entirety on different levels of granularity. Comparisons can be based on a species to species level at the most granular level, a bulk property level like average carbon oxidation state (OSc) at the least granular level, or distributive properties like vapor pressure distributions at some intermediate level of granularity. It behooves us to explore comparisons across a range of granularity to assess the type and value of information that can be gleaned at each level. It is important to put this task into the context of the bigger picture; chemists may wish to see more granular improvements in mechanisms whereas climate modelers may wish to see improvements in less granular properties which could be useful to parametrize their models.

Just as mechanisms can help elucidate uncertainties in chamber experiments, chamber data can be used to refine GECKO-A's predictive capabilities. Both mechanisms and chamber data analysis will greatly benefit from a chamber TSC measurement by providing a top-down constrain on speciated measurements and mechanism outputs. In summary, TSC measurements, speciated chamber measurements, and mechanistic simulations of VOC oxidation can be used together to improve our understanding of chamber oxidation systems, complex chemistry, mechanism behavior, and ultimately reduce key uncertainties in how radical chemistry and SOA formation affect Earth's climate and human health.

2. Research Questions

In this thesis, we probe the completeness and accuracy of speciated organic chamber measurements and chemical mechanistic models. We perform this via the development of a new instrument to measure TSC and the comparison of multiple chamber experiments to GECKO-A simulations. Specifically, this work aims to address the following questions:

(1) Are measurements of organic species accurate and complete in a chamber experiment when accounting for wall losses?

(2) How do we compare large chamber mechanistic datasets in a way that provides useful information for reducing uncertainty and error in both measurements and models?

(3) How can mechanisms reduce ambiguity in speciated chamber measurements?

(4) How well do mechanisms understand a few select complex SOA oxidation systems?

(5) How can chamber measurements improve GECKO-A by suggesting changes to SARs?

These questions will be addressed in the following chapters:

Chapter 2: This chapter focuses on Question 1 by constructing, developing, and characterizing an instrument to measure TSC in an air sample. The instrument, known as the Oxy-Cat, uses heated palladium and platinum catalysts to convert organic species to CO_2. A differential CO_2 monitor then measures the amount of CO_2 generated from the organic species which serves as the measure of TSC in the sampled air mass. Calibration studies of several species spanning a range of volatility and chemical complexity are presented. The objective of this chapter is to show that the Oxy-Cat will convert a diverse set of VOCs entire to CO_2 and that it is capable of measuring concentrations of VOCs at chamber-relevant levels down to 10ppbC.

Chapter 3: This chapter focuses on Questions 2 and 3 by developing new methodologies for comparing time series speciated datasets from chamber studies and mechanistic simulations. Initial comparisons focus on direct species-to-species analyses of the butane oxidation system which suggest the likelihood of decomposition reactions taking place inside the PTR-MS. Subsequent comparisons are based on distributive properties of the gas phase of chamber and GECKO-A SOA, namely carbon number and OSc distributions. These distributions are combined for a more granular examination of the similarities and differences between the chamber and modeled systems, and an error metric is developed to quantify the degree to which the two systems are similar. This chapter lays the foundations for a more in-depth examination of the chemical differences between the systems in Chapter 4. The objectives of this chapter are to show that the comparison methodology yields insights into the differences between observed and

modeled chemistry and that the error metric we developed can be used to compare measurement-mechanism agreement across different VOC oxidation systems.

Chapter 4: This chapter focuses on Questions 4 and 5 by using the metrics developed in Chapter 3 to analyze the similarities and discrepancies between chamber experiments and GECKO-A simulations of the α-pinene, 1,2,4-trimethylbenzene (TMB), and isoprene oxidation systems. Specific hypotheses based on an analysis of existing mechanisms for each system are discussed as possible reasons for observed differences. These hypotheses are translated into proposed edits to GECKO-A's SARs, primarily those related to the fate of the alkoxy radical, ozonolysis, and nitrate yields. GECKO-A simulations are performed with the suggested SAR alterations, and changes to observed agreement across all systems are discussed. No single set of changes to any system uniformly improves agreement across all three oxidation systems which highlights the need for closer examination of specific reaction pathways to increase the accuracy of mechanisms. The objectives of this chapter are to show how GECKO-A and our novel chamber comparison methodology can be used to identify classes of reactions to which chamber-GECKO agreement are sensitive.

3. References

Ahmadov, R., S. McKeen, M. Trainer, R. Banta, A. Brewer, S. Brown, P. M. Edwards, et al. 2015. "Understanding High Wintertime Ozone Pollution Events in an Oil- and Natural Gas-Producing Region of the Western US." *Atmospheric Chemistry and Physics* 15 (1): 411–29. https://doi.org/10.5194/ACP-15-411-2015.

Apel, E. C., L. K. Emmons, T. Karl, F. Flocke, A. J. Hills, S. Madronich, J. Lee-Taylor, et al. 2010. "Chemical Evolution of Volatile Organic Compounds in the Outflow of the Mexico City Metropolitan Area." *Atmospheric Chemistry and Physics* 10 (5): 2353–76. https://doi.org/10.5194/ACP-10-2353-2010.

Aumont, Bernard, Marie Camredon, Camille Mouchel-Vallon, Stéphanie La, Farida Ouzebidour, Richard Valorso, Julia Lee-Taylor, and Sasha Madronich. 2013. "Modeling the Influence of Alkane Molecular Structure on Secondary Organic Aerosol Formation." *Faraday Discussions* 165: 105. https://doi.org/10.1039/c3fd00029j.

Aumont, Bernard, S. Szopa, and Sasha Madronich. 2005. "Modelling the Evolution of Organic Carbon during Its Gas-Phase Tropospheric Oxidation: Development of an Explicit Model Based on a Self Generating Approach." *Atmospheric Chemistry and Physics Discussions* 5 (1): 703–54. https://doi.org/10.5194/acpd-5-703-2005.

Bates, Kelvin H., and Daniel J. Jacob. 2019. "A New Model Mechanism for Atmospheric Oxidation of Isoprene: Global Effects on Oxidants, Nitrogen Oxides, Organic Products, and Secondary Organic Aerosol." *Atmospheric Chemistry and Physics* 19 (14): 9613–40. https://doi.org/10.5194/ACP-19-9613-2019.

Camredon, M., B. Aumont, J. Lee-Taylor, and S. Madronich. 2007. "The SOA/VOC/NOx System: An Explicit Model of Secondary Organic Aerosol Formation." *Atmos. Chem. Phys.* 7 (21): 5599–5610. https://doi.org/10.5194/acp-7-5599-2007.

Cappa, Christopher D., Shantanu H. Jathar, Michael J. Kleeman, Kenneth S. Docherty, Jose L. Jimenez, John H. Seinfeld, and Anthony S. Wexler. 2016. "Simulating Secondary Organic Aerosol in a Regional Air Quality Model Using the Statistical Oxidation Model - Part 2: Assessing the Influence of Vapor Wall Losses." *Atmospheric Chemistry and Physics* 16 (5): 3041–59. https://doi.org/10.5194/ACP-16-3041-2016.

Debevec, Cécile, Stéphane Sauvage, Valérie Gros, Karine Sellegri, Jean Sciare, Michael Pikridas, Iasonas Stavroulas, et al. 2018. "Driving Parameters of Biogenic Volatile Organic Compounds and Consequences on New Particle Formation Observed at an Eastern Mediterranean Background Site." *Atmospheric Chemistry and Physics* 18 (19): 14297–325. https://doi.org/10.5194/ACP-18-14297-2018.

Dockery, Douglas W., C. Arden Pope, Xiping Xu, John D. Spengler, James H. Ware, Martha E. Fay, Benjamin G. Ferris, and Frank E. Speizer. 1993. "An Association between Air Pollution and Mortality in Six U.S. Cities." *New England Journal of Medicine* 329 (24): 1753–59. https://doi.org/10.1056/NEJM199312093292401.

Donahue, N. M., W. Chuang, S. A. Epstein, J. H. Kroll, D. R. Worsnop, A. L. Robinson, P. J. Adams, and S. N. Pandis. 2013. "Why Do Organic Aerosols Exist? Understanding Aerosol Lifetimes Using the Two-Dimensional Volatility Basis Set." *Environmental Chemistry* 10 (3): 151–57. https://doi.org/10.1071/EN13022.

Ghude, Sachin D., D. M. Chate, C. Jena, G. Beig, R. Kumar, M. C. Barth, G. G. Pfister, S. Fadnavis, and Prakash Pithani. 2016. "Premature Mortality in India Due to PM $_{2.5}$ and Ozone Exposure." *Geophysical Research Letters* 43 (9): 4650–58. https://doi.org/10.1002/2016GL068949.

Heald, C L, and J H Kroll. 2020. "The Fuel of Atmospheric Chemistry: Toward a Complete Description of Reactive Organic Carbon." *Sci. Adv* 6. https://www.science.org.

III, C Arden Pope, Dockery, Douglas W. 2006. "Health Effects of Fine Particulate Air Pollution : Lines That Connect." *Air & Waste Manage. Association* 56 (6): 709–42. https://doi.org/10.1080/10473289.2006.10464545.

"Initial List of Hazardous Air Pollutants with Modifications | US EPA." n.d. Accessed December 5, 2021. https://www.epa.gov/haps/initial-list-hazardous-air-pollutants-modifications.

IPCC. 2014. "Climate Change 2014 Synthesis Report." *Contribution of Working Groups I, II and III to the Fifth Assessment Report of the Intergovernmental Panel on Climate Change*, 1–151.

Isaacman-VanWertz, Gabriel, Paola Massoli, Rachel O'Brien, Christopher Lim, Jonathan P. Franklin, Joshua A. Moss, James F. Hunter, et al. 2018. "Chemical Evolution of Atmospheric Organic Carbon over Multiple Generations of Oxidation." *Nature Chemistry* 10 (4): 462–68. https://doi.org/10.1038/s41557-018-0002-2.

Jenkin, Michael E., Sandra M. Saunders, and Michael J. Pilling. 1997. "The Tropospheric Degradation of Volatile Organic Compounds: A Protocol for Mechanism Development." *Atmospheric Environment* 31 (1): 81–104. https://doi.org/10.1016/S1352-2310(96)00105-7.

Jordan, C. E., P. J. Ziemann, R. J. Griffin, Y. B. Lim, R. Atkinson, and J. Arey. 2008. "Modeling SOA Formation from OH Reactions with C8-C17n-Alkanes." *Atmospheric Environment* 42 (34): 8015–26. https://doi.org/10.1016/j.atmosenv.2008.06.017.

Knote, C., A. Hodzic, and J. L. Jimenez. 2015. "The Effect of Dry and Wet Deposition of Condensable Vapors on Secondary Organic Aerosols Concentrations over the Continental US." *Atmospheric Chemistry and Physics* 15 (1): 1–18. https://doi.org/10.5194/acp-15-1-2015.

Koss, Abigail R., Manjula R. Canagaratna, Alexander Zaytsev, Jordan E. Krechmer, Martin Breitenlechner, Kevin J. Nihill, Christopher Y. Lim, et al. 2020. "Dimensionality-Reduction Techniques for Complex Mass Spectrometric Datasets: Application to Laboratory Atmospheric Organic Oxidation Experiments." *Atmospheric Chemistry and Physics* 20 (2): 1021–41. https://doi.org/10.5194/ACP-20-1021-2020.

Krechmer, Jordan E., Douglas A. Day, and Jose L. Jimenez. 2020. "Always Lost but Never Forgotten: Gas-Phase Wall Losses Are Important in All Teflon Environmental Chambers." *Environmental Science and Technology* 54 (20): 12890–97. https://doi.org/10.1021/ACS.EST.0C03381/SUPPL_FILE/ES0C03381_SI_001.PDF.

Krechmer, Jordan E., Demetrios Pagonis, Paul J. Ziemann, and Jose L. Jimenez. 2016. “Quantification of Gas-Wall Partitioning in Teflon Environmental Chambers Using Rapid Bursts of Low-Volatility Oxidized Species Generated in Situ.” *Environmental Science and Technology* 50 (11): 5757–65. https://doi.org/10.1021/ACS.EST.6B00606/SUPPL_FILE/ES6B00606_SI_001.PDF.

Kroll, Jesse H., and John H. Seinfeld. 2008. “Chemistry of Secondary Organic Aerosol: Formation and Evolution of Low-Volatility Organics in the Atmosphere.” *Atmospheric Environment* 42 (16): 3593–3624. https://doi.org/10.1016/j.atmosenv.2008.01.003.

Laden, Francine, Joel Schwartz, Frank E. Speizer, and Douglas W. Dockery. 2006. “Reduction in Fine Particulate Air Pollution and Mortality.” *American Journal of Respiratory and Critical Care Medicine* 173 (6): 667–72. https://doi.org/10.1164/rccm.200503-443OC.

La, Y. S., M. Camredon, P. J. Ziemann, R. Valorso, A. Matsunaga, V. Lannuque, J. Lee-Taylor, A. Hodzic, S. Madronich, and B. Aumont. 2016. “Impact of Chamber Wall Loss of Gaseous Organic Compounds on Secondary Organic Aerosol Formation: Explicit Modeling of SOA Formation from Alkane and Alkene Oxidation.” *Atmospheric Chemistry and Physics* 16 (3): 1417–31. https://doi.org/10.5194/acp-16-1417-2016.

Lee-Taylor, J., S. Madronich, B. Aumont, A. Baker, M. Camredon, A. Hodzic, G. S. Tyndall, E. Apel, and R. A. Zaveri. 2011. “Explicit Modeling of Organic Chemistry and Secondary Organic Aerosol Partitioning for Mexico City and Its Outflow Plume.” *Atmospheric Chemistry and Physics* 11 (24): 13219–41. https://doi.org/10.5194/acp-11-13219-2011.

Molina, L. T., S. Madronich, J. S. Gaffney, E. Apel, B. de Foy, J. Fast, R. Ferrare, et al. 2010. “An Overview of the MILAGRO 2006 Campaign: Mexico City Emissions and Their Transport and Transformation.” *Atmospheric Chemistry and Physics* 10 (18): 8697–8760. https://doi.org/10.5194/ACP-10-8697-2010.

Pai, Sidhant J., Colette L. Heald, Jeffrey R. Pierce, Salvatore C. Farina, Eloise A. Marais, Jose L. Jimenez, Pedro Campuzano-Jost, et al. 2020. “An Evaluation of Global Organic Aerosol Schemes Using Airborne Observations.” *Atmospheric Chemistry and Physics* 20 (5): 2637–65. https://doi.org/10.5194/ACP-20-2637-2020.

Pankow, J.F., and W.E. Asher. 2008. “SIMPOL.1: A Simple Group Contribution Method for Predicting Vapor Pressures and Enthalpies of Vaporization of Multifunctional Organic Compounds.” *Atmospheric Chemistry and Physics* 8: 2773–96. https://doi.org/10.5194/acpd-7-11839-2007.

Park, Rokjin J., Yujin J. Oak, Louisa K. Emmons, Cheol Hee Kim, Gabriele G. Pfister, Gregory R. Carmichael, Pablo E. Saide, et al. 2021. “Multi-Model Intercomparisons of Air Quality Simulations for the KORUS-AQ Campaign.” *Elementa* 9 (1). https://doi.org/10.1525/ELEMENTA.2021.00139/116310.

Saunders, S. M., M. E. Jenkin, R. G. Derwent, and M. J. Pilling. 2003. “Protocol for the Development of the Master Chemical Mechanism, MCM v3 (Part A): Tropospheric Degradation of Non-Aromatic Volatile Organic Compounds.” *Atmospheric Chemistry and Physics* 3 (1): 161–80. https://doi.org/10.5194/ACP-3-161-2003.

Seinfeld, JH., and SN. Pandis. 2006. *Atmospheric Chemistry and Physics: From Air Pollution to Climate Change*. Edited by Inc. John Wiley and Sons. *John Wiley & Sons.* 3rd ed. John Wiley and Sons, Inc. https://doi.org/10.1080/00139157.1999.10544295.

Shrivastava, Manish, Christopher D. Cappa, Jiwen Fan, Allen H. Goldstein, Alex B. Guenther, Jose L. Jimenez, Chongai Kuang, et al. 2017. "Recent Advances in Understanding Secondary Organic Aerosol: Implications for Global Climate Forcing." *Reviews of Geophysics* 55 (2): 509–59. https://doi.org/10.1002/2016RG000540.

Sindelarova, K, C Granier, I Bouarar, A Guenther, S Tilmes, T Stavrakou, J.-F Müller, U Kuhn, P Stefani, and W Knorr. 2014. "Global Data Set of Biogenic VOC Emissions Calculated by the MEGAN Model over the Last 30 Years." *Atmos. Chem. Phys* 14: 9317–41. https://doi.org/10.5194/acp-14-9317-2014.

Vereecken, L., and J. Peeters. 2010. "A Structure–Activity Relationship for the Rate Coefficient of H-Migration in Substituted Alkoxy Radicals." *Physical Chemistry Chemical Physics* 12 (39): 12608–20. https://doi.org/10.1039/C0CP00387E.

Yee, Lindsay D., Jill S. Craven, Christine L. Loza, Katherine A. Schilling, Nga Lee Ng, Manjula R. Canagaratna, Paul J. Ziemann, Richard C. Flagan, and John H. Seinfeld. 2012. "Secondary Organic Aerosol Formation from Low-NO_x Photooxidation of Dodecane: Evolution of Multigeneration Gas-Phase Chemistry and Aerosol Composition." *The Journal of Physical Chemistry A* 116 (24): 6211–30. https://doi.org/10.1021/jp211531h.

Ye, Penglin, Xiang Ding, Jani Hakala, Victoria Hofbauer, Ellis S. Robinson, and Neil M. Donahue. 2016. "Vapor Wall Loss of Semi-Volatile Organic Compounds in a Teflon Chamber." *Https://Doi.Org/10.1080/02786826.2016.1195905* 50 (8): 822–34. https://doi.org/10.1080/02786826.2016.1195905.

Zhang, X., R. H. Schwantes, M. M. Coggon, C. L. Loza, K. A. Schilling, R. C. Flagan, and J. H. Seinfeld. 2014. "Role of Ozone in SOA Formation from Alkane Photooxidation." *Atmospheric Chemistry and Physics* 14 (3): 1733–53. https://doi.org/10.5194/acp-14-1733-2014.

Ziemann, P. J. 2011. "Effects of Molecular Structure on the Chemistry of Aerosol Formation from the Oh-Radical-Initiated Oxidation of Alkanes and Alkenes." *International Reviews in Physical Chemistry* 30 (2): 161–95. https://doi.org/10.1080/0144235X.2010.550728.

II. Development and Characterization of an Instrument to Measure Total Suspended Carbon for Chamber Experiments

1. Introduction

As we discussed in Chapter 1, SOA oxidation studies are frequently conducted in environmental chambers (Kroll and Seinfeld 2008). All of the physical experiments discussed in this work were conducted in the MIT environmental chamber in the Kroll lab. The surfaces of the chamber system itself, including the Teflon walls, outlet sample line tubing, and instrument inlets, are of particular importance to the work in this chapter. While an SOA oxidation experiment is being conducted, VOCs, SVOCs, IVOCs, and LVOCs are simultaneously being oxidized and partitioning between the gas phase, the particle phase, and also the "wall phase" which is a condensed organic phase on chamber system surfaces (La et al. 2016). Both gasses and particles may be lost to chamber surfaces (Park et al. 2001; Krechmer, Day, and Jimenez 2020; Zhang et al. 2014). Suspended particle and gas measurements are commonplace in environmental chamber experiments and often contain the most important data an environmental chamber experiment can provide, but the organic species on chamber surfaces are unable to be measured in-situ.

Surface losses pose challenges to the accurate and complete interpretation of gas- and particle-phase chamber data. This is especially problematic for SVOC's and IVOC's which comprise the bulk of SOA as they are likely more susceptible to chamber depositional losses (Lopez-Hilfiker et al. 2015). These losses further complicate our understanding of the underlying chemistry behind the formation and oxidative evolution of SOA as highly oxygenated species likely partition more into the particle phase due to their lower vapor pressures (Donahue et al. 2013; Hallquist et al. 2009; Donahue et al. 2006). Indeed, some SOA modelling studies under-predict observed SOA yields and have suggested chamber depositional losses as (Cappa et al. 2016). A more recent comparison of GEOS-Chem model predictions and 15 aircraft campaigns suggested little systemic underprediction of SOA but also little correlation between observed

and modeled SOA (Pai et al. 2020). These discrepancies may arise from many factors including missing emissions inventories in models and unaccounted aerosol cloud processing, but another potential set of culprits is errors in SOA yields because model SOA yield inputs are determined in large part from chamber studies (Y. B. Lim et al. 2010; Ervens, Turpin, and Weber 2011; Loza et al. 2010; Zhang et al. 2014).

The physical reasoning behind chamber particle losses are generally well-understood and can be modeled as a first-order decay if the particle size distribution is known (Park et al. 2001; Crump and Seinfeld 1981). Air masses within chambers are commonly assumed to be in a turbulent flow regime because of air's low kinematic viscosity and corresponding high Reynold's number even for low air flow velocities (Welty 2008). This turbulent flow creates a boundary layer at the chamber wall surfaces through which particles can diffuse and finally settle on the walls themselves (Crump and Seinfeld 1981; Park et al. 2001). The thickness of the boundary later and thus the rate of particle diffusion through said layer depend on the dynamics of chamber mixing which are usually unknown of poorly understood, so empirical studies analyzing loss rates of polydisperse particle populations must be performed to provide constraints on particle deposition rates as a function of particle size (Ng et al. 2007; M. D. Keywood et al. 2004). Once particles deposit on surfaces they may remain there, re-aerosolize, or evaporate either partially or completely, and some particles that have deposited may remain in the chamber even after repeated chamber flushing and baking (McGarvey and Shorten 2000).

Vapor deposition rates are more difficult to parametrize, and until recently, few studies have been conducted to characterize these losses. Most vapor deposition models essentially treat chamber walls as one large particle into which gas-phase species may partition (Matsunaga et al. 2010; La et al. 2016). However, even these models are inadequate and usually do not account for important factors such as relative humidity and chamber age (Loza et al. 2010). Moreover, partitioning models in general such as the commonly used model described in Pankow, 1994 often under predict particle-phase concentrations of certain organic species such as methyl-tetrols because of myriad factors including particle-phase

oligomerization, particle phase inhomogeneity (i.e. varying viscosities and composition with radial position within the particle) , and unknown particle-phase activity coefficients (Pankow 1994; Isaacman-VanWertz et al. 2016). Consequently, empirical observations are currently required to quantify vapor losses to walls for each individual compound in each chamber. Depositional losses are combated by adding ammonium sulfate seed particles to the chamber before the organic species is injected, but commonly used seed:chamber surface area ratios of $<1x10^{-3}$ may not be adequate to effectively prevent significant wall losses (Zhang et al. 2014). Evidently there is still a great deal of work that must be done before vapor wall losses are as well characterized as particle wall losses which provides powerful motivation for the work presented below which focuses on directly quantifying bulk depositional losses.

We can quantify bulk depositional losses to chamber surfaces by measuring the Total Suspended Carbon (TSC) content of the SOA in the chamber. TSC is itself a bulk property which represents the total concentration of carbon in the gas and particle phases in an SOA sample. Measuring TSC in combination with an initial measurement or knowledge of the amount of carbon injected into a chamber system allows one to calculate the amount of carbon, if any, lost to chamber surfaces over the course of an SOA oxidation experiment. A measurement of TSC by itself is also useful as a top-down measurement to constrain the various bottom-up speciated measurements made by gas monitors and mass spectrometry instruments. This constraint can inform chamber researchers if they have accurately measured all of the suspended carbon contained within gas- and particle-phase organic species or if they may be under or overestimating the amount of TSC in the chamber from with bottom-up measurements. Previous studies have been performed using OH reactivity instead of TSC as the top-down constraint and in many instances have shown significant discrepancies between bottom-up measurements and the top-down constraint (Sinha et al. 2007; Hansen et al. 2015). Thus, the development of new techniques and instruments for establishing top-down constraints on aerosol systems is critically important for allowing for

intercomparisons of different top-down constraints and for assessing whether all carbon in a system has been properly quantified.

The work presented herein describes the development and characterization of a TSC measurement apparatus hereafter referred to as the Oxy-Cat (short for 'Oxidizing Catalyst'). The Oxy-Cat's design is based on two previous apparatuses created to measure total gaseous carbon in ambient air and consists of three main components; a catalyst composed of palladium on glass wool, a tube furnace to house the catalyst, and a CO_2 analyzer (Maris et al. 2003; Veres et al. 2010). Heated palladium catalysts are commonly employed in organic chemistry to oxidize organic chemicals, and when the oxidations occur when significant oxygen is present and with sufficient reaction time, carbonaceous species are converted completely to CO_2 (Veres et al. 2010; Maris et al. 2003). It is currently unknown how efficient the catalyst is at oxidizing various species or even if it in fact is able to oxidize all species, so a significant portion of the research presented in this paper focuses on calibrating the catalyst. Once the catalyst has fully oxidized the organic species, the CO_2 analyzer can measure the total carbon concentration in the sampled aerosol. As of yet, no system like the Oxy-Cat has been used in environmental chamber experiments (except for experiments conducted in smaller Potential Aerorosl Mass (PAM) oxidation flow reactor experiments).

2. Design and Methodology

The Oxy-Cat system is comprised of three main components: the palladium catalyst; the tube furnace to house the catalyst; and the CO_2 monitor. Figure 1 displays the basic design of the Oxy-Cat. 1 Lpm zero air passes through the heated inlet line (~20 cm of 1/4" stainless steel tubing wrapped in heat tape, held at 150 °C). VOC solutions are injected into the heated zero air stream. The gas stream then passes through the heated Pd catalysts ("Hi Sens Catalyst" from Shimadzu, 10% Pd on glass wool) and Pt catalysts ("Platinum screen, TOC" from Shimadzu). 24 Pt screen and two sets of Pd on glass wool catalysts were used. The catalysts were housed in a tube furnace (Supelco 2-3800 set to 500 °C). The gas stream

then exits the tube furnace and enters a cooling coil region (1/4" copper tubing; three coils). Lastly, the gas stream enters the sample cell of the CO_2 (LI-7000, LI-COR Biosciences). The LI-7000 has two cells which measure CO_2, one reference cell and one sample cell. The sample cell is sampling gas that has been put through the heated catalyst region which is designed to convert all organic carbon to CO_2, and the reference cell is sampling gas that is not passing through the heated catalyst. The measurement from the reference cell is subtracted from the measurement of the sample cell in order to determine the difference in the concentration of CO_2 between the two cells which is thus the measurement of TSC that we desire. The LI-7000 a rated nominal precision of ±1% and an empirically determined differential limit of detection of approximately 10 ppbC.

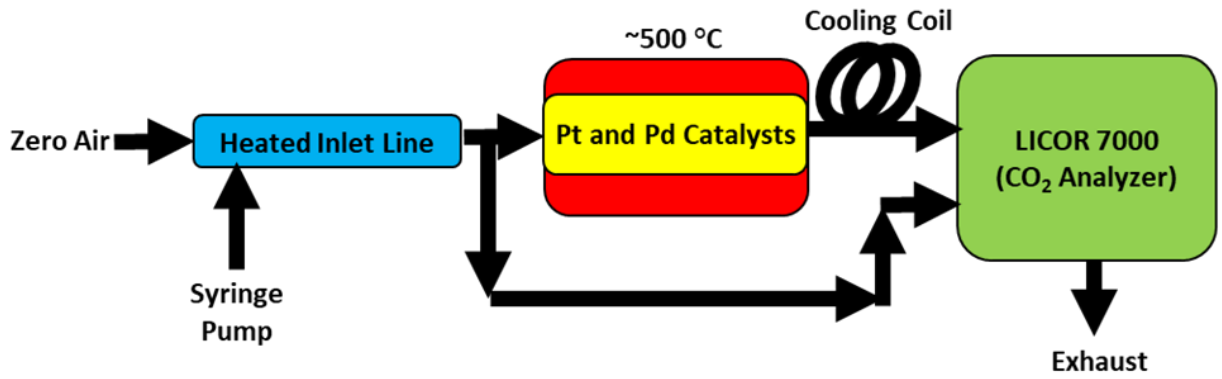

Figure 1: A basic schematic of the Oxy-Cat system. The major components are a heated inlet, heated platinum and palladium catalysts, and the LICOR 7000 CO2 monitor. The LICOR 7000 contains two measurement cells: the sample cell measures CO_2 from the air stream going through the heated catalyst region; the reference cell measures CO2 from the air stream which bypasses the catalysts.

The Oxy-Cat was calibrated with VOC injections via syringe pump as shown in Figure 1. The syringe pump used was a Harvard Apparatus PHD Ultra Syringe Pump with an accompanying Hamilton glass 50 µL syringe. Dilute solutions of water-soluble VOCs prepared in Milli-Q water were injected in the heated inlet line at different rates to produce air samples of varying TSC. It was necessary to dilute the organics prior to injection to ensure that the expected CO_2 concentration would be in a relevant range to most chamber experiments (10-500 ppbC) The injected VOC solutions were vaporized in the heated inlet line and mixed with a zero air stream. The gas stream is then split with roughly half of the gas (0.5 Lpm) traveling to the

reference cell of the LI-7000 and the other half of the gas traveling through the heated catalyst region to the sample cell of the LI-7000.

Expected CO_2 concentrations were calculated assuming ideal gas behavior and complete and rapid evaporation of all injected material. Expected CO_2 concentrations were set by varying the volumetric injection rate of the diluted organic solutions. Blanks of Milli-Q water were run at each volumetric injection rate and used to establish baseline CO_2 levels. The net flow rate (zero air plus vaporized dilute organic solution) was measured with a Mesa Labs DryCal® Defender 510 flow meter placed inline after each of the LI-7000's cells. Zero air flow rates were adjusted with a needle valve placed inline before the heated inlet line to account for changes in flow rates at different organic solution injection rates because of significant influences on the net flow rate from the evaporation of the organic solution. CO_2 measurements were recorded at a rate of 1Hz and were averaged over at least a 30 second interval once the measurements had stabilized to obtain final values. The averaged CO_2 measurements were then compared to the expected CO_2 concentrations to determine the degree of oxidation for each organic species.

3. Results: Calibration and Characterization

An example of the raw data obtained from the LI-7000 from a calibration study involving a syringe pump injection of methanol is shown below in Figure 2. There is noise in the signal immediately preceding and following the start of the methanol injection (represented by the spike in the data), and averaging the signal over a two-minute period yields an uncertainty in the measurement of ±2.5 ppbC, two orders of magnitude less than the initial carbon content upon injection of a precursor VOC.

In addition to measuring small changes in aerosol carbon content, it was crucial to ensure that the Oxy-Cat was not biased against VOC's which are more difficult to oxidize. Methanol, acetone, benzene, glutaric acid, pinonic acid, and dichloromethane were chosen as calibrants because of the diversity of functional groups and vapor pressures they encompass. Of particular note is the inclusion of glutaric acid

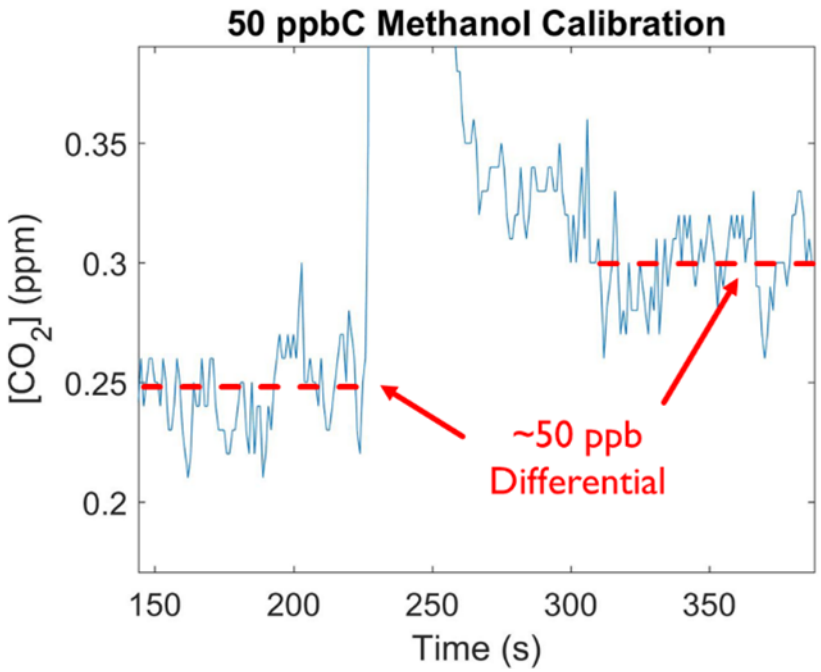

Figure 2: Raw data obtained from the Oxy-Cat system for the calibration of 50ppb methanol. The start of the syringe pump injections is clearly visible in the spike near 225 seconds. A 50 ppbC increase in the differential CO_2 measurement is observed after injection.

and pinonic acid which are IVOC's and thus more susceptible to wall losses than the other species included in the calibrations. Figure 3 displays the calibration results, and it is readily apparent that all species displayed complete conversion to CO_2 across the chosen span of concentrations.

One species of particular importance in Figure 3 that was not fully oxidized is perfluorooctane. All of the other species on which the Oxy-Cat was calibrated are at least somewhat water soluble which made it possible to create dilute solution in MilliQ water. However, we still need to ensure that the Oxy-Cat can convert a variety of non-water-soluble and nonpolar VOC's entirely to CO_2 as well. Perfluorooctane is nonpolar and liquid at room temperature which means it can be used as a solvent to create dilute solutions of non-water-soluble VOCs. It is readily apparent that the observed formation of CO_2 from the oxidation of perfluorooctane is at least three orders of magnitude less than expected. This is promising for perfluorooctane's use as a solvent since the solvent should not contribute to the differential CO_2 signal measured by the LI-7000.

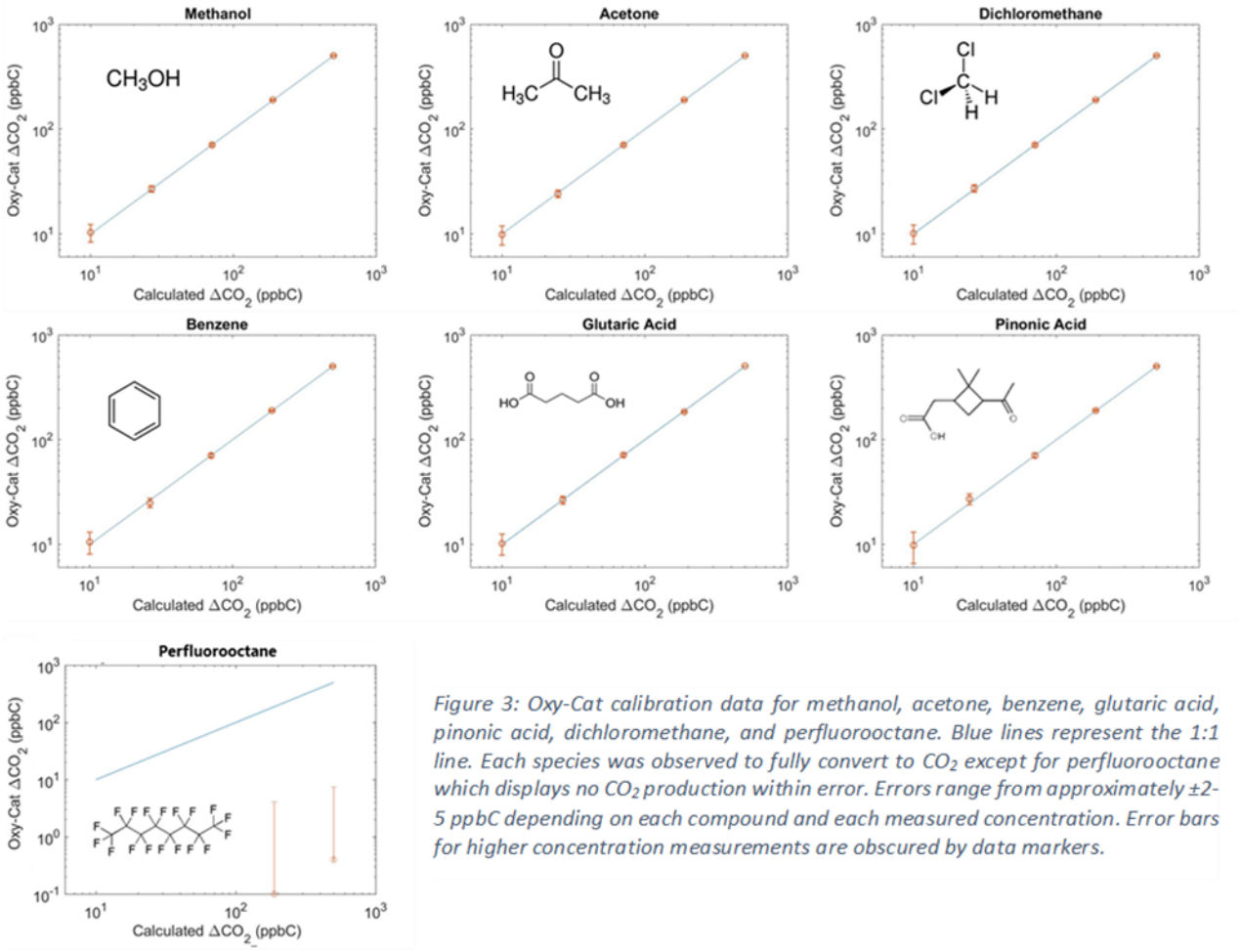

Figure 3: Oxy-Cat calibration data for methanol, acetone, benzene, glutaric acid, pinonic acid, dichloromethane, and perfluorooctane. Blue lines represent the 1:1 line. Each species was observed to fully convert to CO_2 except for perfluorooctane which displays no CO_2 production within error. Errors range from approximately ±2-5 ppbC depending on each compound and each measured concentration. Error bars for higher concentration measurements are obscured by data markers.

4. Discussion and Future Work

The data presented in Figures 2 and 3 suggest that the Oxy-Cat is capable of oxidizing a wider range of organic species across a range of size, chemical complexity, volatility. The Oxy-Cat is capable of measuring gas-phase TSC in concentrations ranging from 500 ppbC down to 10 ppbC, which spans the range of concentrations that are commonly seen in chamber experiments. TSC measurements are precise to within ±2-5 ppbC which corresponds to a less than 1% uncertainty for a typical chamber study.

The work in this chapter is a positive proof of concept to demonstrate that the Oxy-Cat is capable of oxidizing several different VOCs and that it is able to measure their concentrations with high precision down to 10ppbC ±2-5 ppbC. However, some work must still be completed before the Oxy-Cat is ready to

be used during chamber experiments to constrain TSC. Notably absent in Figure 3 are nonpolar species which are not water-soluble. Relatively hydrophilic species were chosen because water does not contain carbon, and so when the VOC calibrant mix is injected via syringe pump, the solvent will not contribute significantly to the observed CO_2 signal. Were we to have used a common organic solvent like hexane, the solvent's conversion to CO_2 would completely mask the signal from the VOC under analysis. Future work regarding calibrations of nonpolar and non-water-soluble VOC may be performed with perfluorooctane. Figure 3 shows that perfluorooctane oxidizes approximately three orders of magnitude less than we would expect were it to be fully converted to CO_2 by the heated catalysts. This means that perfluorooctane may be used as a nonpolar solvent for nonpolar VOC calibrations to confirm that they too may be fully oxidized.

Particle-phase calibrations must also be performed because organic species often condense onto seed particles over the course of a normal chamber experiment. These particle-phase species are also considered a component of TSC. I propose that initial stages of this future work can be performed using purely organic particles of squalane ($C_{30}H_{62}$). Squalane particles of this nature have generated in our lab by flowing air through a tub containing liquid squalane in a tube furnace, and they would serve as a good model system for calibration purposes (C. Y. Lim et al. 2017). Squalane is also a branched alkane which is of particular interest to this proposal. Although particle-phase VOC oxidation may at first appear to be different than gas-phase VOC oxidation, it is worth remembering that the catalysts is kept at ~500 °C which we believe is sufficient to vaporize and/or decompose organic particles. However, more work on a variety of different particles, including oxygenated and aged aerosol particles, should be performed to verify this assumption.

Our ultimate goal for the Oxy-Cat is for it to be used in any chamber study in which a measure of TSC would help constrain other measurements. Labs often perform chamber experiments in which they attempt to achieve carbon closure which means that they attempt to measure all oxidation products completely and accurately. However, those measurements may be uncertain due to uncertainties

stemming from the calibration used to convert instrument signal to concentration (e.g. Isaacman-VanWertz et al. 2018). The Oxy-Cat can help constrain these measurements by providing an upper bound of TSC against which bottom-up speciated measurements can be compared. Further work must be performed to demonstrate the Oxy-Cat's ability to provide this constraint. Chamber experiments designed to achieve carbon closure should be performed in tandem with the Oxy-Cat as proofs of concept. The process of attaching the Oxy-Cat to the chamber poses challenges. Some of these challenges may include gas and particle losses on Oxy-Cat tubing and other surfaces which would need to be minimized for the Oxy-Cat to provide an accurate measure of TSC regardless of the VOC system under observation. Another potential challenge could arise in the form of negative pressure leaks (e.g. room air entering into the Oxy-Cat apparatus via small openings in tubing joints) which render the Oxy-Cat measurements useless because of high indoor CO_2 concentrations. These chamber characterization studies will require collaboration across multiple labs and potentially multiple universities in order to obtain a suite of instruments capable of achieving carbon closure.

Once these remaining steps are taken, the Oxy-Cat will be ready to be adapted and optimized for use in any future chamber study. Several benefits will arise from implementing the Oxy-Cat in chamber experiments. As discussed in Section 1, vapor losses have been difficult to parametrize, and they may differ substantially from chamber to chamber. The Oxy-Cat will allow each lab to measure wall losses in-situ to better constrain all gas- and particle-phase bottom up measurements, for example, by measuring wall losses of VOCs across a range of volatilities to create a vapor deposition model as a function of volatility. Even if this parametrization is not performed, the Oxy-Cat can still be utilized to place an upper bound on all speciated measurements to reduce uncertainty. This clearly has important implications for the results of every chamber experiment, namely that measurements can be corrected and reported with increased accuracy and precision, particularly for studies focused on SOA yield and/or studies which involve significant formation of SVOCs, IVOCs, and LVOCs which are particularly susceptible to gas-phase

wall loss. Improvements in SOA yield studies from chamber will increase the accuracy of and decrease uncertainties in regional and global chemical transport models which rely on chamber studies to parametrize SOA particle formation (Zhang et al. 2014).

5. References

Cappa, Christopher D., Shantanu H. Jathar, Michael J. Kleeman, Kenneth S. Docherty, Jose L. Jimenez, John H. Seinfeld, and Anthony S. Wexler. 2016. "Simulating Secondary Organic Aerosol in a Regional Air Quality Model Using the Statistical Oxidation Model - Part 2: Assessing the Influence of Vapor Wall Losses." *Atmospheric Chemistry and Physics* 16 (5): 3041–59. https://doi.org/10.5194/ACP-16-3041-2016.

Crump, James G., and John H. Seinfeld. 1981. "Turbulent Deposition and Gravitational Sedimentation of an Aerosol in a Vessel of Arbitrary Shape." *Journal of Aerosol Science* 12 (5): 405–15. https://doi.org/10.1016/0021-8502(81)90036-7.

Donahue, N. M., W. Chuang, S. A. Epstein, J. H. Kroll, D. R. Worsnop, A. L. Robinson, P. J. Adams, and S. N. Pandis. 2013. "Why Do Organic Aerosols Exist? Understanding Aerosol Lifetimes Using the Two-Dimensional Volatility Basis Set." *Environmental Chemistry* 10 (3): 151–57. https://doi.org/10.1071/EN13022.

Donahue, N. M., A. L. Robinson, C. O. Stanier, and S. N. Pandis. 2006. "Coupled Partitioning, Dilution, and Chemical Aging of Semivolatile Organics." *Environmental Science and Technology* 40 (8): 2635–43. https://doi.org/10.1021/es052297c.

Ervens, B., B. J. Turpin, and R. J. Weber. 2011. "Secondary Organic Aerosol Formation in Cloud Droplets and Aqueous Particles (AqSOA): A Review of Laboratory, Field and Model Studies." *Atmospheric Chemistry and Physics* 11 (21): 11069–102. https://doi.org/10.5194/acp-11-11069-2011.

Hallquist, M, J C Wenger, U Baltensperger, Y Rudich, D Simpson, M Claeys, J Dommen, et al. 2009. "The Formation, Properties and Impact of Secondary Organic Aerosol: Current and Emerging Issues." *Atmos. Chem. Phys. Atmospheric Chemistry and Physics* 9 (July): 5155–5236. https://doi.org/10.5194/acp-9-5155-2009.

Hansen, R. F., M. Blocquet, C. Schoemaecker, T. L??onardis, N. Locoge, C. Fittschen, B. Hanoune, P. S. Stevens, V. Sinha, and S. Dusanter. 2015. "Intercomparison of the Comparative Reactivity Method (CRM) and Pump-Probe Technique for Measuring Total OH Reactivity in an Urban Environment." *Atmospheric Measurement Techniques* 8 (10): 4243–64. https://doi.org/10.5194/amt-8-4243-2015.

Isaacman-VanWertz, Gabriel, Paola Massoli, Rachel O'Brien, Christopher Lim, Jonathan P. Franklin, Joshua A. Moss, James F. Hunter, et al. 2018. "Chemical Evolution of Atmospheric Organic Carbon over Multiple Generations of Oxidation." *Nature Chemistry* 10 (4): 462–68. https://doi.org/10.1038/s41557-018-0002-2.

Isaacman-VanWertz, Gabriel, Lindsay D. Yee, Nathan M. Kreisberg, Rebecca Wernis, Joshua A. Moss, Susanne V. Hering, Suzane S. de Sá, et al. 2016. "Ambient Gas-Particle Partitioning of Tracers for Biogenic Oxidation." *Environmental Science & Technology* 50 (18): 9952–62. https://doi.org/10.1021/acs.est.6b01674.

Krechmer, Jordan E., Douglas A. Day, and Jose L. Jimenez. 2020. “Always Lost but Never Forgotten: Gas-Phase Wall Losses Are Important in All Teflon Environmental Chambers.” *Environmental Science and Technology* 54 (20): 12890–97. https://doi.org/10.1021/ACS.EST.0C03381/SUPPL_FILE/ES0C03381_SI_001.PDF.

Kroll, Jesse H., and John H. Seinfeld. 2008. “Chemistry of Secondary Organic Aerosol: Formation and Evolution of Low-Volatility Organics in the Atmosphere.” *Atmospheric Environment* 42 (16): 3593–3624. https://doi.org/10.1016/j.atmosenv.2008.01.003.

La, Y. S., M. Camredon, P. J. Ziemann, R. Valorso, A. Matsunaga, V. Lannuque, J. Lee-Taylor, A. Hodzic, S. Madronich, and B. Aumont. 2016. “Impact of Chamber Wall Loss of Gaseous Organic Compounds on Secondary Organic Aerosol Formation: Explicit Modeling of SOA Formation from Alkane and Alkene Oxidation.” *Atmospheric Chemistry and Physics* 16 (3): 1417–31. https://doi.org/10.5194/acp-16-1417-2016.

Lim, C. Y., E. C. Browne, R. A. Sugrue, and J. H. Kroll. 2017. “Rapid Heterogeneous Oxidation of Organic Coatings on Submicron Aerosols.” *Geophysical Research Letters* 44 (6): 2949–57. https://doi.org/10.1002/2017GL072585.

Lim, Y. B., Y. Tan, M. J. Perri, S. P. Seitzinger, and B. J. Turpin. 2010. “Aqueous Chemistry and Its Role in Secondary Organic Aerosol (SOA) Formation.” *Atmospheric Chemistry and Physics* 10 (21): 10521–39. https://doi.org/10.5194/acp-10-10521-2010.

Lopez-Hilfiker, F. D., C. Mohr, M. Ehn, F. Rubach, E. Kleist, J. Wildt, Th. F. Mentel, et al. 2015. “Phase Partitioning and Volatility of Secondary Organic Aerosol Components Formed from α-Pinene Ozonolysis and OH Oxidation: The Importance of Accretion Products and Other Low Volatility Compounds.” *Atmospheric Chemistry and Physics* 15: 7765–76. https://doi.org/10.5194/acp-15-7765-2015.

Loza, Christine L, Arthur W H Chan, Melissa M Galloway, and Frank N Keutsch. 2010. “Characterization of Vapor Wall Loss in Laboratory Chambers.” *Environmental Science & Technology* 44 (13): 5074–78.

Maris, Christophe, Myeong Y Chung, Richard Lueb, Udo Krischke, Richard Meller, Matthew J Fox, and Suzanne E Paulson. 2003. “Development of Instrumentation for Simultaneous Analysis of Total Non-Methane Organic Carbon and Volatile Organic Compounds in Ambient Air.” *Atmospheric Environment* 37 (2): 149–58. https://doi.org/10.1016/S1352-2310(03)00387-X.

Matsunaga, Aiko, Paul J Ziemann, Aiko Matsunaga, and Paul J Ziemann. 2010. “Gas-Wall Partitioning of Organic Compounds in a Teflon Film Chamber and Potential Effects on Reaction Product and Aerosol Yield Measurements Gas-Wall Partitioning of Organic Compounds in a Teflon Film Chamber and Potential Effects on Reaction Product And.” *Aerosol Science and Technology* 44: 881–92. https://doi.org/10.1080/02786826.2010.501044.

McGarvey, Linda J., and Charles V. Shorten. 2000. “The Effects of Adsorption on the Reusability of Tedlar® Air Sampling Bags.” *AIHAJ - American Industrial Hygiene Association* 61 (3): 375–80. https://doi.org/10.1080/15298660008984546.

M. D. Keywood, V. Varutbangkul, R. Bahreini, and R. C. Flagan, and J. H. Seinfeld*. 2004. “Secondary Organic Aerosol Formation from the Ozonolysis of Cycloalkenes and Related Compounds.” https://doi.org/10.1021/ES035363O.

Ng, N. L., J. H. Kroll, A. W. H. Chan, P. S. Chhabra, R. C. Flagan, and J. H. Seinfeld. 2007. “Secondary Organic Aerosol Formation from M-Xylene, Toluene, and Benzene.” *Atmospheric Chemistry and Physics* 7 (14): 3909–22. https://doi.org/10.5194/acp-7-3909-2007.

Pai, Sidhant J., Colette L. Heald, Jeffrey R. Pierce, Salvatore C. Farina, Eloise A. Marais, Jose L. Jimenez, Pedro Campuzano-Jost, et al. 2020. “An Evaluation of Global Organic Aerosol Schemes Using Airborne Observations.” *Atmospheric Chemistry and Physics* 20 (5): 2637–65. https://doi.org/10.5194/ACP-20-2637-2020.

Pankow, J. F. 1994. “An Absorption Model of Gas/Particle Partitioning of Organic Compounds in the Atmosphere.” *Atmospheric Environment* 28 (2): 185–88. https://doi.org/10.1016/1352-2310(94)90093-0.

Park, S. H., H. O. Kim, Y. T. Han, S. B. Kwon, and K. W. Lee. 2001. “Wall Loss Rate of Polydispersed Aerosols.” *Aerosol Science and Technology* 35 (3): 710–17. https://doi.org/10.1080/02786820152546752.

Sinha, V., J. Williams, J. N. Crowley, and J. Lelieveld. 2007. “The Comparative Reactivity Method – a New Tool to Measure Total OH Reactivity in Ambient Air.” *Atmospheric Chemistry and Physics Discussions* 7 (6): 18179–220. https://doi.org/10.5194/acpd-7-18179-2007.

Veres, P., J. B. Gilman, J. M. Roberts, W. C. Kuster, C. Warneke, I. R. Burling, and J. De Gouw. 2010. “Development and Validation of a Portable Gas Phase Standard Generation and Calibration System for Volatile Organic Compounds.” *Atmospheric Measurement Techniques* 3 (3): 683–91. https://doi.org/10.5194/amt-3-683-2010.

Welty, James R. 2008. *Fundamentals of Momentum, Heat, and Mass Transfer*. John Wiley & Sons.

Zhang, Xuan, Christopher D. Cappa, Shantanu H Jathar, Renee C. McVay, Joseph J. Ensberg, Michael J. Kleeman, John H. Seinfeld, and Christopher D. Cappa. 2014. “Influence of Vapor Wall Loss in Laboratory Chambers on Yields of Secondary Organic Aerosol.” *Proceedings of the National Academy of Sciences of the United States of America* 111 (16): 1–6. https://doi.org/10.1073/pnas.1404727111.

III. Multiparameter Quantitative Comparisons of Smog Chamber and Chemical Mechanistic Datasets

1. Introduction

As we have discussed in the previous chapters, experiments studying the chemistry of SOA formation and evolution are frequently conducted in controlled environments known as environmental chambers (Kroll and Seinfeld 2008). The MIT chamber used in this work is composed of a Teflon bag in a temperature-controlled room surrounded by UV lights which catalyze the all-important photolytic reactions which drive oxidation reactions (Seinfeld and Pandis 2006). We study specific oxidation systems by injecting a single organic species into the chamber along with seed particles and oxidant precursors like HONO which photolyze to form OH and NO radicals. With this framework, chamber experiments allow us to examine isolated chemical oxidation systems in a variety of different ways and at different levels of granularity.

On the least granular side of the analysis spectrum, chamber studies are conducted to measure overarching system properties like O:C ratios and SOA yield from a specific VOC precursor oxidation system (Docherty et al. 2021; Zhang et al. 2014; Aiken et al. 2008; Gkatzelis et al. 2018). Some of these studies are particularly useful for parametrizing SOA production in chemical transport models, and other studies involving measurements of elemental ratios can provide evidence regarding the degree to which SOA is oxidized. On the most granular side of the analysis spectrum, chamber experiments can be conducted to measure specific products in a VOC oxidation system to better characterize production and degradation rate constants (Ma et al. 2007). These experiments are quite useful for elucidating specific chemical reactions, particularly those which lead to the production and degradation of major products like pinic acid and pinonaldehyde in the α-pinene oxidation system (Ma et al. 2007). Both highly granular and highly coarse chamber analyses provide useful information, but it is not possible to simultaneously gain deep and broad understandings of the oxidation system using simply one of these analyses.

A third and particularly relevant class of chamber experiments falls in the category of holistic measurement studies which aim to achieve "carbon closure." These chamber studies are performed with a suite of instruments selected to measure every major organic and inorganic species in the gas- and particle-phases to obtain a more complete view of the evolution of VOC oxidation system over time. These studies are difficult to perform because of the extreme complexity of VOC oxidation product mixtures, so until recently these studies had only been performed for simple systems like short-chain alkane oxidation (Calvert 2008). Advanced in analytical capabilities including the introduction of new CIMS measurement techniques have recently allowed our lab to conduct carbon closure studies on α-pinene oxidation (Gabriel Isaacman-VanWertz et al. 2018). The α-pinene study tracked carbon over the course of an eight-hour chamber experiment which translates to roughly one day in the atmosphere. Speciated measurements were catenated into distributions based on different properties including each species' average carbon oxidation state (OSc), number of carbons per species, and each species' vapor pressure. Examining the carbon number over time is a useful proxy for understanding the fragmentation of the VOC precursor's carbon backbone, and exploring the OSc distribution is a useful proxy for understanding the degree to and manner in which the species in the system are functionalizing.

Computational mechanisms are another useful tool that researchers use to understand how a chemical oxidation system may behave in different circumstances. A mechanism's greatest advantage lies in its predictive capabilities, allowing researchers to test their understanding of and potential additions Additionally, it usually requires much less time to perform a box model simulation than it does to perform a chamber experiment and analyze CIMS data. One of the best-known computational mechanism in the field of atmospheric chemistry is the Master Chemical Mechanism (MCM) which contains a set of thousands of explicitly defined chemical reactions of dozens of VOCs (Jenkin, Saunders, and Pilling 1997; Saunders et al. 2003). MCM has been used in different studies at different levels of granularity, just like chamber experiments. For example, MCM has been used to model bulk SOA production along with O:C

and N:C ratios in a chemical transport model for the Houston, Texas region (Li et al. 2015). MCM can also be used more granularly, for example, to characterize specific organonitrate species in the particle-phase of SOA formed from the nitrate radical initiated oxidation of limonene (Faxon et al. 2018). Both of these examples involve the comparison of MCM to an observationally derived dataset. This is a requirement in order to validate the results from the mechanism, and this comparison can also be used to improve the mechanism itself by constraining it to the observational data.

Explicit mechanisms like MCM are inherently limited because If a certain reaction exists in reality but has not been explicitly defined in the mechanism, the mechanism will be incomplete. Self-generating mechanisms are less susceptible to these limitations because they attempt to predict every possible reaction and their corresponding rates even if they are not already contained in an explicit mechanism. For example, GECKO-A, a self-generating mechanism, incorporates the known reactions contained in MCM and then generates its own reactions and predicts rates using SARs (Bernard Aumont, Szopa, and Madronich 2005; Camredon et al. 2007). GECKO-A examines every bond in a given molecule and predicts how it may react under different scenarios. Unimolecular reactions including, but not limited to, alkoxy radical decomposition and isomerization and bimolecular reactions including reaction with OH, NO, O_3 are all considered. If a reaction and its rate are contained within MCM or have been empirically studied and reported, GECKO-A will use the reported values (Bernard Aumont et al. 2012). However, if a reaction is not explicitly known, GECKO-A will use SARs to predict said reaction and rate. SARs are essentially a set of rules to predict the activation energy for a reaction, rules which have been determined via quantum chemical calculations using a training set of reactions for which rate and activation energies are known (Vereecken and Peeters 2010; Vereecken and Peeters 2009; Peeters, Fantechi, and Vereecken 2004). One of GECKO-A's useful advantages is that these SARs may be edited to test their effects on predicted chemistry.

GECKO-A results have been compared to empirical observations on several occasions. For example, GECKO-A has shown an ability to reproduce empirical results on SOA yields from alkane oxidation studies which has helped validate the mechanisms that GECKO-A creates for alkane oxidation (Bernard Aumont et al. 2012). However, GECKO-A also indicated that a large fraction of alkane SOA particulate matter is composed of multifunctional organic nitrates which have previously not been empirically detected in the concentrations the model suggested (Bernard Aumont et al. 2013). The same study showed that GECKO-A does not do a good job of describing the formation of highly oxygenated organic aerosol most likely because of missing reaction pathways (i.e. RO_2 isomerization) for which SARs dis not exist at that time in GECKO-A. We must remain wary that all mechanisms, and particularly those with capabilities to predict unknown or uncharacterized reactions like GECKO-A can, require validation to be taken as truth.

The main goal of this chapter is to develop a methodology by which measurements and computational mechanistic results can be compared to provide mutual improvements. To date, no study has compared entire product distributions from chamber and mechanistic datasets. Chamber experiments provide an anchor in reality, but the chamber and instruments themselves often introduce uncertainty into the results. These uncertainties can arise from depositional losses as we discussed in Chapter 2, but they can also arise from chemical transformations which occur to certain species upon detection. Evidence of decomposition of organic hydroperoxides on instrument surfaces and decomposition of organic nitroperoxides upon protonation in the PTR ionization region have been reported (Rivera-Rios et al. 2014; Leglise et al. 2019). Additionally, alcohol dehydration has been reported to occur in the PTR-MS (Brown et al. 2010). Anecdotal evidence from collaborators Abby Koss and Alexander Zaytsev suggests that aldehyde functional groups may also undergo decomposition, and perhaps other functional groups may undergo decomposition as well. Through correlative analysis of the time series of each species, mechanisms can provide suggestions as to the true structures and identities

of decomposed species. On the other hand, GECKO-A results must be checked against physical measurements for validation purposes. Comprehensive chamber experiments like those we perform at MIT provide an unprecedented way to perform these comparisons since we can compare data every level of granularity to suggest areas in which GECKO-A can improve.

The overall result of the work described in the rest of this chapter is to provide a method to generate two kinds of targeted insights from chamber-mechanism comparisons: (1) improvements in understanding how the act of measuring organic species with CIMS instruments affects the ways in which we should identify them; (2) suggested improvements in GECKO-A's mechanism generator, particularly in how it predicts reactions and rates using SARs.

2. Materials and Methods

2.1. Chamber Experimental Design

High-NOx experiments were conducted in the 7.5 m^3 Teflon Kroll lab chamber (Hunter et al. 2014). The UV lights (Q-Labs) used in the chamber for the experiments described herein have a peak wavelength of 340 nm, different from the 351 nm peak wavelength lights from Hunter et al. The chamber was operated in semi-batch mode with a makeup zero air flow of 10-12 Lpm to account for the instrument sample flow. The chamber was run under dry conditions (maximum RH of ~2%), and the temperature was held at 291.0±0.5 K. The low RH is better for comparisons with GECKO-A simulations because the gas-particle partitioning module in GECKO cannot account for most heterogeneous reactions or water uptake, both of which would increase the uncertainty between the measurement-mechanism comparisons (Camredon et al. 2007; Mouchel-Vallon et al. 2013; Lee-Taylor et al. 2011).

Photochemical oxidation experiments were performed using butane and α-pinene as the VOC precursors, nitrous oxide (HONO) as the source of OH (and NO), and dry ammonium sulfate particles (2.5–5.7×10^4 cm^{-3}) as condensation nuclei. The dry ammonium sulfate particles were added first, followed by

2 µL of hexafluorobenzene (C_6F_6) which served as the dilution tracer because of its exceedingly slow reaction kinetics with OH. HONO was then generated in a bubbler by adding 2-4 µL of sulfuric acid (H_2SO_4) via syringe pump to a solution of sodium nitrate ($NaNO_2$). HONO was added to the chamber in a 15 Lpm zero air stream to be added to the chamber, resulting in HONO mixing ratios of ~25-35 ppbV. Lastly, precursor VOCs were added by injecting 2-4 µL into a heated inlet with a zero air flow rate of 15 Lpm. All reagents and seed particles were allowed to mix in the chamber for several minutes to allow for more even distribution throughout the chamber. UV lights were then turned on to catalyze the production of OH and NO from HONO photolysis, thereby begging the experiment. Measurements were collected over the course of ~7.5 hrs. Three subsequent additions of HONO to the chamber occurred in for both precursor experiments so as to promote further oxidation and aging.

2.2. Chamber Instrumentation

The temperature, relative humidity, ozone (2B Technologies), CO (Teledyne) and HONO and nitrogen oxides (NOx) (Thermo Fischer Scientific) were monitored throughout the course of the experiments. An aerosol mass spectrometer (AMS) (Aerodyne Research Inc.) was calibrated with ammonium nitrate and was used to measure total organic particle-phase mass assuming a particle collection efficiency of 1. Gas-phase compounds, including the precursors, were measured with a suite of chemical ionization high-resolution time-of-flight mass spectrometers (CIMS). The I^- CIMS (Aerodyne Research Inc.) was operated as described in Lee et al., 2014. H_3O^+ and NH_4^+ CIMS (PTR3, IONICON Analytik) measurements were also performed. Each CIMS instrument used a 3/16" Teflon sampling line with a 2 Lpm flow rate. Estimations of uncertainties in quantification for all of the species detected via CIMS are as follows: identified compounds, 10% uncertainty; PTR and NH_4^+ CIMS, 30% uncertainty; and I-CIMS, 2.5x uncertainty.

2.3. GECKO-A Mechanistic Simulations

GECKO-A was used to generate chemical oxidation mechanisms and perform 1-D box model simulations for the chamber experiments described in Section 3.2. All mechanisms were created to include all reactions, products, and intermediates leading up to and including fourth-generation oxidation products. Detailed descriptions of how GECKO-A generates mechanisms can be found in Aumont et al., 2005, Camredon et al. 2007, and Valorso et al. 2011. GECKO-A simulations were run on a remote Linux server (Digital Ocean) operating Ubuntu 18.04. GECKO-A itself is written in FORTRAN 77 and FORTRAN 90 (some parts of the code have not been updated to the more recent version of FORTRAN).]

GECKO-A simulations must be "tuned" for the best comparisons to chamber data. Tuning a GECKO-A simulation involves matching the precursor, ozone, NO_x, and particulate mass concentration time series to the time series measured in the chamber. Matching these key parameters ensures that the reaction conditions in the GECKO-A simulation are as close as possible to those experienced in the chamber. This serves to anchor the comparative analysis (main focus of Section 2.4) to chamber observations, allowing for comparisons to focus on differences in chemistry instead of differences arising from potential discrepancies in ambient conditions. Light intensity is the main tuning parameter used for these GECKO-A simulations because it is largely responsible for controlling ozone, HONO, and NO_x concentrations as they are sensitive to the chamber's photolytic conditions. Light intensity is scaled linearly across the UV light spectrum input which was obtained from the manufacturer of the lights (Q-Labs). An iterative process is used to tune the light intensity scaling factor and all other tuning parameters.

The other two major tuning parameters are linear multipliers controlling the rate of losses of gas-phase species to the walls and the mass accommodation coefficient for gas-particle uptake. These parameters are tuned to match the ozone concentrations and particulate SOA yield as observed in the chamber as best as possible.

2.4. Chamber-Mechanism Comparisons: Development of and Insights from Novel Methods

This section focuses on the butane oxidation system as the basis on which the pinene oxidation system comparisons will be conducted. Butane is a relatively simple molecule comprised of a linear alkane chain of only four carbon atoms, and butane oxidation is believed to be well characterized by GECKO-A because of the extensive work done with GECKO-A to model alkane oxidation (B. Aumont et al. 2012). This simplicity and relatively high level of confidence in GECKO-A's ability to model butane oxidation makes the butane system a reasonable choice as the starting point for building our comparison methodology. The PTR was the only CIMS-based instrument taking measurements during the chamber experiment, and there is a high degree of confidence that the PTR measured all expected major gas-phase products from butane oxidation because the PTR is adept at measuring species with four or fewer carbons, relatively high-volatility species, and species with O:C ratios ranging from 0-1 (G. Isaacman-VanWertz et al. 2017). No significant concentrations of organic particle-phase species were formed or were expected to have formed in the chamber.

Butane oxidation simulations were performed in GECKO-A and tuned according to the methods provided in Section 2.3. Since CIMS can not distinguish between compositional isomers (except in cases where the CIMS reagent ion may preferably associate with specific functional groups), all GECKO-A compositional isomers were lumped together before comparing GECKO-A and chamber data. After isomer lumping was performed and all time series were corrected for dilution, an average of the concentrations of each isomer in GECKO-A and the chamber were taken across the duration of the experiment. These average concentrations were then plotted against each other as shown in Figure 1.

Several features are immediately apparent in Figure 1; the compositional isomer group of Methyl Ethyl Ketone (MEK), butanal, and tetrahydrofuran (THF) has the highest average concentration in both datasets and almost falls exactly on the 1:1 line. Several other major species (e.g. acetaldehyde) fall within one order of magnitude of the 1:1 line which implies that GECKO-A has done a reasonable job of

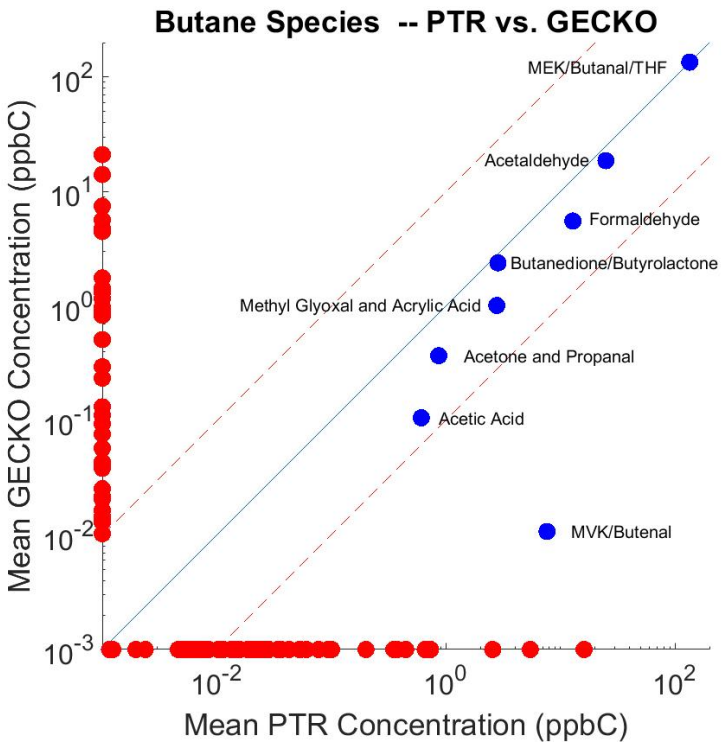

Figure 1: A first-pass comparison of the averages of the concentrations of compositional isomers in the chamber and GECKO-A butane oxidation experiments. Major identifiable species that are found in both datasets are represented by blue dots which fall in the middle of the plot. All species which only appear in the GECKO-A or chamber dataset, but not both, are represented by red markers which fall on the axis belonging to their representative dataset. The blue line represents the 1:1 line, and each of the red dashed lines represent plus/minus one order of magnitude deviation from the 1:1 line.

replicating the chemistry leading to the formation of those species. However, there are several species which only appear in one dataset and not the other, including some species with average concentrations greater than 1 ppbC, which is the heuristic that we are using to define what is considered to be a "major species". Another concerning feature in Figure 1 is how the Methyl Vinyl Ketone (MVK) and butenal compositional isomer group is in very poor agreement between the two datasets.

We begin exploring reasons for the observed discrepancies by examining the largest outlier in the PTR dataset which is represented by the greatest magnitude red point on the PTR axis. This isomer has the chemical formula C_4H_8 which corresponds may correspond to a few different species (e.g. cyclobutene and methyl cyclopropane) but most likely corresponds to butene. However, butene is not expected to be a major product of butane oxidation even though it is identified as one of the species with the highest

concentrations in the chamber experiment. We will now explore the hypothesis that even though butene is the species that is detected by the PTR, it is actually a different species that undergoes a decomposition reaction inside the PTR itself.

One of the major species in the GECKO-A dataset that does not appear in the PTR dataset is butylnitrate ($C_4H_9NO_3$). If butylnitrate were to decompose along the same lines as an alcohol (which ejects H_2O upon protonation) we could expect it to do so according to the reaction scheme shown in Figure 2. If this occurs, we would expect to detect butylnitrate as butene.

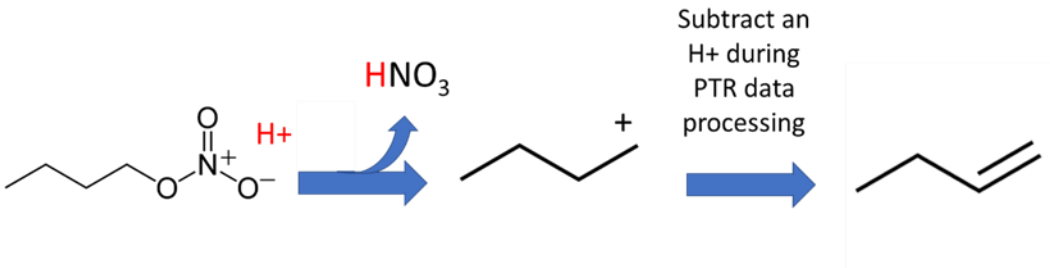

Figure 2: Proposed reaction scheme for the decomposition of butylnitrate inside a PTR. One of the steps in the normal course of processing PTR data is to subtract an H+ from the detected ion to account for the association of an H+ in the PTR's ionization region. In this case, the subtraction of an H+ introduces what appears to be the carbon-carbon double bond in butene.

We must now compare the time series of butylnitrate from the GECKO-A dataset with the time series of butene as detected by the PTR. Figure 3 displays two related ways to compare the time series. The overlaid time series in panel A suggest a strong correlation, and panel B plots the concentrations in each dataset at each measurement time point against each other to determine the correlation coefficient. The r^2 of 0.995 between the GECKO-A and chamber datapoints (compared to an average r^2 of 0.755 for correlating butylnitrate with all other major PTR species) provides strong evidence in support of our hypothesis that butylnitrate undergoes decomposition inside to PTR to end up being detected as butene.

This insight changes the way that we must think about performing comparisons between GECKO-A and chamber data because isomer-to-isomer comparisons could suffer if decomposition reactions occur

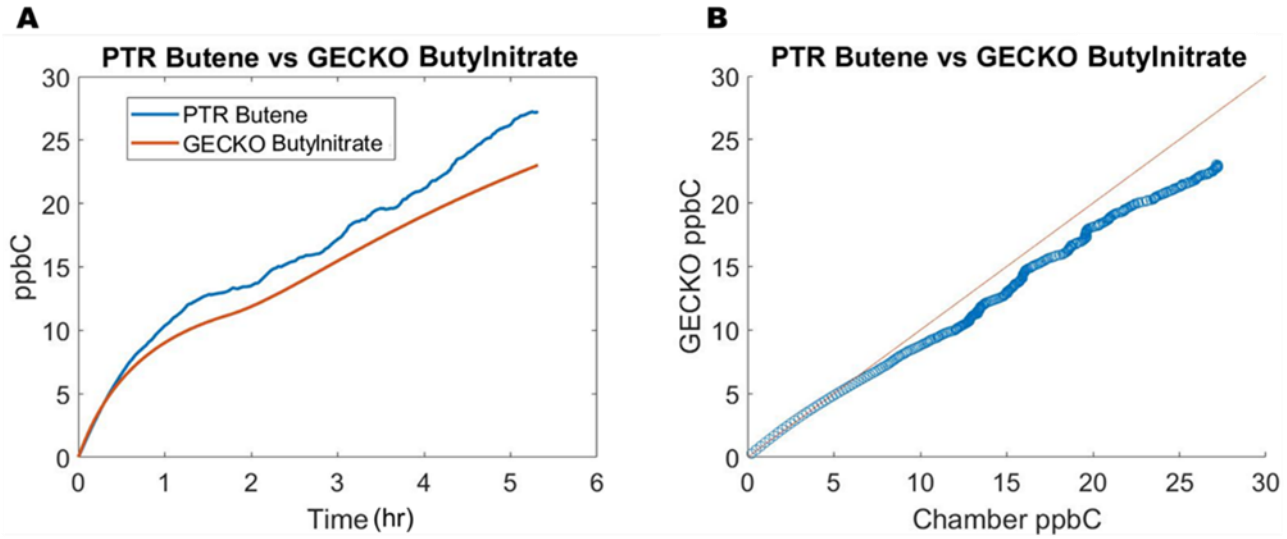

Figure 3: This figure displays the time series (A) and correlation plot (B) for comparing the PTR "butene" and GECKO-A C2PAN species. Panel A displays the time series of the PTR butene signal and GECKO-A butylnitrate. There is an apparent and close correlation between the two. This correlation is further explored in Panel B which plots the concentration of the two species in each dataset at each minute of the experiment. The diagonal orange line represent the 1:1 line. The high r^2 value of 0.995 provides strong evidence that the butene signal in the PTR actually comes from butylnitrate decomposing inside the instrument.

in the PTR (or any other CIMS in other experiments). We must also explore the possibility that other functional groups may decompose including peroxyacyl nitrates (PANs), alcohols, and aldehydes, and we will begin this process by examining the largest GECKO-only species which is peroxyacetyl nitrate, the peroxyacyl nitrate with a total of two carbons (henceforth referred to as C2PAN). The same two correlation plots from Figure 3 are adapted in Figure 4 to compare GECKO-A C2PAN with its posited decomposition product from the PTR, ketene (C_2H_2O). The decomposition results in a loss of the PAN functional group along with one hydrogen atom from PTR data processing for a total loss of HNO_4. Although the absolute concentrations between the species are not as similar as they were in the butylnitrate/butene comparison, the r^2 between the two species is 0.997 (compared to an average r^2 of 0.736 for correlating C2PAN with all other major PTR species) which provides strong evidence that PANs also decompose prior to detection via mass spectrometry.

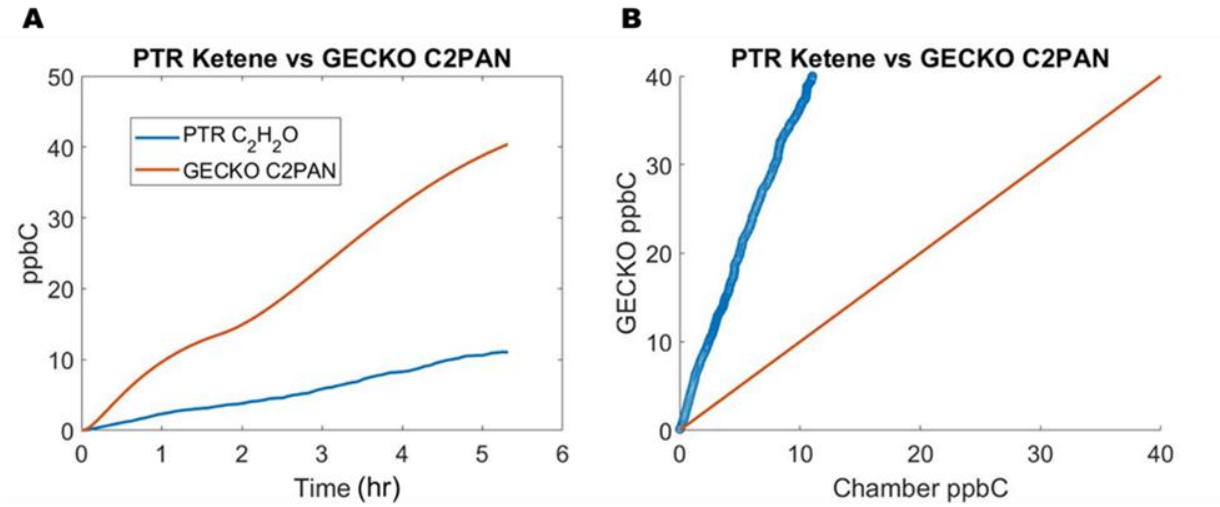

Figure 4: This figure displays the time series (A) and correlation plot (B) for comparing the PTR "ketene" and GECKO-A C2PAN species. Panel A displays the time series of the PTR ketene signal and GECKO-A C2PAN. The correlation between the two is somewhat apparent, but the magnitude of the concentrations for the two species is not the same. This correlation is further explored in Panel B which plots the concentration of the two species in each dataset at each minute of the experiment. The diagonal orange line represent the 1:1 line. The high r^2 value of 0.997 provides strong evidence that the ketene signal in the PTR actually comes from C2PAN decomposing.

The compositional isomer set of MVK and butenal in the PTR dataset does not have one lone species in the GECKO-A dataset against which to compare it but rather multiple potential decomposition precursor species. Multiple GECKO-A species including nitrates, PANs, alcohols, and aldehydes could undergo decomposition reactions to yield either MVK or butenal, and Figure 5 displays the contributions of each set of potential decomposition reactions in the same was as was presented in Figures 3 and 4. Panel A reflects the complexity of performing a decomposition analysis when multiple decomposition reactions may be responsible for the species that is/are detected by the PTR. There is not a sole clear potential decomposition contributor to the detected MVK/butenal, and it is likely that two or more types of decomposition reactions are responsible for the detected MVK/butenal signal. Panel B explore two different possible correlations, one including all three potential decomposition reaction pathways and one which only considers decomposition involving the loss of a PAN group or a dehydration which involves

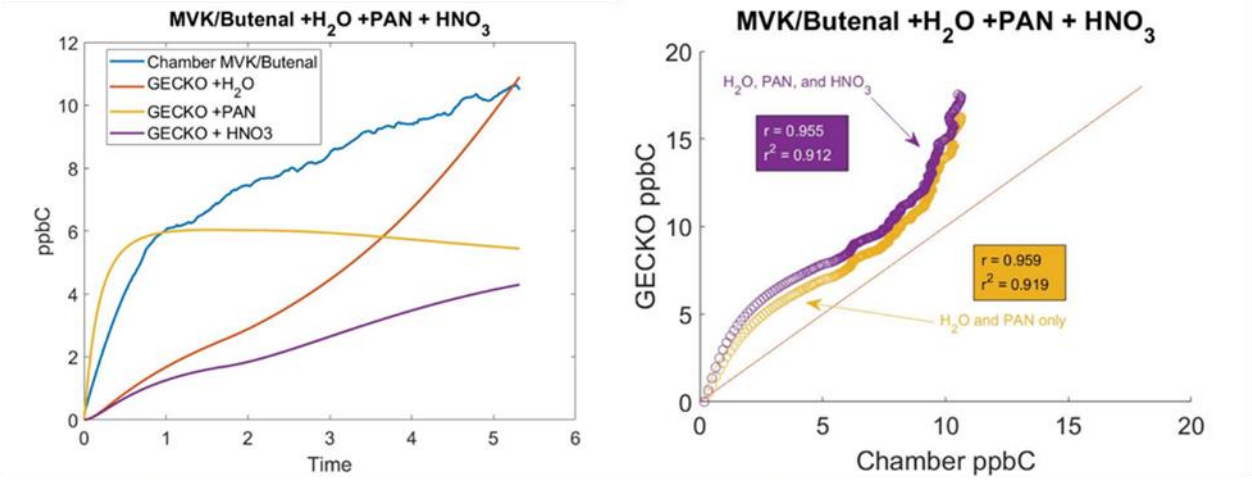

Figure 5: MVK/Butenal correlation diagrams. Panel A shows the measured MVK/butenal compositional isomer set compared to three different precursor traces from GECKO assuming either a dehydration reaction for alcohols and/or aldehydes, a loss of HNO_4 for PANs, and a loss of HNO_3 for organonitrates. No single set of decomposition precursors from GECKO match the chamber trace. Panel B plots the concentration of chamber MVK/butenal at each minute of the experiment against the sum of the concentrations of all three potential decomposition precursors as well as the sum of just the "+H_2O" and "+PAN" decomposition precursors. Both have r^2 values greater than 0.9 which indicates both strongly correlate with the chamber trace.

the loss of either an alcohol or aldehyde group. The correlation coefficients for both correlations are greater than 0.9 which still suggests evidence that decomposition reactions are responsible for the high detected concentrations of MVK/butenal.

We have now explored three different instances in which decomposition reactions have plausibly transformed organic species between the time they were sampled from the chamber and the time they were detected by the TOF-MS back end of the PTR. We can now say with some confidence that we are observing decomposition in the PTR, and we can apply the same decomposition correction method to every compositional isomer group. The results of these corrections are presented in Figure 6 which shows a marked improvement in the agreement between the GECKO-A and chamber datasets. No more species with average concentration greater than 1 ppbC remain on the chamber axis, and the two largest species on the GECKO axis in Figure 1 (C2PAN and butylnitrate) now have a good match in the chamber dataset.

The process of checking every set of compositional isomers against decomposition reactions involving a dehydration, loss of HNO_3, and/or loss of HNO_4 is necessary yet time consuming. It is useful to remember that we are using the butane oxidation system as the basis on which to construct our

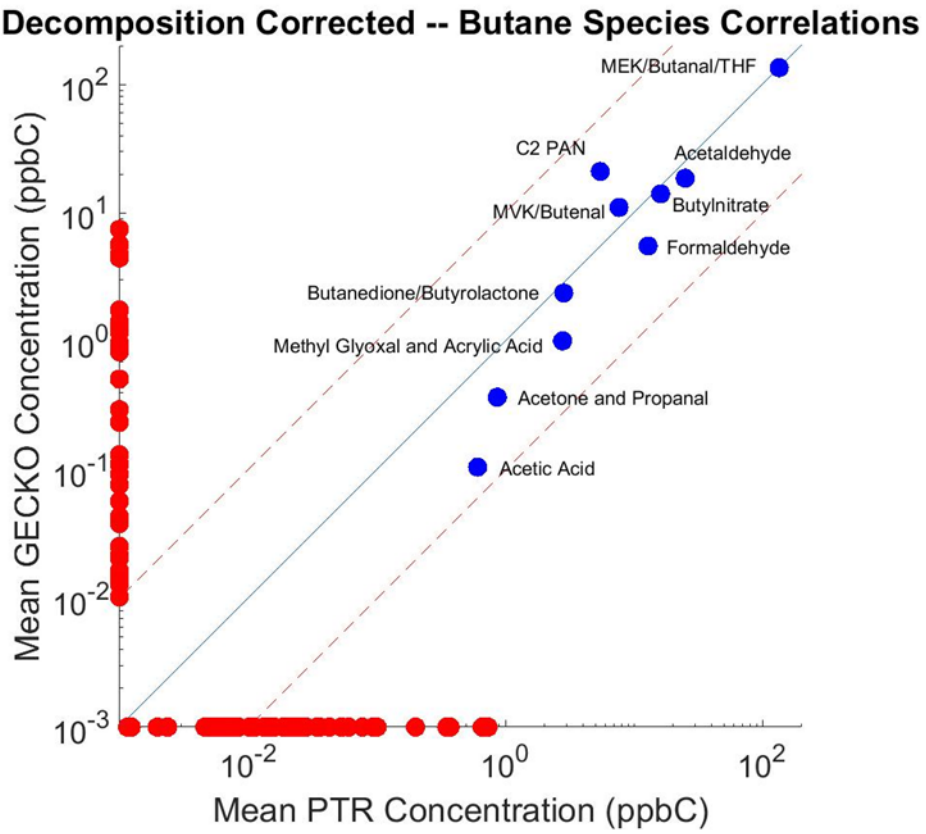

Figure 6: Each set of compositional isomers has been matched to each of their potential decomposition precursors and then replotted in the same way as presented in Figure 1. There is a marked improvement in the agreement between the chamber and GECKO-A data once decomposition is considered. Special note should be taken of the improvement and/or appearance of the C2PAN, butylnitrate, and MVK/butenal points close to the 1:1 line.

comparison methodology because it is the simplest of all of the oxidation systems that we will consider. The α-pinene, 1,2,4-TMB, and isoprene systems each contain significantly more products with more functional groups than are found in the butane system, so the time it takes to manually perform decomposition corrections will quickly become untenable as we scale up in complexity. More complex oxidation systems derived from precursors with more than four carbons (like butane) are more likely to contain multifunctional species whose susceptibilities to one or more decomposition reactions may not be easily determinable as was the case for the butane system species. Instead of performing manual corrections however, we can perform bulk corrections on all species in the GECKO-A datasets by assuming 100% decomposition of species that contain nitrate, alcohol, aldehyde, and PAN functional groups. This is a fairly bold assumption to make, especially since we are not certain if and/or how functional groups may

decompose in other CIMS instruments. Instead of spending considerable time and effort determining or estimating the extent to which different functional group and multifunctional species may decompose, we can instead group the species in each dataset in a way that will not be as susceptible to these considerations.

Grouping the species by carbon number (Cnum) and average carbon oxidation state (OSc) provides an avenue that allows us to avoid performing manual decomposition corrections on each set of compositional isomers. Cnum and OSc are also useful proxies for understanding the dichotomy of backbone fragmentation and functionalization which is critical for understanding the evolution of a VOC oxidation system (e.g. Gabriel Isaacman-VanWertz et al. 2018). Species with the same Cnum and similar OSc fall along similar lines in the fragmentation and functionalization continuum which supports our decision to group species in this manner. It is important to note that the only way we can reliably use Cnum and OSc instead of doing direct isomer-to-isomer comparisons is if our chamber measurements capture all of the organic gas-phase carbon in the system. If not, these comparisons will be incomplete and could yield misleading data.

CIMS instruments are soft ionization techniques which tend to leave the carbon backbone of each species intact (except for large molecules like sesquiterpenes), so Cnum is unlikely to change upon detection with an instrument. OSc is calculated using Equation 1:

$$\overline{OSc} = 2\frac{O}{C} - \frac{H}{C} - 5\frac{N}{C} \quad (1)$$

The OSc calculation uses elemental ratios and assumes an oxidation state of -2 for each oxygen atom, +1 for reach hydrogen atom, and +5 for each nitrogen atom. These assumptions hold true for almost every functional group except for ones in which there is a peroxide bond in which each oxygen has an oxidation state of -1. Most importantly, when species undergo a decomposition reaction their average OSc will remain the same with the exception of PAN decomposition products because of the aforementioned peroxide linkage which is found in a PAN. This means that we only need to correct PAN species for

decomposition, and since PANs known to be highly prone to thermal and other modes of decomposition, we feel comfortable performing bulk corrections for PAN decomposition without having to worry about the degree to which these species may decompose.

Grouping the species in the chamber and GECKO-A datasets for the butane oxidation systems by Cnum and OSc yields Figure 7. Each species' OSc is rounded to the nearest 0.5 before being added to their respective Cnum and OSc bin. In comparison to Figure 6, Figure 7 shows similar qualitative agreement with less complexity. More major species and compositional isomer groups have left the axes and into the center of the plot which means that more of the carbon in each dataset is being used in the overall comparison. Only 1.8% of chamber carbon and 21.7% of GECKO-A carbon remain on the axes.

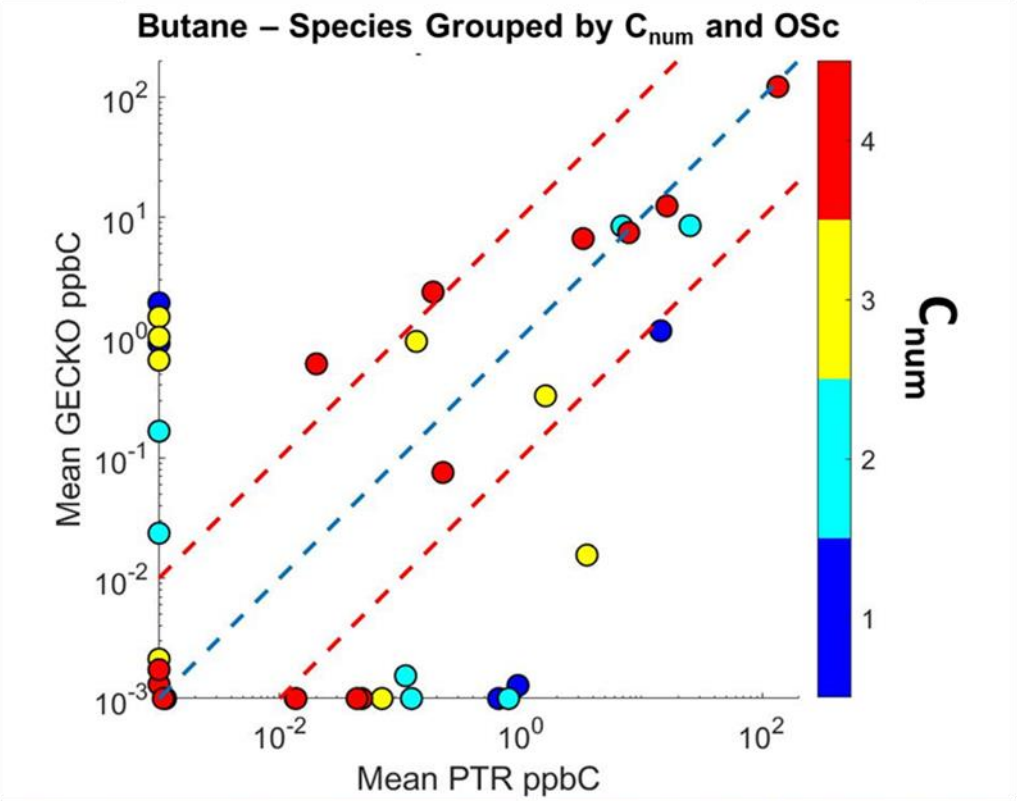

Figure 7: Grouping butane oxidation system species by Cnum and OSc in which each group is colored by Cnum. Grouping in this manner does not qualitatively alter the agreement presented in Figure 6. More major species are pulled off the GECKO axis to the center of the plot compared to Figure 6.

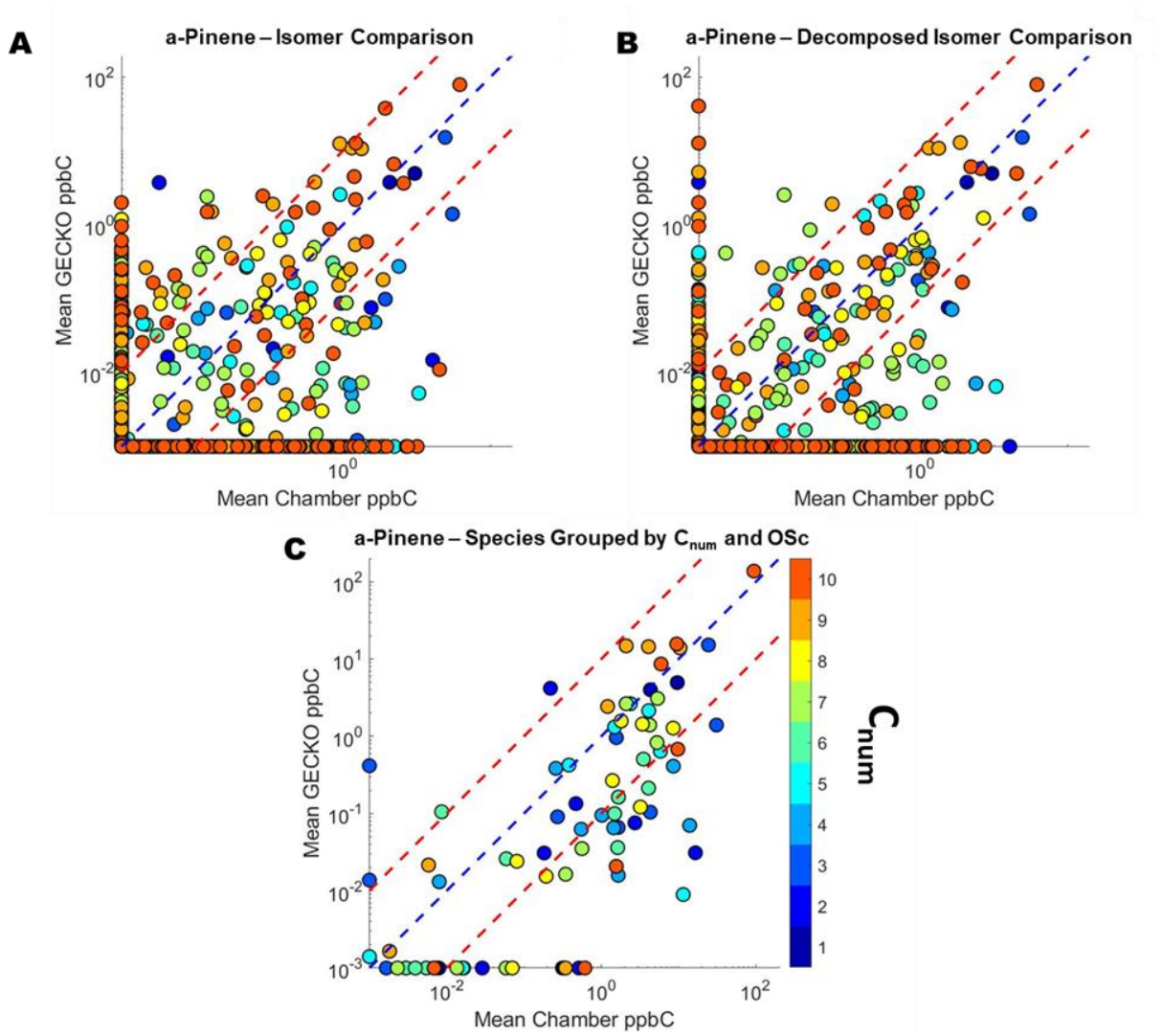

Figure 8: The evolution of chamber and GECKO-A α-pinene dataset comparisons. The prima facie comparison of compositional isomer sets in each dataset is in Panel A, the decomposition corrected compositional isomer set comparison is in Panel B, and the grouped Cnum and OSc comparison is in Panel C. Each point is colored by Cnum. There is a clear reduction in scatter going from Panel A to B which is even more apparent upon binning in Panel C. Panel C allows for a comparison of all major species in both datasets since no points fall on the axes with average concentrations greater than 1 ppbC.

We may now apply this novel comparison method to a more complex oxidation system, α-pinene. The three stages of the evolution of the comparison methodology are shown in Figure 8. There is an obvious decrease in the degree of scatter moving from Panel A to B, but the clearest reduction in complexity comes once species are binned by OSc and Cnum in Panel C. In Panel A, 5.9% of GECKO-A carbon is on the axis, and 25.5% or chamber carbon is on the axis. In Panel C all major species are off the axes with only 1.3% of GECKO-A carbon and 1.4% of chamber carbon remaining on the axes. This means that this binned comparison involves all major species and the vast majority of carbon in both datasets.

Another benefit we reap by progressing from a prima facie isomer-to-isomer comparison to the binned-by-OSc-and-Cnum comparison is that we no longer have to be concerned about any decomposition reactions that may take place in any of the CIMS instruments except for PAN decomposition reactions. Even so, the presence of a PAN may not change the OSc bin into which a compound is sorted. Equation 1 tells us that a PAN decomposition will correct a species' OSc identification by -2/Cnum, so only PAN compounds which are within 2/C of the lower bound of the OSc bin in which they were sorted will change OSc bin upon decomposition correction implementation.

Although Figure 8 represents a significant improvement in the way we are able to compare large chamber and mechanistic datasets, some information is obfuscated in the process. The data are averaged over the course of the experiment, and the binned plots do not contain information related to the behavior of the species within each bin at each time. It is also unclear whether uncertainties in CIMS calibrations could be responsible the differences and similarities between chamber and GECKO-A data. In order to assess these points of concern we can examine the Cnum and OSc distributions separately at every point in time. The distributions are examined separately so the visualizations can be shown in two dimensions as opposed to a single three-dimensional plot where species are grouped jointly by Cnum and OSc. Uncertainties in the calibration of each species as detected by each CIMS were estimated as outlined in Section 2.2.

Figures 9 and 10 display the differences between the chamber and GECKO-A datasets in each Cnum and OSc bin respectively at each time point in the experiment. GECKO-A concentrations in each bin were subtracted from chamber concentrations in each bin. If that subtraction results in a positive value it means that the concentration of secondary carbon in that bin is higher in the chamber dataset than the concentration of secondary carbon in the same bin in the GECKO-A dataset. Conversely, if the subtraction results in a negative number, the concentration in that bin is higher in the GECKO-A dataset than it is in the chamber dataset.

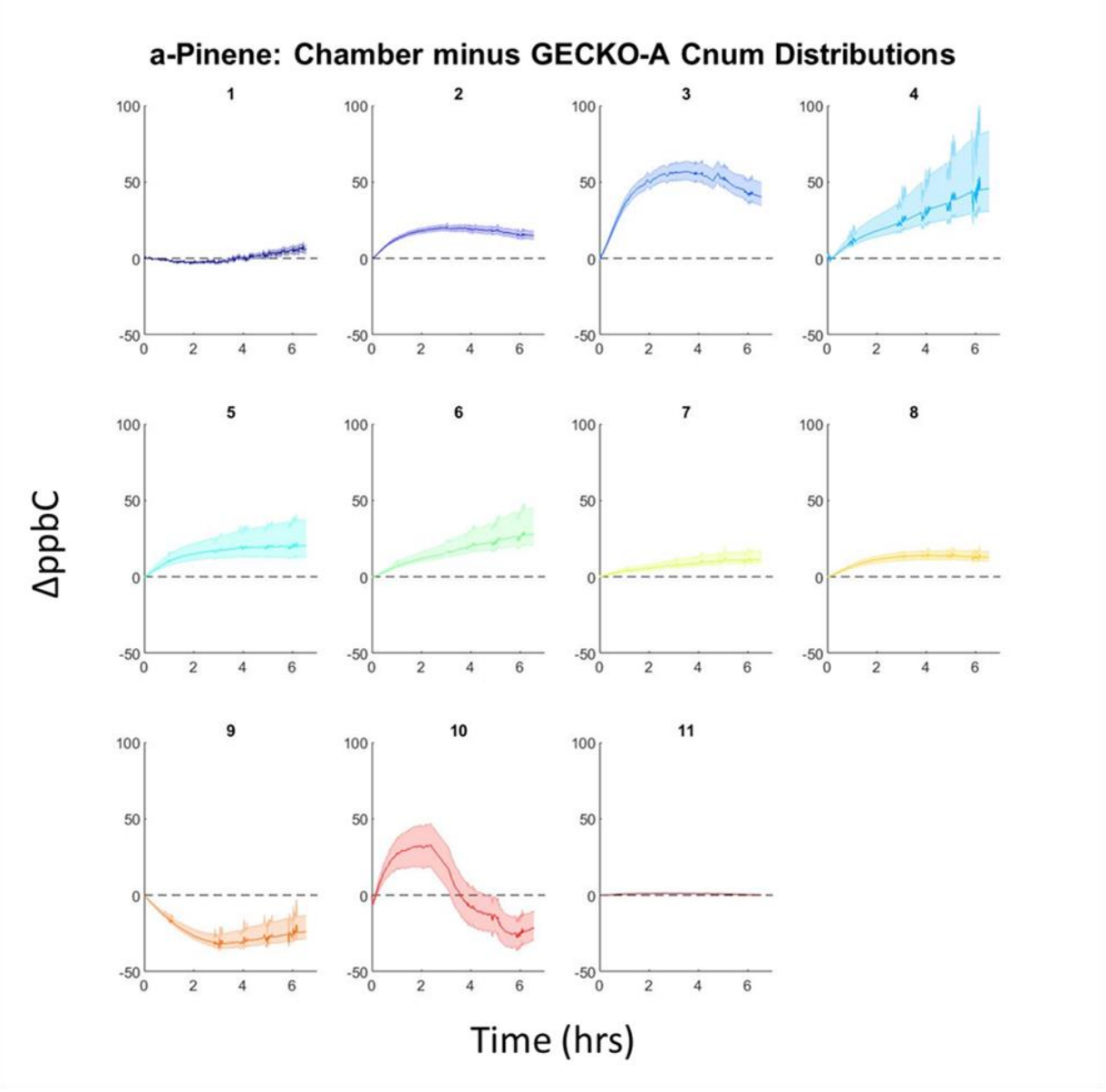

Figure 9: Absolute differences in the concentrations of secondary gas-phase carbon in each Cnum bin between the chamber and GECKO-A datasets. Positive values indicated greater concentrations in the chamber dataset, and negative values indicate greater concentrations in the GECKO-A dataset. Shaded regions represent one standard deviation uncertainty. Uncertainties for each bin are derived from the CIMS calibration uncertainties of the species in each bin. Bin "11" represents all species with 11 or more carbons; these species are not found in the GECKO dataset but are found in minor concentrations in the chamber dataset.

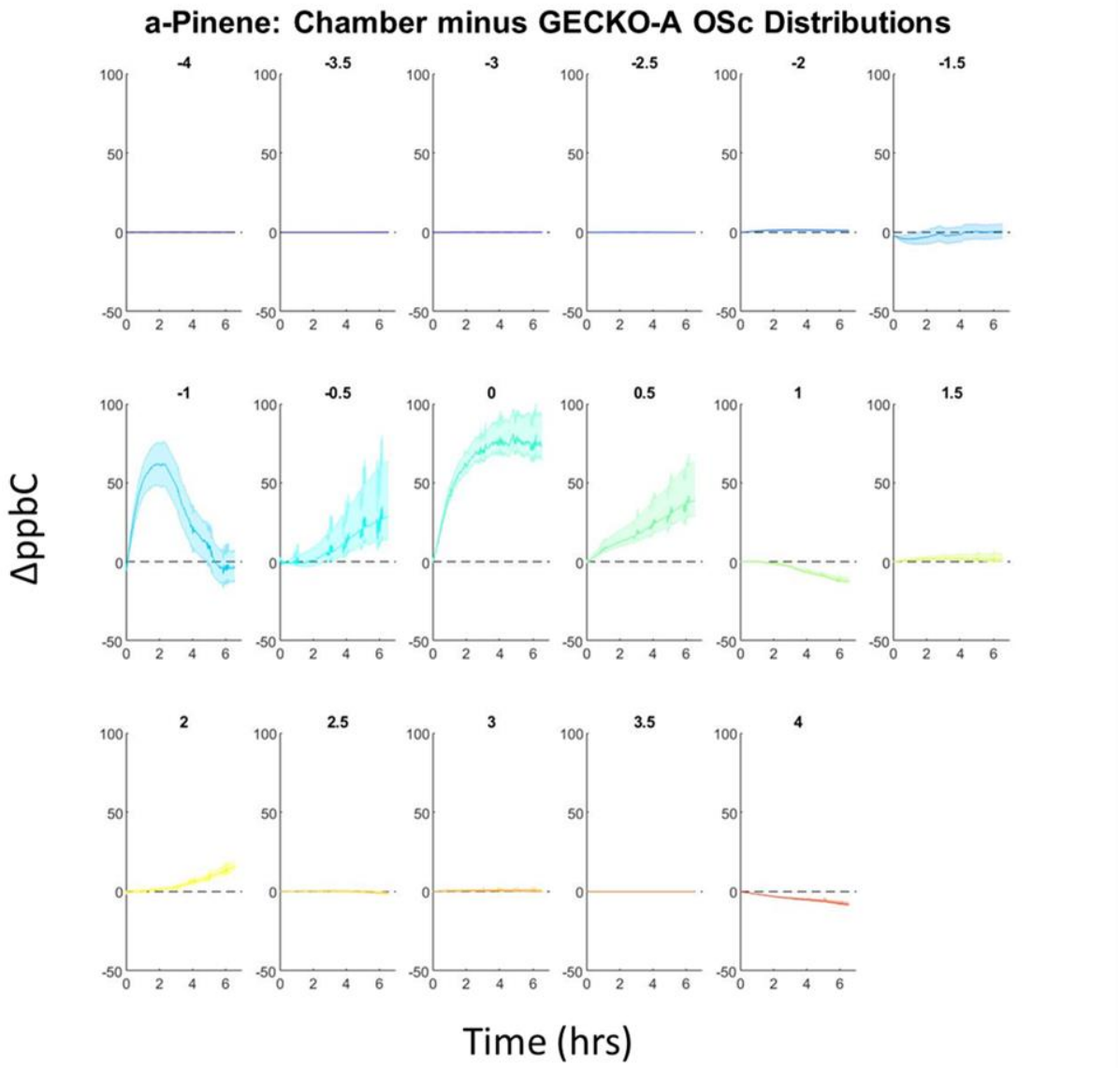

Figure 10: Absolute differences in the concentrations of secondary gas-phase carbon in each OSc bin between the chamber and GECKO-A datasets. Positive values indicated greater concentrations in the chamber dataset, and negative values indicate greater concentrations in the GECKO-A dataset. Shaded regions represent one standard deviation uncertainty. Uncertainties for each bin are derived from the CIMS calibration uncertainties of the species in each bin.

Both Figures 9 and 10 suggest that the uncertainties in the calibrations of the species detected by CIMS instruments can not be the main source of discrepancy observed between the chamber and GECKO-A. Most of the shaded regions for each bin do not overlap with the zero line which means that, within one standard deviation uncertainty, it is not expected for the concentrations in each bin to be the same. It is also important to address the issue that there appears to be much more secondary gas-phase carbon in the chamber dataset than there is in the GECKO-A dataset. Although many parameters were used to tune the GECKO-A model to match the chamber experiment as best as possible, total secondary gas-phase carbon was not a parameter that was utilized. As discussed in Section 1, GECKO-A incorporates wall losses of gaseous species, and since we did not have the Oxy-Cat (Chapter 2) on hand to measure TSC in the chamber, we were unable to tune GECKO-A to TSC. Since GECKO-A was tuned to match the chamber's SOA time series, GECKO-A's apparent underestimate of TSC is likely caused by an overestimate of vapor wall losses. This potential source of error must be accounted for when we discuss the overall agreement between the two datasets.

Finally, we wish to develop a way to quantifiably express the degree to which the GECKO-A and chamber datasets disagree. In other words, we want to create an error metric that can be used to understand how any changes in GECKO-A's mechanism generator quantitatively affect the overall agreement between GECKO-A and chamber measurements. This will be particularly useful for the work described in the next chapter. Another motivation for creating this error metric is so we can begin to quantitatively compare agreement between the two datasets across different VOC precursor oxidation systems. This will help determine which oxidation systems are well captured by GECKO-A and which systems GECKO-A struggles to model.

The method of binning species by Cnum and OSc is used to calculate the error metric. The error metric is calculated at every time point in the experiment, so concentrations in each bin will not be averaged over the entire timespan of the experiment like in Figure 8. We also normalized each dataset to

the amount of secondary carbon at each time point in each respective dataset; this is important because the amount of TSC in each dataset in each precursor VOC oxidation system is different, so normalization is required in order to compare error metrics across systems. The final decision we must make is whether to calculate the error metric using a partial distribution function or a cumulative distribution function. The partial distribution function method involves taking the sum of the absolute value of the difference between the values in each normalized Cnum-OSc bin in each dataset, and then taking that value and dividing it by the maximum possible error which is 2. We have selected to use the partial distribution (as opposed to the cumulative distribution) method because it will not be sensitive to the maximum Cnum in each precursor system and will therefore allow for a more even comparison across precursor systems. The final equation for the error metric is shown below in Equation 2:

$$Error = \sum_{1}^{Cnum\ max} \sum_{OSc\ bin\ -4}^{OSc=4} \left| [Chamber]_{Cnum,OSc\ bin} - [GECKO]_{Cnum,OSc\ bin} \right| /2 \qquad (2)$$

Applying Equation 2 to the α-pinene system results in Figure 11. The error metric is bound between 0 and 1, so the maximum and minimum values of approximately 0.25 and 0.5 are reasonable. The error grows over time which is expected because as time advances, GECKO-A is less likely to accurately capture later-generation chemistry due to gaps in specific knowledge of later-generation chemical reactions and their corresponding rates.

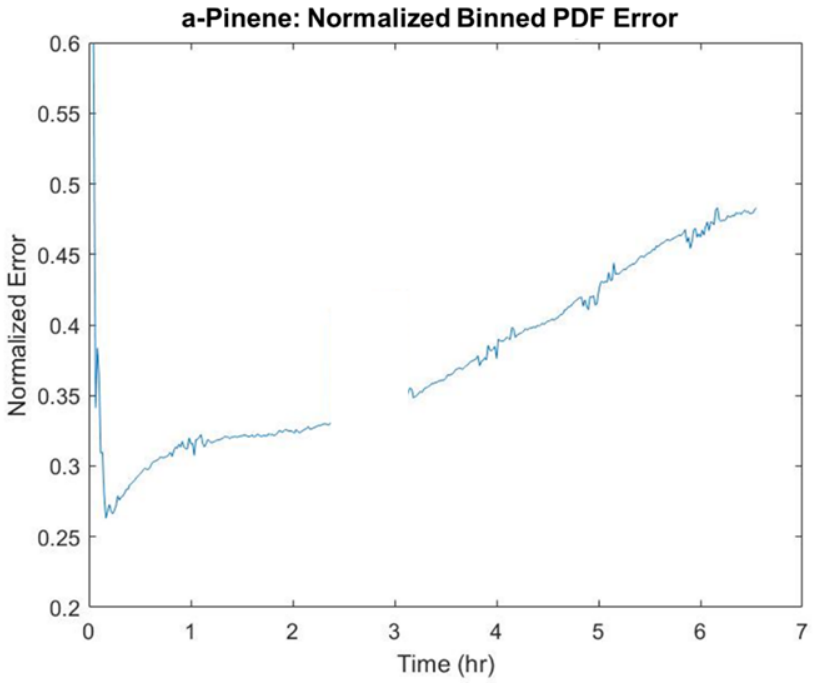

Figure 11: The error metric at each time point is plotted for the a-pinene oxidation system. Initial error values start high and quickly fall within the first few minutes of the comparison because initial errors are prone to small differences in the small concentrations of secondary carbon in each bin in the two datasets. The gap in the data from approximately 2.5-3 hrs exists because there is no CIMS data for pinonaldehyde between those times, and it is a major product which significantly influences the value of the error.

3. Discussion and Further Work

We began by examining the relatively simple butane oxidation system in order to better understand how GECKO-A (and more broadly, mechanisms in general) can be used to disambiguate chamber data. We explored multiple different potential decomposition reactions, and we found evidence to suggest that organic compounds with nitrate, PAN, alcohol, and aldehyde functional groups may all undergo decomposition reactions via detection with the PTR-MS. It is unclear exactly where the decompositions occur, but we hypothesize that they may occur in the ionization region of the PTR. It is also unclear whether these reactions may occur in other CIMS instruments, and the extent to which these decompositions may occur is also unknown. However, this work has provided useful evidence showing that species may transform upon detection with a CIMS instrument and also that comparing chamber

datasets to GECKO-A results can help elucidate the correct structures and identities of a variety of different compounds.

The uncertainty surrounding potential decompositions complicate efforts to compare chamber and GECKO-A datasets, so we began grouping species by Cnum and OSc. It is important to highlight that this grouping was only reasonable because we believe that we have the instrumentation to measure all major organic gas-phase species formed over the course of a chamber experiment. The only functional group that required decomposition correction was the PAN group because the peroxide oxygens in PAN have an oxidation state of -1 instead of -2. This binning simplified the comparison methodology while maintaining important information; Cnum and OSc may be used as proxies for understanding the tradeoff between fragmentation and functionalization. This binning is thus a suitable and utile basis for our comparisons.

Once the species in each dataset were binned, we ensured that the differences we observed between the chamber and GECKO-A data in Figure 8 could not be explained by uncertainties in calibrations for CIMS measurements. While the one standard deviation uncertainty for some bins was rather large (i.e. the uncertainty in the Cnum = 4 bin in Figure 9 was ±26 ppbC at the end of the experiment), even those uncertainties were not large enough to account for the discrepancies in the distributions between the chamber and GECKO-A. We can therefore conclude that the observed discrepancies are not arising from uncertainties in chamber measurements and more likely arise from differences between observed and modeled chemistry and/or partitioning.

Lastly, we developed an error metric to quantify the degree to which the chamber and GECKO-A datasets disagrees with each other. The true utility of this work lies ahead in Chapter 4 in which we will discuss how changes to the chemistry in a GECKO-A might affect overall agreement with the chamber experiment. Data from figures like Figure 8 highlights areas of large measurement-mechanism disagreement which can in turn suggest that certain chemical reactions are missing from the mechanism

or that the mechanism does not accurate predict the rates of those reactions. GECKO-A can then be accordingly edited to attempt to better match empirical observations.

This work has broad implications across our field. CIMS instrument users now have a generalized, straightforward, and efficient way to compare empirically derived results to mechanisms. GECKO-A and mechanism users in general also benefit from this work because it describes for the first time a way to holistically compare chamber and mechanism datasets on all levels of granularity, ranging from species-to-species comparisons, distribution comparisons, and ensemble property comparisons. Mechanisms must be continuously validated and improved based on empirical data, and this work specifically devises a method to quantify the degree to which mechanisms are improved following alterations. This work also provides a way to target those edits based on discrepancies in Cnum and OSc distributions which may arise from missing chemistry in mechanisms and/or inaccurate SARs parametrization. Improvements in mechanisms are ultimately beneficial for improving the accuracy of chemical transport and global climate models.

4. References

Aiken, Allison C., Peter F. Decarlo, Jesse H. Kroll, Douglas R. Worsnop, J. Alex Huffman, Kenneth S. Docherty, Ingrid M. Ulbrich, et al. 2008. "O/C and OM/OC Ratios of Primary, Secondary, and Ambient Organic Aerosols with High-Resolution Time-of-Flight Aerosol Mass Spectrometry." *Environmental Science and Technology* 42 (12): 4478–85. https://doi.org/10.1021/ES703009Q.

Aumont, Bernard, Marie Camredon, Camille Mouchel-Vallon, Stéphanie La, Farida Ouzebidour, Richard Valorso, Julia Lee-Taylor, and Sasha Madronich. 2013. "Modeling the Influence of Alkane Molecular Structure on Secondary Organic Aerosol Formation." *Faraday Discussions* 165: 105. https://doi.org/10.1039/c3fd00029j.

Aumont, Bernard, S. Szopa, and Sasha Madronich. 2005. "Modelling the Evolution of Organic Carbon during Its Gas-Phase Tropospheric Oxidation: Development of an Explicit Model Based on a Self Generating Approach." *Atmospheric Chemistry and Physics Discussions* 5 (1): 703–54. https://doi.org/10.5194/acpd-5-703-2005.

Aumont, B., R. Valorso, C. Mouchel-Vallon, M. Camredon, J. Lee-Taylor, and S. Madronich. 2012. "Modeling SOA Formation from the Oxidation of Intermediate Volatility N-Alkanes." *Atmospheric Chemistry and Physics* 12 (16): 7577–89. https://doi.org/10.5194/acp-12-7577-2012.

Brown, P., P. Watts, T. D. Märk, and C. A. Mayhew. 2010. "Proton Transfer Reaction Mass Spectrometry Investigations on the Effects of Reduced Electric Field and Reagent Ion Internal Energy on Product Ion Branching Ratios for a Series of Saturated Alcohols." *International Journal of Mass Spectrometry* 294 (2–3): 103–11. https://doi.org/10.1016/J.IJMS.2010.05.028.

Calvert, Jack G. (Jack George). 2008. *Mechanisms of Atmospheric Oxidation of the Alkanes*. Oxford University Press. https://global.oup.com/academic/product/mechanisms-of-atmospheric-oxidation-of-the-alkanes-9780195365818?cc=us&lang=en&.

Camredon, M., B. Aumont, J. Lee-Taylor, and S. Madronich. 2007. "The SOA/VOC/NOx System: An Explicit Model of Secondary Organic Aerosol Formation." *Atmos. Chem. Phys.* 7 (21): 5599–5610. https://doi.org/10.5194/acp-7-5599-2007.

Docherty, Kenneth S., Robert Yaga, William T. Preston, Mohammed Jaoui, Theran P. Reidel, John H. Offenberg, Tadeusz E. Kleindienst, and Michael Lewandowski. 2021. "Relative Contributions of Selected Multigeneration Products to Chamber SOA Formed from Photooxidation of a Range (C10–C17) of n-Alkanes under High NOx Conditions." *Atmospheric Environment* 244 (January): 117976. https://doi.org/10.1016/J.ATMOSENV.2020.117976.

Faxon, Cameron, Julia Hammes, Michael le Breton, Ravi Kant Pathak, and Mattias Hallquist. 2018. "Characterization of Organic Nitrate Constituents of Secondary Organic Aerosol (SOA) from Nitrate-Radical-Initiated Oxidation of Limonene Using High-Resolution Chemical Ionization Mass Spectrometry." *Atmospheric Chemistry and Physics* 18 (8): 5467–81. https://doi.org/10.5194/ACP-18-5467-2018.

Gkatzelis, Georgios I., Ralf Tillmann, Thorsten Hohaus, Markus Müller, Philipp Eichler, Kang Ming Xu, Patrick Schlag, et al. 2018. “Comparison of Three Aerosol Chemical Characterization Techniques Utilizing PTR-ToF-MS: A Study on Freshly Formed and Aged Biogenic SOA.” *Atmospheric Measurement Techniques* 11 (3): 1481–1500. https://doi.org/10.5194/AMT-11-1481-2018.

Hunter, James F., Anthony J. Carrasquillo, Kelly E. Daumit, and Jesse H. Kroll. 2014. “Secondary Organic Aerosol Formation from Acyclic, Monocyclic, and Polycyclic Alkanes.” *Environmental Science and Technology* 48 (17): 10227–34. https://doi.org/10.1021/ES502674S.

Isaacman-VanWertz, Gabriel, Paola Massoli, Rachel O’Brien, Christopher Lim, Jonathan P. Franklin, Joshua A. Moss, James F. Hunter, et al. 2018. “Chemical Evolution of Atmospheric Organic Carbon over Multiple Generations of Oxidation.” *Nature Chemistry* 10 (4): 462–68. https://doi.org/10.1038/s41557-018-0002-2.

Isaacman-VanWertz, G., P. Massoli, R. E. O’Brien, J. B. Nowak, M. R. Canagaratna, J. T. Jayne, D. R. Worsnop, et al. 2017. “Using Advanced Mass Spectrometry Techniques to Fully Characterize Atmospheric Organic Carbon: Current Capabilities and Remaining Gaps.” *Faraday Discussions* 200 (0): 579–98. https://doi.org/10.1039/C7FD00021A.

Jenkin, Michael E., Sandra M. Saunders, and Michael J. Pilling. 1997. “The Tropospheric Degradation of Volatile Organic Compounds: A Protocol for Mechanism Development.” *Atmospheric Environment* 31 (1): 81–104. https://doi.org/10.1016/S1352-2310(96)00105-7.

Kroll, Jesse H., and John H. Seinfeld. 2008. “Chemistry of Secondary Organic Aerosol: Formation and Evolution of Low-Volatility Organics in the Atmosphere.” *Atmospheric Environment* 42 (16): 3593–3624. https://doi.org/10.1016/j.atmosenv.2008.01.003.

Lee-Taylor, J., S. Madronich, B. Aumont, A. Baker, M. Camredon, A. Hodzic, G. S. Tyndall, E. Apel, and R. A. Zaveri. 2011. “Explicit Modeling of Organic Chemistry and Secondary Organic Aerosol Partitioning for Mexico City and Its Outflow Plume.” *Atmospheric Chemistry and Physics* 11 (24): 13219–41. https://doi.org/10.5194/acp-11-13219-2011.

Leglise, Joris, Markus Mu, Felix Piel, Tobias Otto, and Armin Wisthaler. 2019. “Bulk Organic Aerosol Analysis by Proton-Transfer-Reaction Mass Spectrometry: An Improved Methodology for the Determination of Total Organic Mass, O:C and H:C Elemental Ratios, and the Average Molecular Formula.” https://doi.org/10.1021/acs.analchem.9b02949.

Li, Jingyi, Meredith Cleveland, Luke D. Ziemba, Robert J. Griffin, Kelley C. Barsanti, James F. Pankow, and Qi Ying. 2015. “Modeling Regional Secondary Organic Aerosol Using the Master Chemical Mechanism.” *Atmospheric Environment* 102 (February): 52–61. https://doi.org/10.1016/J.ATMOSENV.2014.11.054.

Ma, Yan, Timothy R. Willcox, Andrew T. Russell, and George Marston. 2007. “Pinic and Pinonic Acid Formation in the Reaction of Ozone with α-Pinene.” *Chemical Communications*, no. 13 (March): 1328–30. https://doi.org/10.1039/B617130C.

Mouchel-Vallon, C., P. Br??uer, M. Camredon, R. Valorso, S. Madronich, H. Herrmann, and B. Aumont. 2013. “Explicit Modeling of Volatile Organic Compounds Partitioning in the Atmospheric

Aqueous Phase." *Atmospheric Chemistry and Physics* 13 (2): 1023–37. https://doi.org/10.5194/acp-13-1023-2013.

Peeters, Jozef, Gaia Fantechi, and Luc Vereecken. 2004. "A Generalized Structure-Activity Relationship for the Decomposition of (Substituted) Alkoxy Radicals." *Journal of Atmospheric Chemistry 2004 48:1* 48 (1): 59–80. https://doi.org/10.1023/B:JOCH.0000034510.07694.CE.

Rivera-Rios, J. C., T. B. Nguyen, J. D. Crounse, W. Jud, J. M. st. Clair, T. Mikoviny, J. B. Gilman, et al. 2014. "Conversion of Hydroperoxides to Carbonyls in Field and Laboratory Instrumentation: Observational Bias in Diagnosing Pristine versus Anthropogenically Controlled Atmospheric Chemistry." *Geophysical Research Letters* 41 (23): 8645–51. https://doi.org/10.1002/2014GL061919.

Saunders, S. M., M. E. Jenkin, R. G. Derwent, and M. J. Pilling. 2003. "Protocol for the Development of the Master Chemical Mechanism, MCM v3 (Part A): Tropospheric Degradation of Non-Aromatic Volatile Organic Compounds." *Atmospheric Chemistry and Physics* 3 (1): 161–80. https://doi.org/10.5194/ACP-3-161-2003.

Seinfeld, JH., and SN. Pandis. 2006. *Atmospheric Chemistry and Physics: From Air Pollution to Climate Change*. Edited by Inc. John Wiley and Sons. *John Wiley & Sons.* 3rd ed. John Wiley and Sons, Inc. https://doi.org/10.1080/00139157.1999.10544295.

Vereecken, L., and J. Peeters. 2009. "Decomposition of Substituted Alkoxy Radicals—Part I: A Generalized Structure–Activity Relationship for Reaction Barrier Heights." *Physical Chemistry Chemical Physics* 11 (40): 9062–74. https://doi.org/10.1039/B909712K.

———. 2010. "A Structure–Activity Relationship for the Rate Coefficient of H-Migration in Substituted Alkoxy Radicals." *Physical Chemistry Chemical Physics* 12 (39): 12608–20. https://doi.org/10.1039/C0CP00387E.

Zhang, Xuan, Christopher D. Cappa, Shantanu H Jathar, Renee C. McVay, Joseph J. Ensberg, Michael J. Kleeman, John H. Seinfeld, and Christopher D. Cappa. 2014. "Influence of Vapor Wall Loss in Laboratory Chambers on Yields of Secondary Organic Aerosol." *Proceedings of the National Academy of Sciences of the United States of America* 111 (16): 1–6. https://doi.org/10.1073/pnas.1404727111.

IV. Comparing Chamber Data to Chemical Mechanistic Simulations Suggests Targeting Pathways for Mechanism Improvements

1. Introduction

Chapters 2 and 3 tackled questions regarding chamber experiments, mechanisms, and how to effectively and efficiently compare the two, but lacking from those chapters was an in-depth discussion of the actual chemistry underpinning SOA formation and evolution. This chapter focuses primarily on investigations of alterations to GECKO-A's mechanism generator in order to provide a better match to chamber observations. We begin with a more thorough explanation of the inner workings of GECKO-A. A simplified diagram of GECKO-A's mechanism generation procedure is shown in Figure 1 (Bernard Aumont, Szopa, and Madronich 2005):

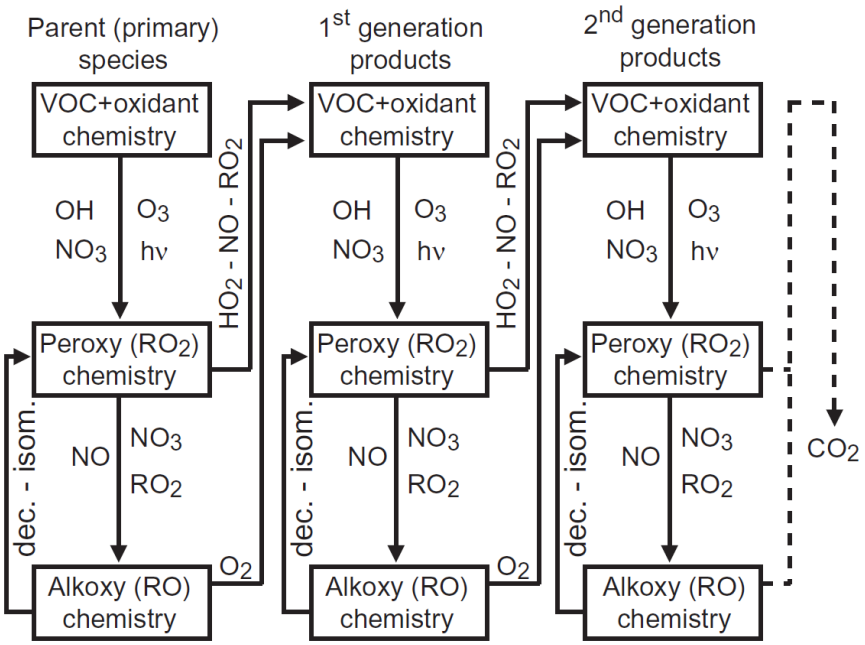

Figure 1: A simplified scheme of the GECKO-A mechanism generator taken from (Bernard Aumont, Szopa, and Madronich 2005). VOC+oxidant reactions leading to the formation of peroxy and alkoxy radicals are performed until stable species is produced. These stable species compose the 1st generation of products. GECKO-A's mechanism generator is run either until all species are converted to CO_2 or the GECKO-A user specifies a terminating generation.

GECKO-A begins generating explicit mechanisms by examining every bond in the precursor VOC (Camredon et al. 2007; Bernard Aumont, Szopa, and Madronich 2005). Each bond may be susceptible to one or more types of reaction including, but not limited to, hydrogen abstraction by an OH radical, ozonolysis, and addition of an OH radical across a double bond. If one or more individual reactions in each class of reactions can be found in MCM (discussed in Chapter 3) or another mechanism like SAPRC, GECKO-A will use the rate constants contained therein (Bernard Aumont, Szopa, and Madronich 2005). If these reactions can not be found in an existing mechanism, GECKO-A will predict the reaction rate using Structure Activity Relationships (SARs) which will be discussed in more depth below. The precursor is likely to undergo more than one reaction, but GECKO-A will only retain reactions which account for at least 2% of the total consumption of the precursor. This is done to retain all major reactions while simultaneously preventing the GECKO-A mechanism from growing too large and computationally unwieldy.

Once all potential reactions have been generated, rates predicted, and reactions filtered, the products from said reactions will be added to the stack to subsequently go through the same process themselves. This process may repeat until all species are eventually reacted to CO_2, but more commonly the GECKO-A user defines a certain product generation as the end generation. This is done for practical purposes since mechanisms including between three and five generations of stable products are usually sufficient to capture the chemistry that is expected to be observed over the length of a normal chamber experiment (B. Aumont et al. 2012).

GECKO-A incorporates thousands of explicitly defined reactions from mechanisms including MCM, but what makes GECKO-A relatively unique is its ability to also generate its own reactions based on a set of rules known as Structure Activity Relationships (SARs) (Bernard Aumont, Szopa, and Madronich 2005; Jenkin, Saunders, and Pilling 1997; Saunders et al. 2003). SARs have been used since the 1970's as a way to predict the rates of reactions which were difficult to study at that time including even simple

alkane oxidation reactions (Baldwin et al. 1977). Needless to say, there have been significant advances in the use and creation of SARs since the Baldwin paper was published.

GECKO-A uses SARs to predict reaction rates by beginning with a well-studied reaction that incorporates a reactive site that resembles the reactive site of interest (Peeters, Fantechi, and Vereecken 2004). The activation energy for that known reaction forms the basis of the SARs-predicted rate constant along with the assumption that the reaction follows Arrhenius kinetics. For example, estimating the rate for a reaction of any double bond with an OH radical would start with the known activation energy of ethene reacting with OH. Modifying factors are then applied (usually additively or multiplicatively) to that activation energy based on the substituents and functional groups that may be adjacent to the bond of interest (Vereecken and Peeters 2009). The values of these modifying factors are most frequently determined using quantum chemical calculations from a training set of molecules that all contain the reactive site of interest but with a variety of permutations of different moieties surrounding the reactive site. The reaction rates and activation energies for the reactions of each molecule in the training set are known quantities, so the results from the quantum chemical prediction can be validated against the empirically known rate values. Once the SARs have been validated, they can be used to predict activation energies and rates for reactions which have yet to be empirically characterized.

It is important to note that SARs can not be used to predict rates for reactions for which a training set does not exist. While the work in this chapter focuses on understanding the extent to which uncertainties and errors in SARs contribute to chamber-GECKO discrepancies, the other major potential source of discrepancy is missing chemistry in GECKO-A. The importance of new chemistry is continuously being elucidated; for example, isomerization of RO_2 species has recently been found to form Highly Oxygenated Organic Molecules (HOMs), but the version of GECKO-A used in this thesis only allows RO_2 species to react with NO_x (Crounse et al. 2013; Bianchi et al. 2019; Barber and Kroll 2021). Adding this class of reactions and others could yield improved chamber-GECKO agreement, but adding new chemistry

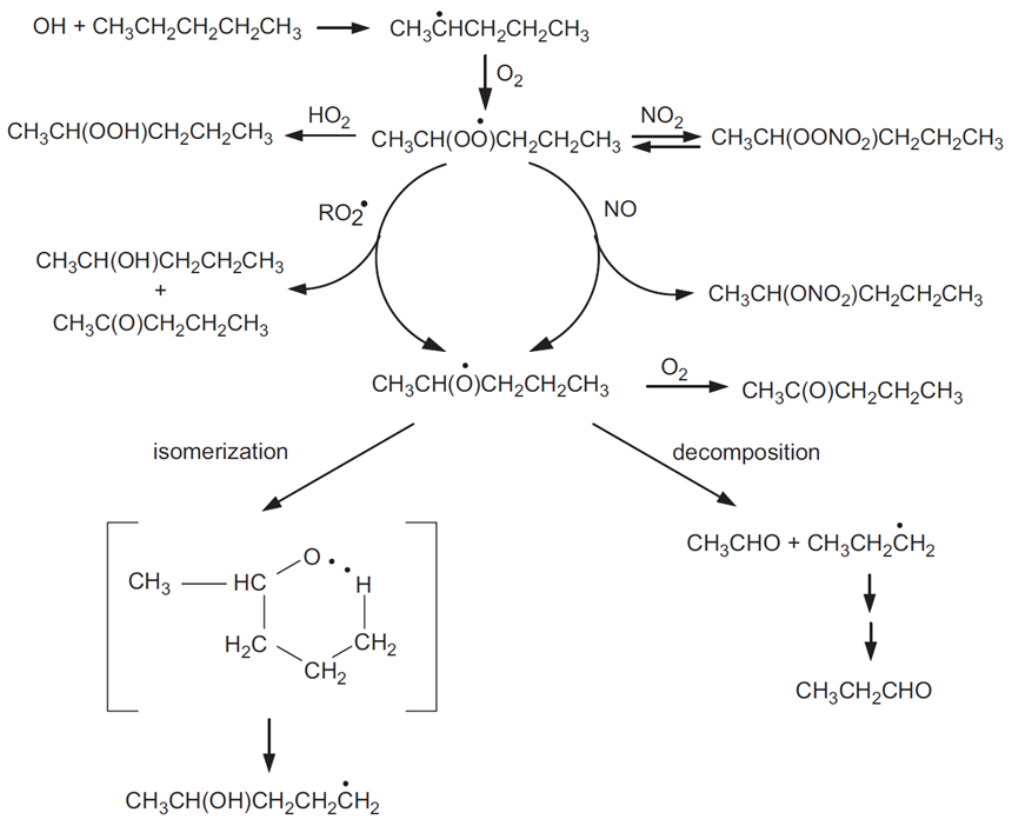

Figure 2: Sample oxidation reaction scheme for n-pentane. Only the first two generations of products are shown. Chamber studies in this work were performed under high-NOx conditions which means organonitrates ($RONO_2$) and alkoxy radicals (RO•) are expected to be formed. Adapted from (Atkinson, Arey, and Aschmann 2008). The fate of alkoxy radicals is critical to understanding the interplay of fragmentation and functionalization.

to GECKO-A is outside the scope of this work. Instead, we will focus on the effects of potential amendments to existing GECKO-A chemistry.

We now turn our attention to specific classes of reactions which are critically important for understanding how VOCs functionalize and fragment. Figure 2 displays an example reaction scheme for n-heptane OH oxidation which highlights the important pathways under consideration in this chapter (Atkinson, Arey, and Aschmann 2008). After an initial hydrogen abstraction and addition of O_2, peroxy radicals (ROO•) may follow four different paths of further oxidation. Since the chamber experiments presented in this work were conducted under high-NOx conditions, we will only be considering peroxy radical reactions with NO_2 and NO. Reactions with NO_2 result in an equilibrium between the peroxy radical

and a peroxynitrate species (Seinfeld and Pandis 2006). Peroxy radical reactions with NO can either result in the formation of an organonitrate species ($RONO_2$) or an alkoxy radical (RO•).

The fate of the alkoxy radical is an important contributor to the dynamic between fragmentation and functionalization (Ziemann 2011). Decomposition reactions encompass the means by which an alkoxy radical undergoes carbon backbone fragmentation, leading to the formation of a stable aldehyde and an alkyl radical. The vapor pressures of these products tend to be higher than that of the parent molecule which decreases the likelihood that they will contribute to SOA particulate formation and growth (Lambe et al. 2012). In contrast, alkoxy radical reactions with O_2 lead to the formation of stable products with carbonyls. The addition of the carbonyl lowers the vapor pressure of the product compared to its parent which in turn makes it more likely to partition into the particle phase. Isomerization is the third and most complex path available to an alkoxy radical (at least four carbons in length). As Figure 2 shows, alkoxy radicals may form a transition state in which the oxygen abstracts an internal molecular hydrogen leading to the formation of an alcohol and an alkyl radical in the same molecule. Essentially this means that the molecule restarts from the top middle of the Figure 2, just with another functional group. Species may undergo any number of rounds of isomerization before a stable species is generated, but the more functionalized a molecule becomes, the more likely it is to undergo decomposition (Lambe et al. 2012; Roger Atkinson, Arey, and Aschmann 2008; Jordan et al. 2008).

We will now examine changes to the above chemistry to posit potential explanations for differences between chamber measurements and mechanistic simulations. Chapter 3 provided new methods to compare chamber and GECKO-A datasets, and in the process we uncovered significant differences in the carbon number (Cnum) and average carbon oxidation state (OSc) distributions of the V-pinene oxidation system which serve as useful proxies for understanding the fragmentation-functionalization dynamic of the system (Isaacman-VanWertz et al. 2018). We determined that the differences between the distributions were not due to CIMS calibration uncertainties. CIMS are also not

prone to fragmenting a molecule's carbon backbone, so although functional groups may decompose the Cnum distribution should remain unaffected. A reasonable explanation for the differences between the datasets is they are derived from differences between observed and simulated chemistry. Alkoxy radical chemistry can serve as a potential driver of the observed differences since the differing fates of the alkoxy radical directly impact the fragmentation-functionalization dynamic. Ozonolysis provides yet another pathway to fragmentation is double bonds are present (Roger Atkinson 2009). Organonitrate and PAN formation may also be important in that they act as sinks or reservoirs of reactive carbon, changing the pace at which a system may proceed toward increased oxidation.

This chapter uses GECKO-A to explore how changes to different reaction pathways influence the degree to which GECKO-A simulations agree with chamber observations. We can then perform a directed sensitivity analysis for the SARs for each of the pathways above in order to determine how important each pathway is to the overall agreement with chamber in terms of Cnum and OSc. Ultimately, this work could help target specific chemical pathways for further scrutiny, thereby improving our understanding of complex mechanisms. More complete and accurate mechanisms then allow for more accurate chemical transport and climate models.

2. Methods

The chamber experiments in this chapter are the same as those discussed in Section 3.2. α-Pinene, 1,2,4-TMB, and isoprene were the precursor VOCs. We used the comparison methodology developed over the course of section 3.2 in order to understand differences in the Cnum and OSc distributions. We then edited one or more SARs in GECKO-A to direct each of the precursors' mechanisms to better match their corresponding chamber datasets. We generated new mechanisms using edited SARs, ran new simulations of each precursor's chamber experiment in GECKO-A's 1-D box model program, and then used the

comparison methodology from Chapter 3 to assess the degree to which the edits improved agreement between the measurements and mechanisms.

Edits were performed on the SARs controlling alkoxy decomposition, alkoxy isomerization, ozonolysis, nitrate yield, and PAN decomposition. Each SAR has a corresponding subroutine in GECKO-A's mechanism generator (except for the two aforementioned alkoxy reaction SARs which share a subroutine). Edits were made by multiplying or dividing the SAR-calculated rate constants for all reactions in each subroutine by 2x, 5x, or 10x. These edits were not necessarily meant to be realistic since it is unlikely that the SAR-calculated rate for every reaction in each class of reactions would be inaccurate in the same direction by upwards of an order of magnitude (Vereecken and Peeters 2010). However, we designed these edits as a proof of concept and wanted to push the mechanisms into a regime in which we would be able to discern obvious effects from our edits.

SARs for each class of reactions were derived from their corresponding sources in Table 1:

SAR/Subroutine	Source	SAR-rate uncertainty
Alkoxy Radical Decomposition	Vereecken and Peeters 2009	5-10x
Alkoxy Radical Isomerization	Vereecken and Peeters 2010	3-5x
Alkoxy Radical + O_2	Roger Atkinson 2007	5.4x
Nitrate Yield	Arey et al. 2001	1.4x
Ozonolysis	Roger Atkinson 1997	unknown
PAN Decomposition	Tyndall et al. 2001 ; R. Atkinson et al. 1999	unknown

Table 1: Sources for GECKO-A SARs and subroutines

Mechanistic simulations were also performed using MCM 3.3.1 in the F0AM box model program in MATLAB (Wolfe et al. 2016). These simulations were performed to understand how GECKO-A performs compared to MCM in terms of accurately reproducing chamber results. MCM was tuned for precursor decay. However, at the time of simulation, MCM and F0AM did not contain modules to account for gas-particle-wall partitioning so all species remain in the gas-phase over the entire course of the simulation.

3. Results

We first compared how GECKO-A and MCM perform for each of the three precursor systems. These comparisons were performed to understand the value added by GECKO-A's SARs to generate reactions which are not explicitly know and are thus not contained within MCM. However, GECKO-A contains MCM and thus reaps the benefits of having its reaction data built-in. The error metric results (based on Chapter 3 methods) for all three tuned and unedited systems are shown in Figure 3. The pinene system shows similar error for MCM and GECKO-A with the MCM error growing larger by the end of the experiment. The isoprene system shows a bit more complex behavior because the GECKO-A error is lower until the end of the experiment when the MCM error becomes lower. Lastly, the 1,2,4-TMB system sees

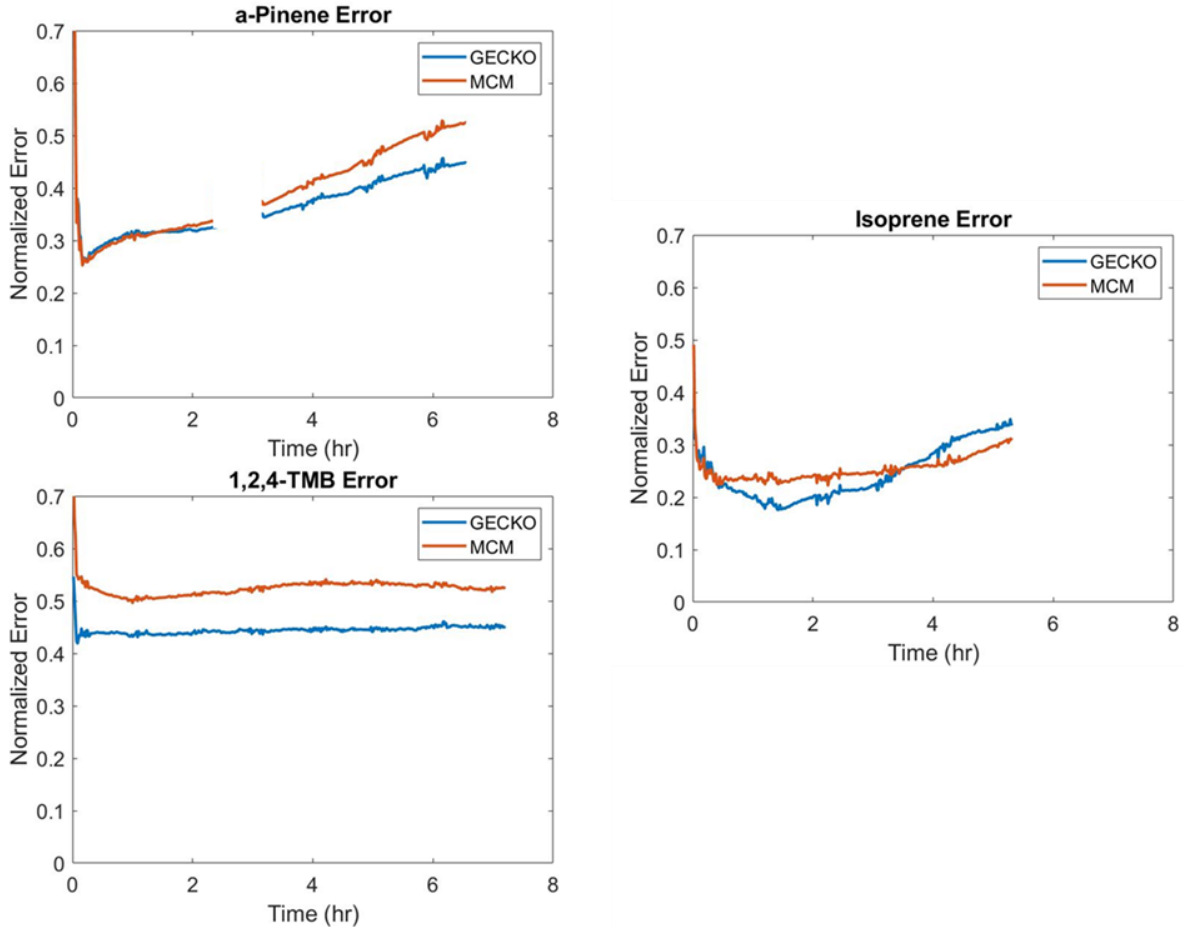

Figure 3: The error metric for GECKO-A and MCM simulations compared to chamber data for all thre precursor systems are displayed. MCM errors tend to be larger than or equal to those for the GECKO-A simulations.

consistently lower error for GECKO-A than for MCM. Overall, GECKO-A performs comparably to MCM and tends to generally reduce chamber-mechanism disagreement. All remaining chamber-mechanism comparisons in this chapter will be performed using GECKO-A since its SARs are editable in a way that MCM is not.

The results of the error metric calculations described in Chapter 3 for the α-pinene, 1,2,4-TMB, and isoprene oxidation systems are shown below in Figure 4. One common feature across all three systems includes a general growth in error over the duration of the experiments. This is what we anticipate to see because our knowledge of higher-generation chemistry is limited compared to our knowledge and parametrization of early-generation reactions. Overall, however, we observe more differences than similarities between the three systems, namely that isoprene appears to have the lowest error in chamber-GECKO agreement followed by α-pinene, and lastly followed by 1,2,4-TMB. This result is

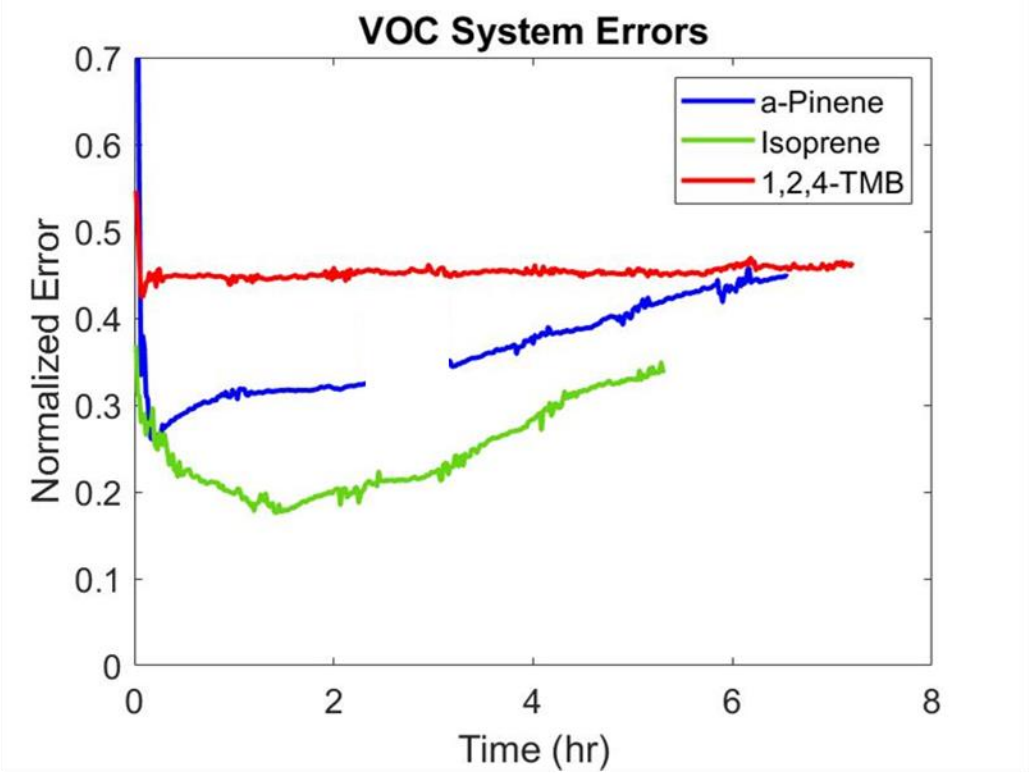

Figure 4: The error metric for each precursor oxidation system at each point in time is displayed here. Isoprene appears to have the lowest disagreement between the chamber and GECKO-A datasets at all but the earliest time points. Pinene has a middling amount of error per our metric, and 1,2,4-TMB has consistently the highest degree of error. The error in all three systems grows over time which implies that GECKO-A is capturing the chemistry and/or dynamics of the system less accurately over time.

consistent with general trends in the field of atmospheric chemistry over the past few decades because isoprene and α-pinene chemistry have been studied extensively while 1,2,4-TMB chemistry has

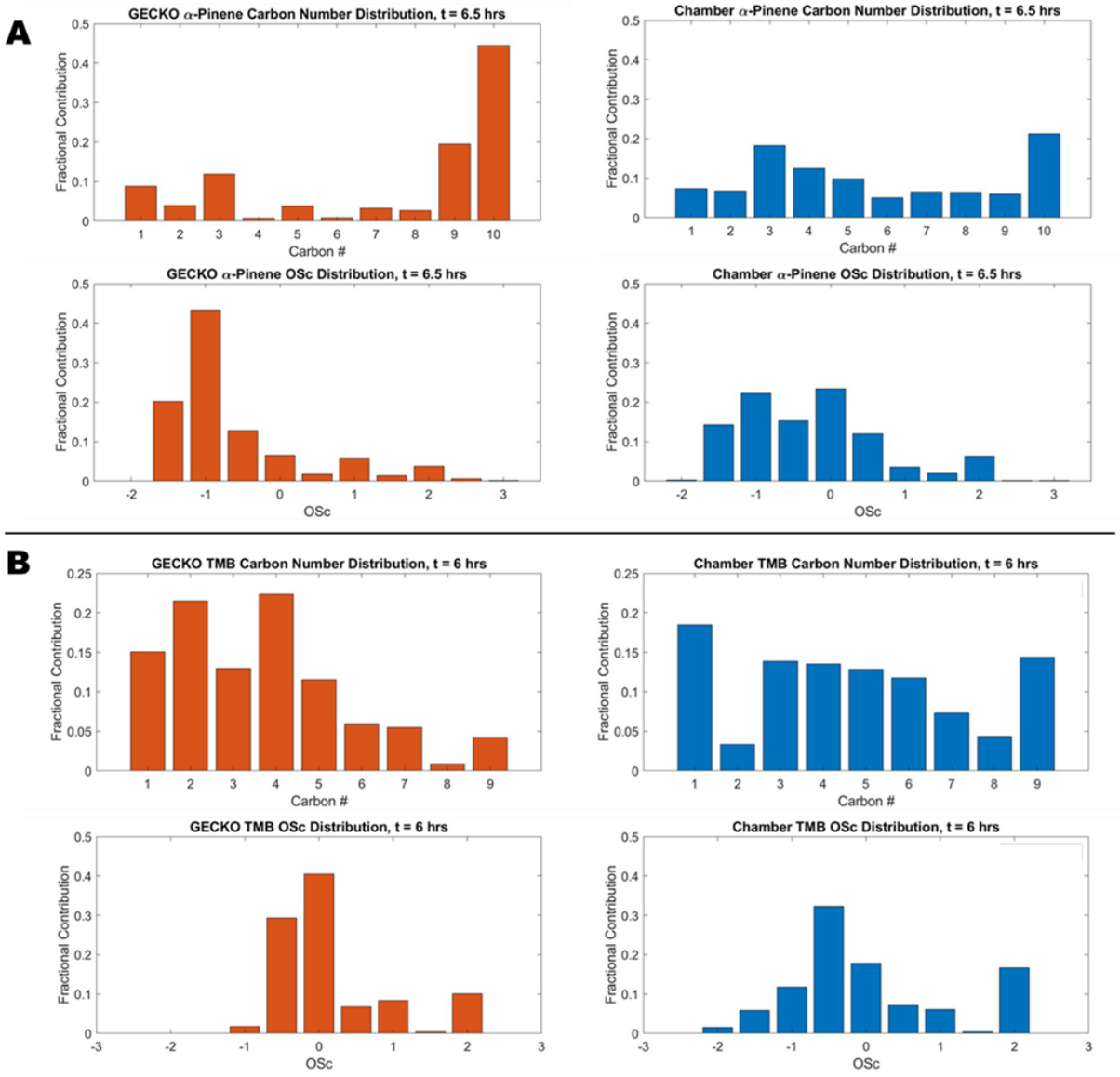

Figure 5: Cnum and OSc distributions at the end of the α-pinene (A) and 1,2,4-TMB (B) oxidation experiments. The pinene comparison shows a clear difference in Cnum and OSc distributions, namely that GECKO-A predicts much less fragmentation and less oxidation than is observed in the chamber. In contrast, the 1,2,4-TMB comparisons shows more fragmentation and more oxidation in GECKO than is observed in the chamber.

comparatively received less attention (e.g. Zhang et al. 2015; Iyer et al. 2021; Archibald et al. 2010; Bates et al. 2014; Bates and Jacob 2019).

We will focus on reducing disagreement between chamber and GECKO-A datasets for the α-pinene and 1,2,4-TMB systems since they displayed the greatest degree of disagreement over the

durations of their experiments. Error reductions were attempted by editing SARs in the GECKO-A mechanism generator, but a closer examination of the pinene and TMB systems were necessary to determine which SARs should be edited. Figure 5 displays histograms of the chamber and GECKO-A Cnum and OSc distributions which are useful to highlight the discrepancies we want to address.

We first consider the discrepancies observed in the pinene comparison from Panel A of Figure 5 which shows that GECKO-A severely underpredicts fragmentation compared to what is observed in the chamber dataset; the Cnum distribution for GECKO-A is skewed right compared to the chamber Cnum distribution. The OSc distributions show a similar yet opposite difference in that GECKO-A predicts less oxidation than occurs in the chamber. Although these histograms are only shown for one point in time near the end of the experiment, Figure 5 shows that the Cnum distribution discrepancies persist and grow over the course of the experiment, consistent with the growth in the Cnum-OSc binned error growth shown in Figure 3.

Based on the differences in the Cnum and OSc distributions, we edited GECKO-A's base case mechanism (i.e. the normal, unedited mechanism) SARs to attempt to yield more fragmentation and more oxidation. Increasing the rate of alkoxy radical decomposition provides a way to increase both fragmentation and functionalization as described in Figure 2. Alkoxy radical isomerization is also important for increasing functionalization, so all alkoxy isomerizations were increased 5x. Increasing ozonolysis rates serves a similar function because ozonolysis breaks a carbon-carbon double bond while oxygenating one of those carbons. Photolysis of carbonyls is another path that could lead to fragmentation, so photolysis rates were increased 2x. PAN decomposition and organonitrate yield SARs were also edited to decrease the amount of reactive carbon effectively trapped in those stable species. Other SARs edits including reducing alkoxy radical decomposition rates by 1/2x and increasing alkoxy radical + O_2 rates by 10x were also considered to test their effects on overall agreement. The error metrics,

Cnum distributions, and OSc distributions for each of these edits are shown in Figures 6, 7, and 8 respectively.

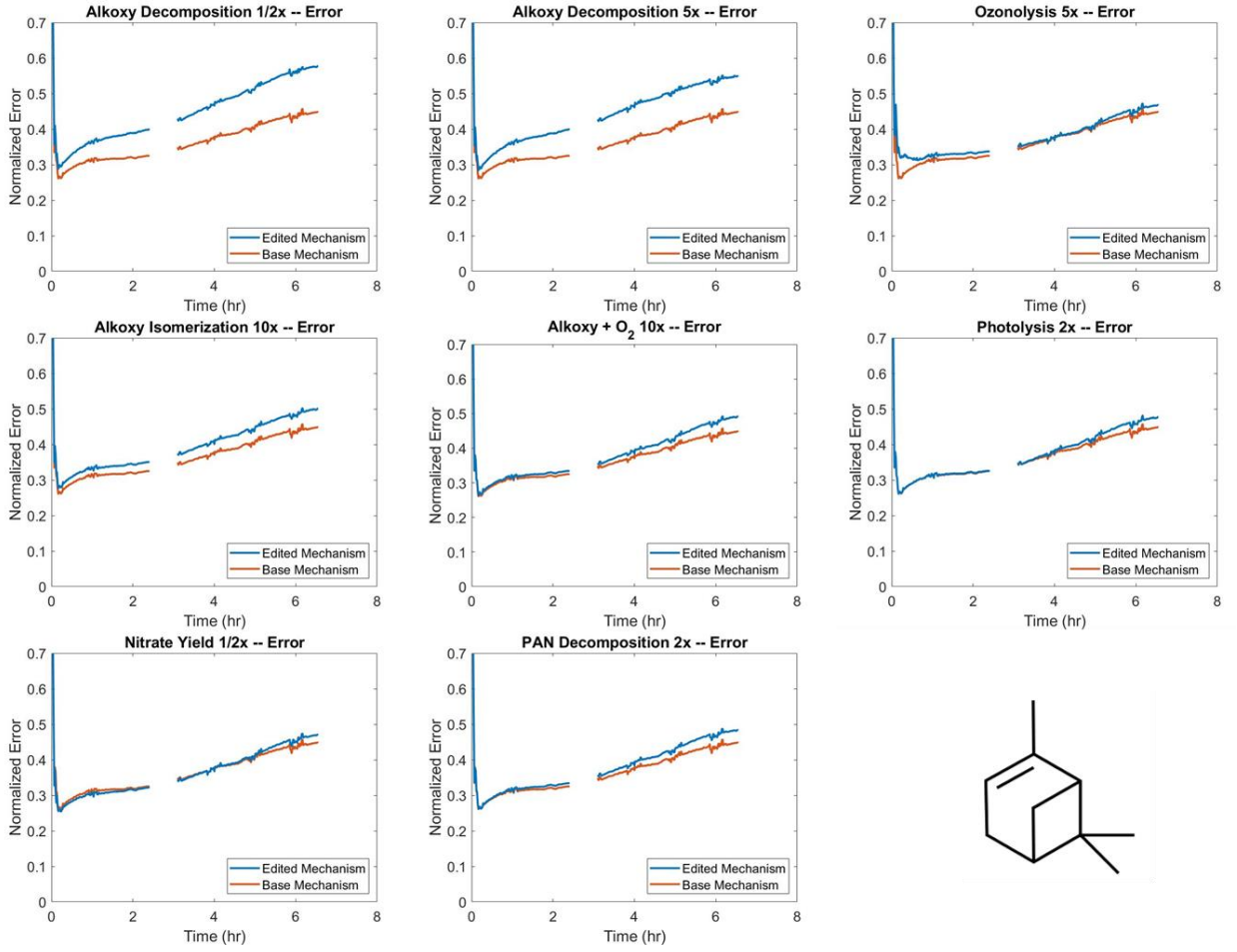

Figure 6: ***α-Pinene Error Metric Results from SARs Edits.*** *The chamber-GECKO comparison errors resulting from each denoted SARs edit to the GECKO-A Base model. Only the SARs edits reducing nitrate yields by 1/2x showed a small reduction in error at the beginning of the experiment. All other SARs edits resulted in an increase in the error metric compared to the Base GECKO-A mechanism. The gaps in the data preceding the 3 hr mark correspond to the period with missing chamber pinonaldehyde measurements.*

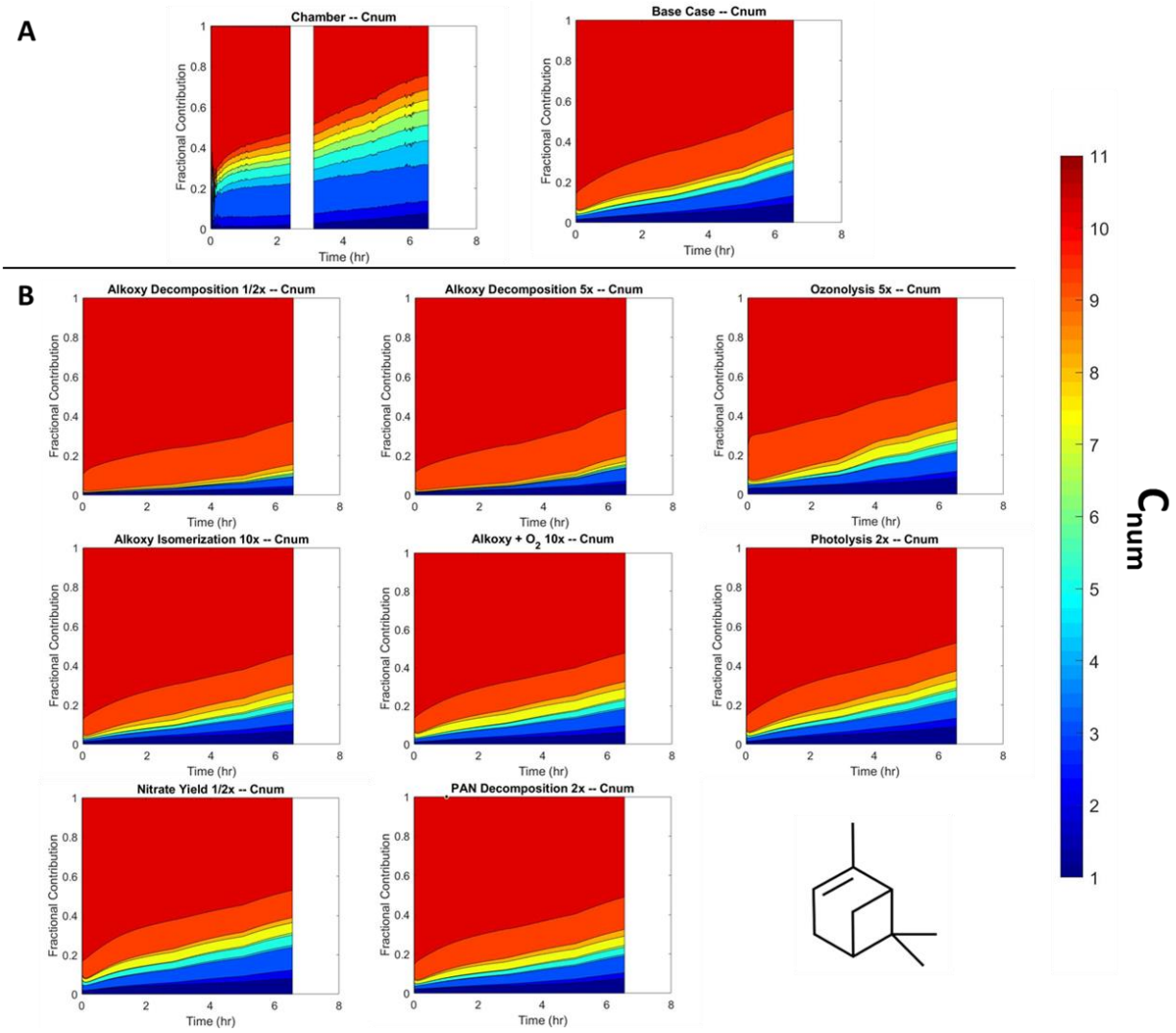

Figure 7: ***α-Pinene Cnum Distributions from SARs Edits.*** *Panel A shows the chamber and GECKO-A Base model Cnum distributions. Panel B shows the Cnum distributions resulting from each denoted SARs edit to the GECKO-A Base model.*

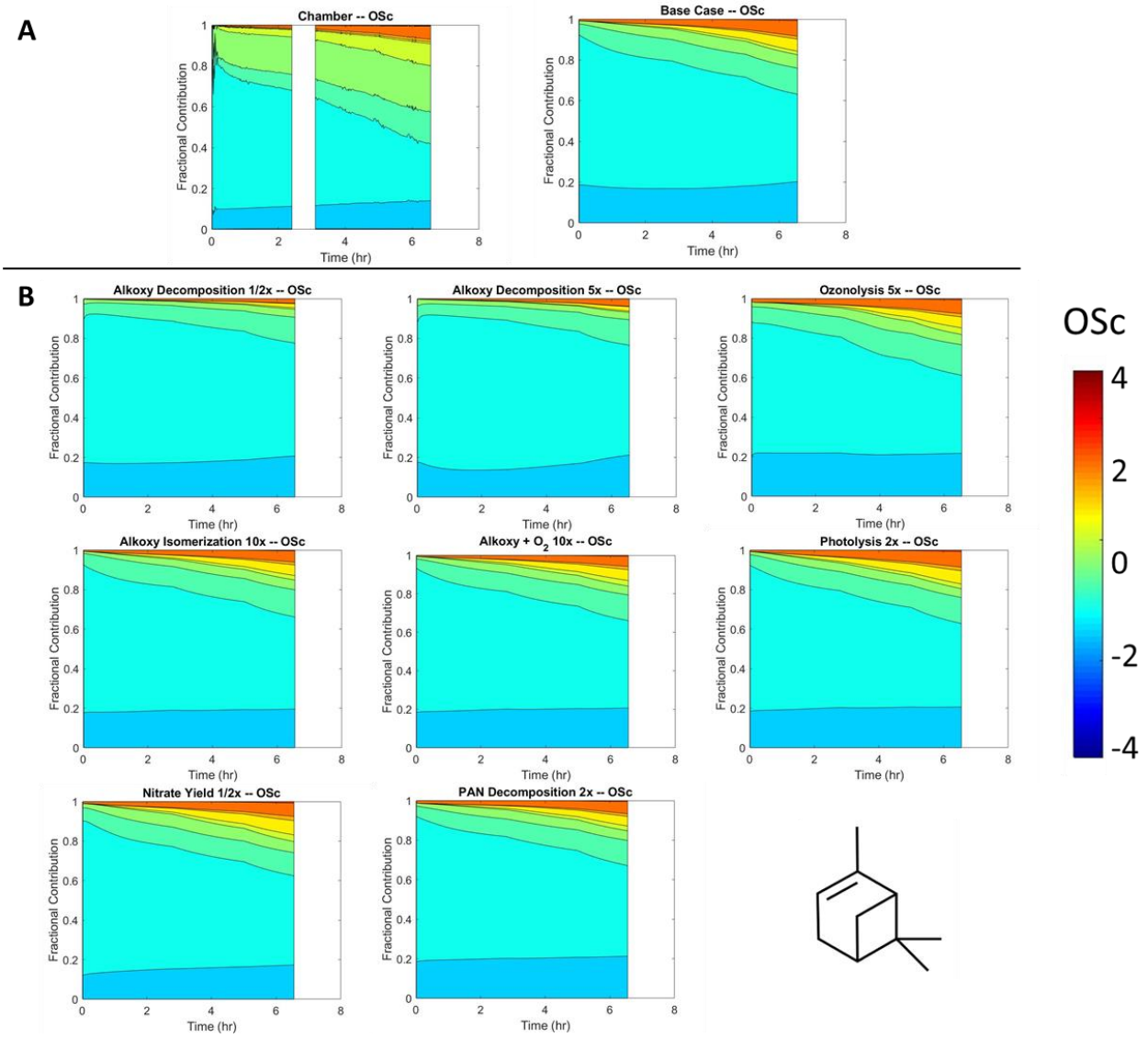

Figure 8: ***α-Pinene OSc Distributions from SARs Edits.*** *Panel A shows the chamber and GECKO-A Base model OSc distributions. Panel B shows the OSc distributions resulting from each denoted SARs edit to the GECKO-A Base model.*

Figure 6 shows that no SARs edit yielded any significant improvements in chamber-GECKO agreement. Dividing nitrate yields in half yielded minor improvements in agreement for the first half of the experiment, but the second half of the experiment showed subsequent decreases in agreement relative to the unedited GECKO-A mechanism. All other SARs edits yielded increases in chamber-mechanism error. Figure 7 displays the Cnum distributions resulting from each SARs edit. Some edits yielded increased fragmentation which helped increase agreement with the chamber Cnum distribution

including increasing ozonolysis rates 5x which increased concentrations of C3, C7, and C8 compounds in GECKO-A. However, the OSc distribution resulting from increasing ozonolysis rates 5x in Figure 8 show little change compared to the base case, and the error metric for ozonolysis shows an overall slight worsening in agreement upon increasing ozonolysis rates. Surprisingly, Figure 7 also shows that both increasing and decreasing alkoxy radical decomposition rates decreased the observed degree of fragmentation. Figure 8 displays the OSc distributions from each GECKO-A mechanism with its associated SAR edit. None of the SARs edits show meaningful improvement in agreement with the chamber distribution, and some including the alkoxy decomposition rate increase and decrease edits show significant worsening in agreement. All of these results, but particularly the error metric results in Figure 6, imply that, at least for the SARs we considered, uncertainties or errors GECKO-A's SARs are not responsible for the discrepancies observed in comparison to chamber data.

We will now consider SARs edits for improving chamber-GECKO-A agreement for the 1,2,4-TMB system. Panel B in Figure 4 shows that GECKO-A predicts more fragmentation and more oxidation than is observed in the chamber. All three alkoxy radical SARs from Table 1 were edited to analyze which would yield reductions in the error metric for the TMB system upon editing. Alkoxy isomerization and reaction with O_2 were increased 10x, and decomposition rates were decreased 1/10x. Figures 9, 10, and 11 display the error metrics, Cnum distributions, and OSc distributions for each SAR edit as well as the combined isomerization and O_2 reaction SARs edit.

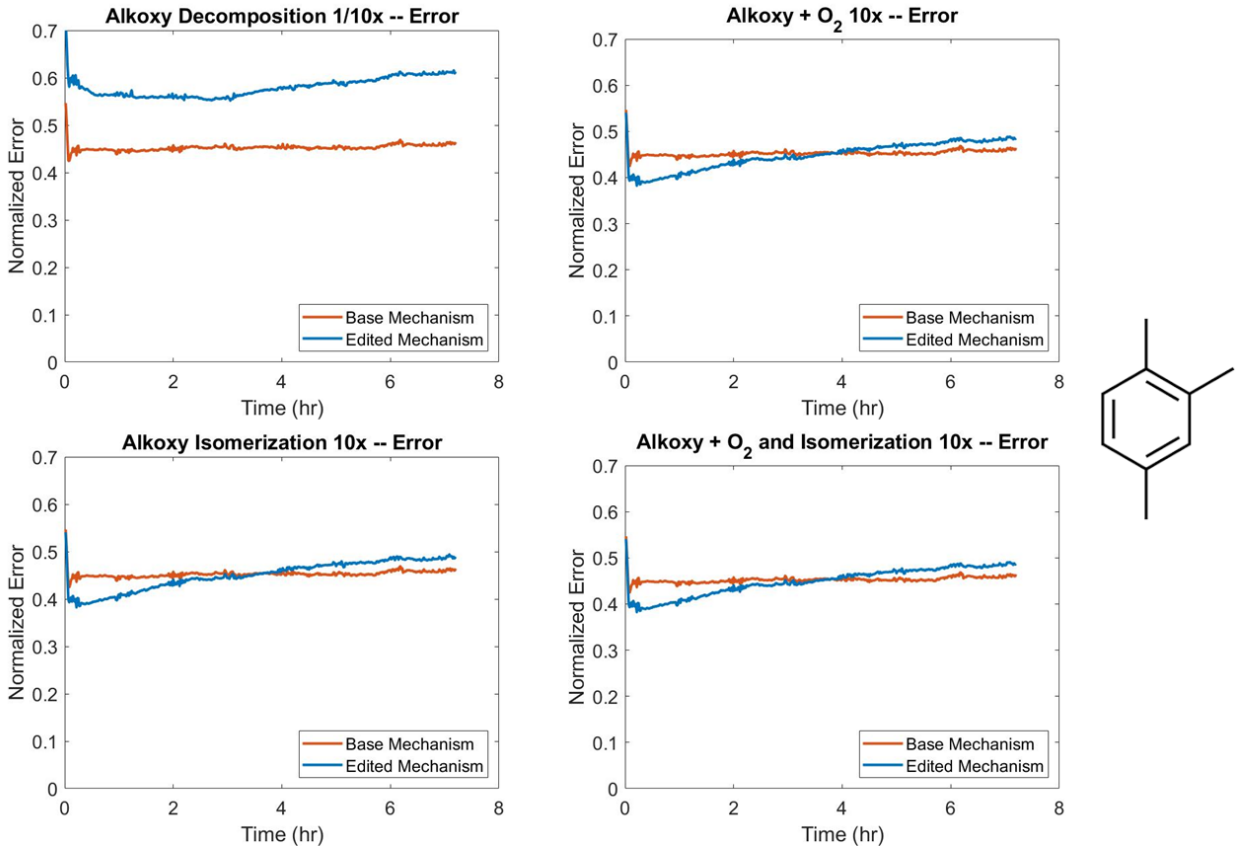

Figure 9: ***1,2,4-TMB Error Metric Results from SARs Edits.*** *The chamber-GECKO comparison errors resulting from each denoted SARs edit to the GECKO-A Base model. Decreasing alkoxy decomposition drastically increased error at all times. Increasing alkoxy + O_2 and alkoxy isomerization rates yielded near-identical improvements. The combination of these two SARs edits does not appreciably change compared to either individual SAR edit.*

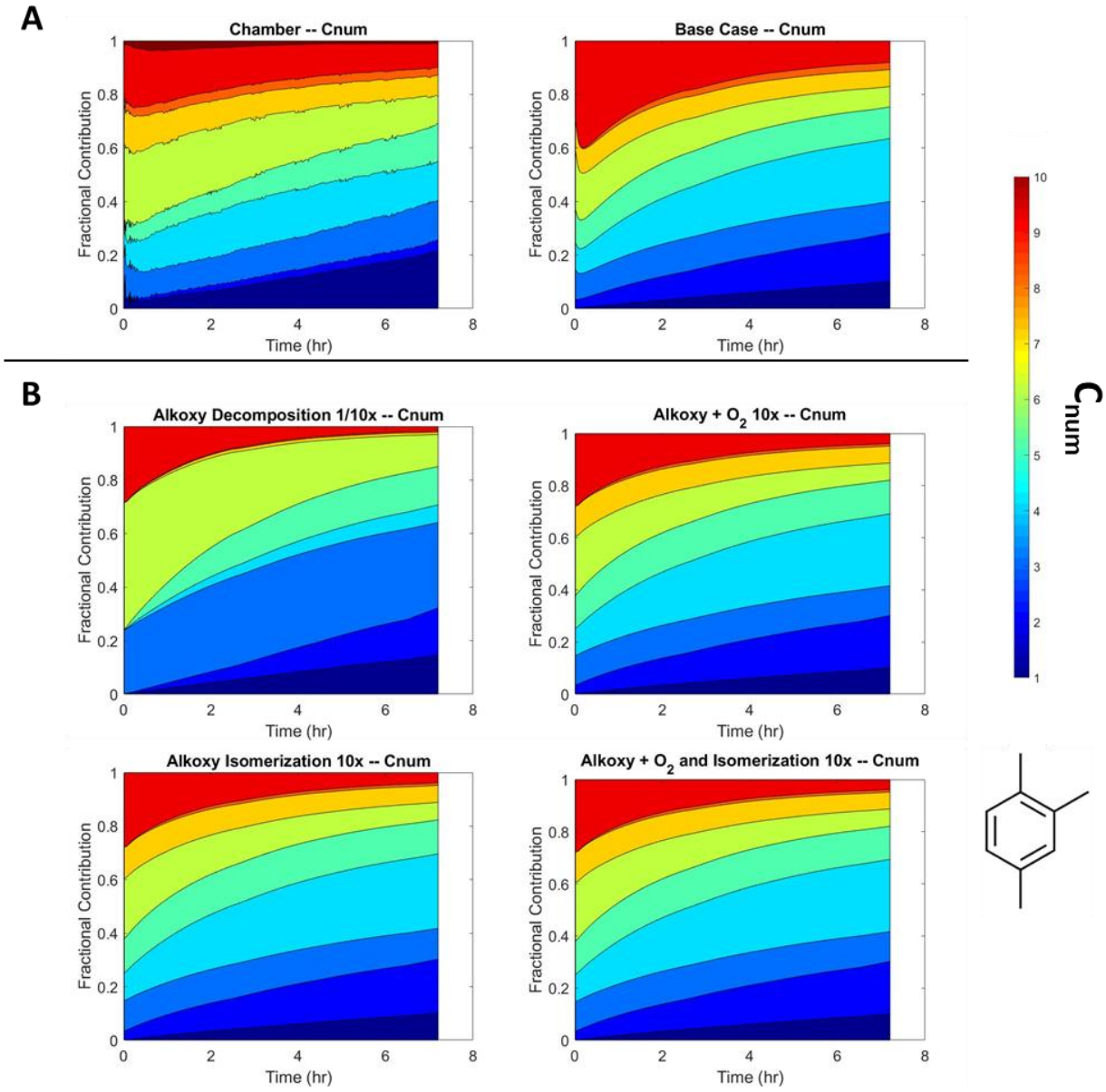

Figure 10: ***1,2,4-TMB Cnum Distributions from SARs Edits.*** *Panel A shows the chamber and GECKO-A Base model Cnum distributions. Panel B shows the Cnum distributions resulting from each denoted SARs edit to the GECKO-A Base model. Very little change is observed compared to the base case except for the SAR edit to decrease alkoxy decomposition 10x.*

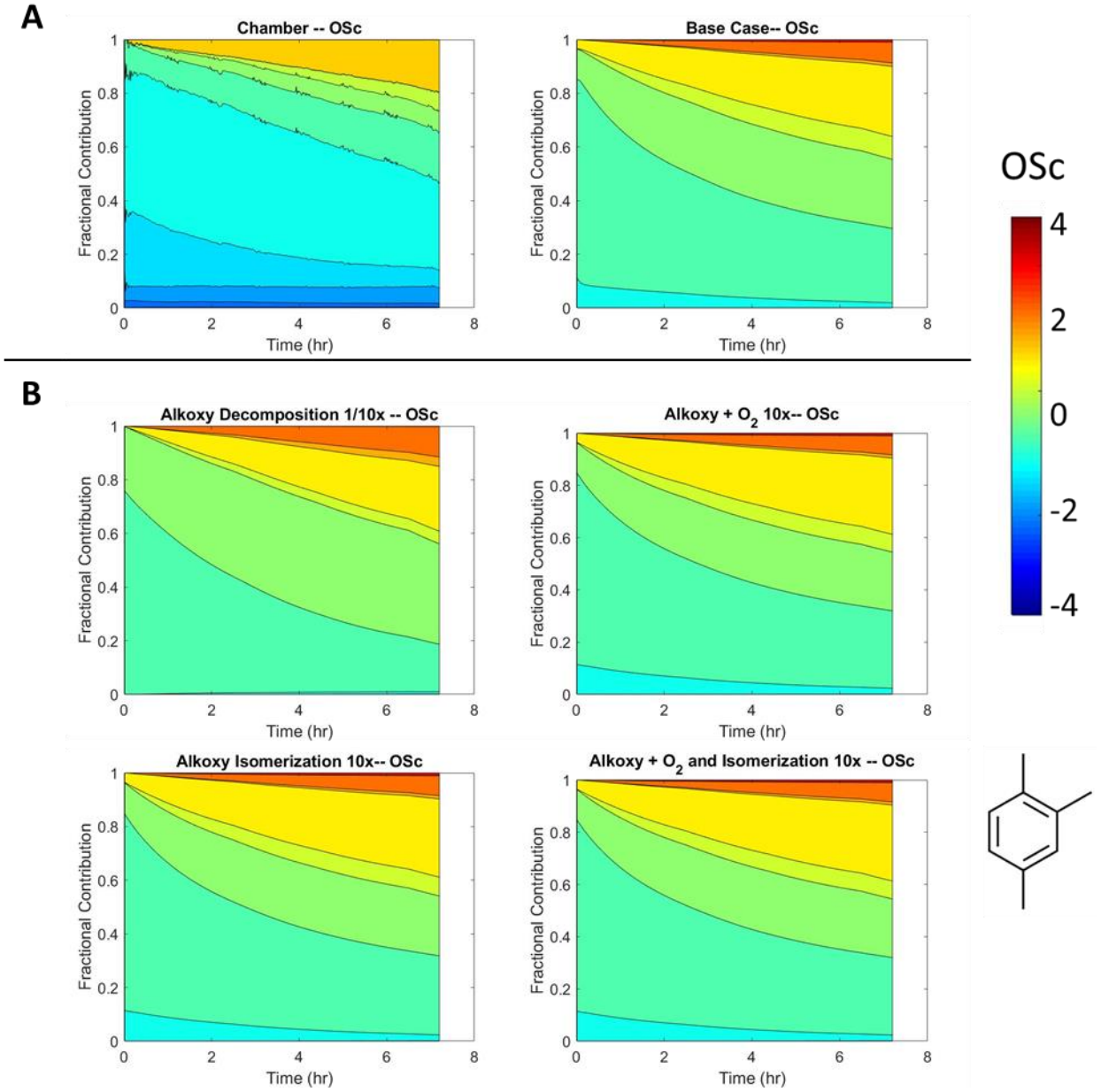

Figure 11: ***1,2,4-TMB OSc Distributions from SARs Edits.*** *Panel A shows the chamber and GECKO-A Base model OSc distributions. Panel B shows the OSc distributions resulting from each denoted SARs edit to the GECKO-A Base model. Very little change is observed compared to the base case except for the SAR edit to decrease alkoxy decomposition 10x.*

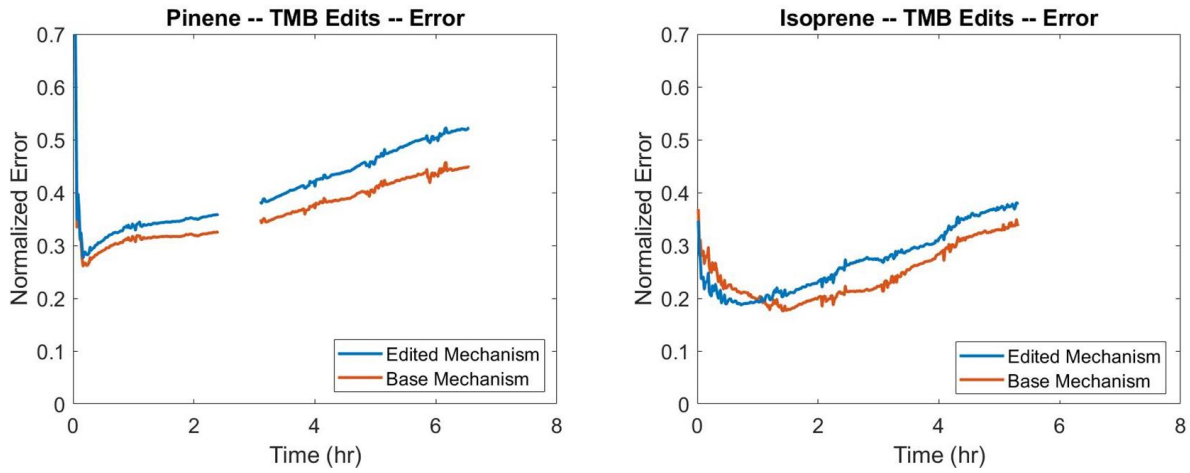

Figure 12: ***Error Metric Plots for α-Pinene and Isoprene Increasing Alkoxy + O_2 and Isomerization 10x.*** *The chamber-GECKO comparison errors for the pinene and isoprene oxidation systems resulting from each denoted SARs edit to the GECKO-A base model.*

Figure 9 shows that the O_2 and isomerization rates edits provided near-identical marginal improvements in the error for the TMB system for the first half of the experiment, but the errors eventually grew to exceed the error of the unedited TMB system. Because both of these edits provided some improvement in overall agreement, we combined the edits to observe how they would affect agreement together. There was no significant difference observed from the combined edits and the individual edits. In terms of alkoxy decomposition, rates by 1/10x substantially increased the error across the entire duration of the experiment, but surprisingly this appears to be because, as shown in Figure 10, this SAR edit led to significantly more fragmentation. This contradicts our preconceived notion that decreasing alkoxy decomposition rates would lead to less fragmentation. Figure 11 suggests none of the edits had a substantial effect on the OSc distribution.

Because a small improvement in overall agreement in the 1,2,4-TMB system was observed upon increasing alkoxy isomerization and O_2 reaction rates, these SARs edits were applied to the α-pinene and isoprene systems to see if the edits could provide benefits to each of the precursor systems we have examined. The error metric results of these edits are presented in Figure 12. The isoprene system sees a small reduction in its initial error compared to its base GECKO-A mechanism, but the edited system's error

quickly grows larger than the base mechanism's error. The pinene system error is noticeably higher with the 1,2,4-TMB system edits than without them. Therefore, no systematic benefits were realized by implementing the beneficial 1,2,4-TMB system edits to the pinene and isoprene systems.

4. Conclusions and Implications

In this chapter, we explored potential changes to GECKO-A SARs in order to increase agreement between GECKO-A simulations and chamber experiments. SARs edits were considered for alkoxy radical decomposition, isomerization, and reaction with O_2. SARs edits were also considered for ozonolysis reactions, PAN decomposition reactions, and nitrate yield calculations. These edits were based on our general understanding of different reaction pathways available to atmospheric species in an oxidizing environment and how each of those pathways contributes to the dynamic of fragmentation and functionalization in each system.

SARs edits were first performed to the α-pinene system in an attempt to reduce the chamber-mechanism discrepancy. The pinene system exhibited a higher degree of fragmentation and oxidation in the chamber than was predicted in GECKO-A. Some SARs-edited systems showed an improvement in Cnum distributions like the "nitrate yield 1/2x" and "photolysis 2x" systems, but no SARs-edited systems yielded significant differences in the OSc distribution. Overall, no SARs edits yielded reduced error compared to the base GECKO-A mechanisms which implies that uncertainties and potential errors in the SARs we examined are not responsible for the chamber-mechanisms discrepancies observed for the α-pinene system.

Edits were also made for the 1,2,4-TMB system based on observations that GECKO-A predicts slightly more fragmentation and oxidation than was observed in the chamber. The SARs for alkoxy radical isomerization and reaction with O_2 were each increased by 10x which led to initial reductions in the error metric compared to the unedited system, and a reduction of alkoxy decomposition rates by 1/10x

surprisingly led to a large increase in error for the duration of the experiment. We had discussed reducing alkoxy decomposition rates to decrease fragmentation in GECKO-A, but this reduction actually led to increased fragmentation. Future work may focus on examining the changes branching ratios and specific reaction rates which led to this surprising result. Because increasing alkoxy isomerization and reaction with O_2 led to a partial reduction in the error of the 1,2,4-TMB system, the same edits were applied to the isoprene and pinene systems. Both systems observed a general increase in error over the duration of their experiments compared to their base mechanisms. Thus, no pan-system benefits were observed for any SARs we examined.

It is possible, albeit computationally intense, to analyze all of the rules that comprise each SAR. This chapter took a sweeping approach to SARs edits by changing the rates of every SARs-predicted reaction in each class of reactions. However, SARs-calculated rates are dependent on the substituents surrounding each reactive site because each substituent contributes their own modifying factor(s). We suggest that future work in this area could be conducted with a Monte-Carlo analysis of all potential SARs of interest in order to map the error metric landscape from a variety of SARs edits combinations of varying orders of magnitude. Similarly, sensitivity analyses could be conducted on the explicitly input reactions from MCM using the uncertainties in their reported rate constants. The SARs edits we performed in this chapter did not change anything regarding the explicitly input reactions.

This work probed the degree to which uncertainties and errors in SARs may be responsible for the discrepancies we observe when comparing GECKO-A results to chamber data. We did not observe that editing any SARs provided benefits across all VOC oxidation systems, and even when errors were reduced from SARs edits for a given oxidation system, the magnitude of those error reductions was minor compared to the overarching discrepancies. These results increase the likelihood that measurement-mechanism discrepancies are driven by missing chemistry in GECKO-A. In section 4.1 we discussed that GECKO-A is not yet completely parametrized for the recently elucidated RO_2 isomerization reaction which

could account for some of the observed discrepancies (Crounse et al. 2013; Bianchi et al. 2019). We also can not preclude the possibility that other important classes of reactions will be elucidated in the future which could account for more discrepancies. Lastly, we can not aver with complete confidence that we edited all relevant SARs in GECKO-A, so other SARs may be important to reduce pan-system chamber-GECKO discrepancies.

One overarching insight we can provide from this work is that GECKO-chamber agreement invariably tends to become worse the longer the system is oxidizing. Much of the work other researchers in our field have conducted has focused on early stage oxidation, in part because most experiments are conducted using the precursor as the initial VOC in the chamber as a practical matter. However, this has unintentionally contributed to a relative dearth in knowledge of reactions that occur after several rounds of oxidation have already happened. Constraints on these reactions which gain importance toward the ends of experiments are needed to reduce measurement-mechanism error and improve our understanding of each VOC oxidation system. One potential way to target these reactions in the future would be to synthesize late-generation products and use them as the initial VOC precursor for the chamber study. Future work may also be conducted by synthesizing chlorinated, iodated, or nitrite precursors to later-generation products which, upon exposure to UV light, will photolyze to form a reactive intermediate which would normally be found in late stage oxidation (Carrasquillo et al. 2014). Chamber studies using these reactive intermediate precursors can then be conducted to measure oxidation products with fewer confounding issues than would occur at the end of a chamber experiment including potential wall losses and significant chamber dilution. Similarly, the Oxy-Cat (Chapter 2) can help constrain the ends of experiments by providing a measurement of TSC which can be used to tune GECKO-A to TSC instead of just SOA yield. Tuning GECKO-A to TSC should yield a more accurate representation of each chamber experiment than we are currently able to attain.

5. References

Archibald, A. T., M. C. Cooke, S. R. Utembe, D. E. Shallcross, R. G. Derwent, and M. E. Jenkin. 2010. "Impacts of Mechanistic Changes on HOx Formation and Recycling in the Oxidation of Isoprene." *Atmospheric Chemistry and Physics* 10 (17): 8097–8118. https://doi.org/10.5194/ACP-10-8097-2010.

Arey, Janet, Sara M. Aschmann, Eric S.C. Kwok, and Roger Atkinson. 2001. "Alkyl Nitrate, Hydroxyalkyl Nitrate, and Hydroxycarbonyl Formation from the NOx−Air Photooxidations of C5−C8 n-Alkanes." *Journal of Physical Chemistry A* 105 (6): 1020–27. https://doi.org/10.1021/JP003292Z.

Atkinson, R., D. L. Baulch, R. A. Cox, R. F. Hampson, J. A. Kerr, M. J. Rossi, and J. Troe. 1999. "Evaluated Kinetic and Photochemical Data for Atmospheric Chemistry, Organic Species: Supplement VII." *Journal of Physical and Chemical Reference Data* 28 (2): 191. https://doi.org/10.1063/1.556048.

Atkinson, Roger. 1997. "Gas-Phase Tropospheric Chemistry of Volatile Organic Compounds: 1. Alkanes and Alkenes." *Journal of Physical and Chemical Reference Data* 26 (2): 215. https://doi.org/10.1063/1.556012.

Atkinson, Roger. 2007. "Rate Constants for the Atmospheric Reactions of Alkoxy Radicals: An Updated Estimation Method." *Atmospheric Environment* 41 (38): 8468–85. https://doi.org/10.1016/J.ATMOSENV.2007.07.002.

Atkinson, Roger, Janet Arey, and Sara M. Aschmann. 2008. "Atmospheric Chemistry of Alkanes: Review and Recent Developments." *Atmospheric Environment* 42 (23): 5859–71. https://doi.org/10.1016/j.atmosenv.2007.08.040.

Aumont, Bernard, S. Szopa, and Sasha Madronich. 2005. "Modelling the Evolution of Organic Carbon during Its Gas-Phase Tropospheric Oxidation: Development of an Explicit Model Based on a Self Generating Approach." *Atmospheric Chemistry and Physics Discussions* 5 (1): 703–54. https://doi.org/10.5194/acpd-5-703-2005.

Aumont, B., R. Valorso, C. Mouchel-Vallon, M. Camredon, J. Lee-Taylor, and S. Madronich. 2012. "Modeling SOA Formation from the Oxidation of Intermediate Volatility N-Alkanes." *Atmospheric Chemistry and Physics* 12 (16): 7577–89. https://doi.org/10.5194/acp-12-7577-2012.

Baldwin, Alan C., John R. Barker, David M. Golden, and Dale G. Hendry. 1977. "Photochemical Smog — Rate Parameter Estimates and Computer Simulations." *J. Phys. Chem.* 81 (25): 2483–92. https://doi.org/10.1021/j100540a027.

Barber, Victoria P., and Jesse H. Kroll. 2021. "Chemistry of Functionalized Reactive Organic Intermediates in the Earth's Atmosphere: Impact, Challenges, and Progress." *The Journal of Physical Chemistry A* 125 (48): 10264–79. https://doi.org/10.1021/ACS.JPCA.1C08221.

Bates, Kelvin H., John D. Crounse, Jason M. st. Clair, Nathan B. Bennett, Tran B. Nguyen, John H. Seinfeld, Brian M. Stoltz, and Paul O. Wennberg. 2014. "Gas Phase Production and Loss of

Isoprene Epoxydiols." *Journal of Physical Chemistry A* 118 (7): 1237–46. https://doi.org/10.1021/JP4107958.

Bates, Kelvin H., and Daniel J. Jacob. 2019. "A New Model Mechanism for Atmospheric Oxidation of Isoprene: Global Effects on Oxidants, Nitrogen Oxides, Organic Products, and Secondary Organic Aerosol." *Atmospheric Chemistry and Physics* 19 (14): 9613–40. https://doi.org/10.5194/ACP-19-9613-2019.

Bianchi, Federico, Theo Kurtén, Matthieu Riva, Claudia Mohr, Matti P. Rissanen, Pontus Roldin, Torsten Berndt, et al. 2019. "Highly Oxygenated Organic Molecules (HOM) from Gas-Phase Autoxidation Involving Peroxy Radicals: A Key Contributor to Atmospheric Aerosol." *Chemical Reviews* 119 (6): 3472–3509. https://doi.org/10.1021/ACS.CHEMREV.8B00395.

Camredon, M., B. Aumont, J. Lee-Taylor, and S. Madronich. 2007. "The SOA/VOC/NOx System: An Explicit Model of Secondary Organic Aerosol Formation." *Atmos. Chem. Phys.* 7 (21): 5599–5610. https://doi.org/10.5194/acp-7-5599-2007.

Carrasquillo, Anthony J, James F Hunter, Kelly E Daumit, and Jesse H Kroll. 2014. "Secondary Organic Aerosol Formation via the Isolation of Individual Reactive Intermediates: Role of Alkoxy Radical Structure." https://doi.org/10.1021/jp506562r.

Crounse, John D., Lasse B. Nielsen, Solvejg Jørgensen, Henrik G. Kjaergaard, and Paul O. Wennberg. 2013. "Autoxidation of Organic Compounds in the Atmosphere." *Journal of Physical Chemistry Letters* 4 (20): 3513–20. https://doi.org/10.1021/JZ4019207/SUPPL_FILE/JZ4019207_SI_001.PDF.

Isaacman-VanWertz, Gabriel, Paola Massoli, Rachel O'Brien, Christopher Lim, Jonathan P. Franklin, Joshua A. Moss, James F. Hunter, et al. 2018. "Chemical Evolution of Atmospheric Organic Carbon over Multiple Generations of Oxidation." *Nature Chemistry* 10 (4): 462–68. https://doi.org/10.1038/s41557-018-0002-2.

Iyer, Siddharth, Matti P. Rissanen, Rashid Valiev, Shawon Barua, Jordan E. Krechmer, Joel Thornton, Mikael Ehn, and Theo Kurtén. 2021. "Molecular Mechanism for Rapid Autoxidation in α-Pinene Ozonolysis." *Nature Communications 2021 12:1* 12 (1): 1–6. https://doi.org/10.1038/s41467-021-21172-w.

Jenkin, Michael E., Sandra M. Saunders, and Michael J. Pilling. 1997. "The Tropospheric Degradation of Volatile Organic Compounds: A Protocol for Mechanism Development." *Atmospheric Environment* 31 (1): 81–104. https://doi.org/10.1016/S1352-2310(96)00105-7.

Jordan, C. E., P. J. Ziemann, R. J. Griffin, Y. B. Lim, R. Atkinson, and J. Arey. 2008. "Modeling SOA Formation from OH Reactions with C8-C17n-Alkanes." *Atmospheric Environment* 42 (34): 8015–26. https://doi.org/10.1016/j.atmosenv.2008.06.017.

Lambe, Andrew T., Timothy B. Onasch, David R. Croasdale, Justin P. Wright, Alexander T. Martin, Jonathan P. Franklin, Paola Massoli, et al. 2012. "Transitions from Functionalization to Fragmentation Reactions of Laboratory Secondary Organic Aerosol (SOA) Generated from the OH Oxidation of Alkane Precursors." *Environmental Science and Technology* 46 (10): 5430–37. https://doi.org/10.1021/es300274t.

Peeters, Jozef, Gaia Fantechi, and Luc Vereecken. 2004. “A Generalized Structure-Activity Relationship for the Decomposition of (Substituted) Alkoxy Radicals.” *Journal of Atmospheric Chemistry 2004 48:1* 48 (1): 59–80. https://doi.org/10.1023/B:JOCH.0000034510.07694.CE.

Saunders, S. M., M. E. Jenkin, R. G. Derwent, and M. J. Pilling. 2003. “Protocol for the Development of the Master Chemical Mechanism, MCM v3 (Part A): Tropospheric Degradation of Non-Aromatic Volatile Organic Compounds.” *Atmospheric Chemistry and Physics* 3 (1): 161–80. https://doi.org/10.5194/ACP-3-161-2003.

Seinfeld, JH., and SN. Pandis. 2006. *Atmospheric Chemistry and Physics: From Air Pollution to Climate Change*. Edited by Inc. John Wiley and Sons. *John Wiley & Sons.* 3rd ed. John Wiley and Sons, Inc. https://doi.org/10.1080/00139157.1999.10544295.

Tyndall, G. S., R. A. Cox, C. Granier, R. Lesclaux, G. K. Moortgat, M. J. Pilling, A. R. Ravishankara, and T. J. Wallington. 2001. “Atmospheric Chemistry of Small Organic Peroxy Radicals.” *Journal of Geophysical Research: Atmospheres* 106 (D11): 12157–82. https://doi.org/10.1029/2000JD900746.

Vereecken, L., and J. Peeters. 2009. “Decomposition of Substituted Alkoxy Radicals—Part I: A Generalized Structure–Activity Relationship for Reaction Barrier Heights.” *Physical Chemistry Chemical Physics* 11 (40): 9062–74. https://doi.org/10.1039/B909712K.

Vereecken, L., and J. Peeters. 2010. “A Structure–Activity Relationship for the Rate Coefficient of H-Migration in Substituted Alkoxy Radicals.” *Physical Chemistry Chemical Physics* 12 (39): 12608–20. https://doi.org/10.1039/C0CP00387E.

Wolfe, Glenn M., Margaret R. Marvin, Sandra J. Roberts, Katherine R. Travis, and Jin Liao. 2016. “The Framework for 0-D Atmospheric Modeling (F0AM) v3.1.” *Geoscientific Model Development* 9 (9): 3309–19. https://doi.org/10.5194/GMD-9-3309-2016.

Zhang, Xuan, Renee C. McVay, Dan D. Huang, Nathan F. Dalleska, Bernard Aumont, Richard C. Flagan, and John H. Seinfeld. 2015. “Formation and Evolution of Molecular Products in α-Pinene Secondary Organic Aerosol.” *Proc. Natl Acad. Sci.* 112 (46): 14168–73. https://doi.org/10.1073/pnas.1517742112.

Ziemann, P. J. 2011. “Effects of Molecular Structure on the Chemistry of Aerosol Formation from the Oh-Radical-Initiated Oxidation of Alkanes and Alkenes.” *International Reviews in Physical Chemistry* 30 (2): 161–95. https://doi.org/10.1080/0144235X.2010.550728.

V. Conclusions, Implications, and Future Directions

1. Summary of Results

Improving our knowledge of the gas-phase oxidation chemistry of VOCs is crucial to refining our understanding of how SOA forms and evolves in the troposphere. Chamber experiments and mechanistic simulations are commonly used to provide the aforementioned improvements we desire, but both measurements and mechanisms have inherent limitations. Chamber species are susceptible to deposition on chamber surfaces, tubing, and instrument inlets, which may result in artificially lowered observed concentrations. This complicates our understanding of the chemistry occurring in the chamber; reaction rates for pathways which lead to the production and consumption of species susceptible to deposition may be underestimated and overestimated, respectively. At the same time, species that make it to detection in a CIMS may decompose, leading to the detection of ions which are not easily attributable to an identifiable compound. Mechanisms, on the other hand, are not completely exhaustive depictions of chemistry which occurs in reality. They are largely parametrized with results from empirical studies and are thus susceptible to any uncertainties and errors which may arise during said studies. However, mechanisms must be validated against empirical evidence if any mechanistic results can be considered reasonable representations of our knowledge of oxidation chemistry. The work in this thesis addressed uncertainties in chamber experiments and mechanistic simulations, and in the process, we gained new insights into the mutual benefits that measurement-mechanism comparisons can provide.

Chapter 2 focused on the development and characterization of an apparatus known as the Oxy-Cat to measure Total Suspended Carbon (TSC) for use in a chamber experiment. The Oxy-Cat consists of a heated inlet line, a tube furnace containing platinum and palladium catalysts, and a differential CO_2 measurement device (LI-7000). We calibrated the Oxy-Cat with seven different precursors to test its ability to convert them fully to CO_2 across a range of concentrations. The VOCs also spanned a range of

volatilities, sizes, and degrees of oxidation. All of the precursors except for perfluorooctane were observed to fully oxidize to CO_2. We discussed that perfluorooctane can be used as the solvent for dilute solutions for future syringe pump calibration studies for nonpolar and non-water-soluble VOC's.

Chapter 3 tackled the question of how to compare large chamber and mechanisms datasets. We utilized GECKO-A to generate the butane and α-pinene mechanisms for these comparisons. A chamber study for butane oxidation was conducted with a PTR-MS, and a chamber study of α-pinene oxidation was conducted with a suite of CIMS and gas monitors designed to achieve carbon closure (except for CO_2 which was not measured). We chose to begin our comparison methodology development by examining the relatively simple and well-characterized butane oxidation system. Prima facie isomer-to-isomer comparisons showed that several major species were found in one, but not both, chamber and GECKO-A datasets. A closer inspection of some chamber-only isomer sets suggested that nitrate, PAN, alcohol, and aldehyde functional groups may decompose in the process of being detected, and close time series correlations with non-decomposed GECKO-A species provided evidence for this assertion.

We grouped species by Cnum and OSc in both datasets to circumvent the decomposition issue and to highlight differences and similarities between measurements and mechanisms in terms of the fragmentation and functionalization dynamic. This dynamic is key to understanding SOA evolution and particle formation potential. We then developed an error metric by, first, normalizing the binned Cnum-OSc distributions at every time point in the experiment to account for differences in TSC between the chamber and GECKO-A. This error is bounded between zero and one and can be used to compare agreement across multiple VOC systems.

Chapter 4 began by discussing error metric results for unedited GECKO-A mechanisms which suggested that the isoprene oxidation system has the highest degree of chamber-GECKO agreement followed by α-pinene and then 1,2,4-TMB. This makes logical sense because isoprene and pinene chemistry have been extensively studied for decades while 1,2,4-TMB has received comparatively less

investigative attention. Isoprene is also a smaller and less complex molecule than the bicyclic α-pinene, so it makes sense for isoprene to display a lower average error as well. We then demonstrated how to use the comparison methodology and error metric developed in Chapter 3 to test edits to GECKO-A's mechanism generator to decrease disagreement with the corresponding chamber dataset. We targeted ozonolysis, alkoxy radical decomposition, alkoxy radical isomerization, alkoxy radical + O_2, nitrate yield, photolysis, and PAN decomposition SARs for amendment because these reaction pathways are important for influencing the fragmentation-functionalization dynamic.

Edits were performed on the α-pinene and 1,2,4-TMB systems because of the relatively high disagreement compared to the relatively low disagreement observed for isoprene. Although some SARs edits marginally improved chamber-GECKO agreement (i.e. increasing alkoxy radical isomerization rates by 10x for the 1,2,4-TMB oxidation system), the vast majority led to increased disagreement. Additionally, no SAR edits were found to provide benefits in all three oxidation systems we examined. These results indicate that improving agreement between observed and modeled chemistry will not be as simple as implementing sweeping SARs changes. Instead, these results indicate that a more targeted approach for each precursor system is required to amend relevant SARs or SARs subsets without decreasing agreement among other systems. Additionally, these results indicate that specific reactions and/or classes reactions which are missing or incomplete in GECKO-A may be responsible for the observed chamber-GECKO discrepancies. For example, RO_2 isomerization chemistry was recently found to be a major contributor to HOMs formation, but RO_2 isomerization SARs were not incorporated in the GECKO-A mechanisms presented in this thesis (Bianchi et al., 2019; Crounse et al., 2013). These missing reaction pathways could be critical for improving chamber-GECKO agreement, thereby improving our overall understanding of atmospheric organic chemistry.

2. Future Directions and Implications

Future work on the OxyCat will initially involve more syringe pump calibration studies with perfluorooctane as the solvent for non-polar and non-water-soluble VOCs. The more difficult work will be to adapt and optimize the Oxy-Cat for use in chamber studies. It is unclear the extent to which vapors and particles may deposit on tubing and other surfaces on their way to the Oxy-Cat's tube furnace, so this will be an important issue to address. Its anticipated use to constrain bottom-up measurements has yet to be proven, so future work must be performed to demonstrate this potential. Once it is ready to be used in chamber experiments, the Oxy-Cat may provide yet another utility in the form of constraining GECKO-A models for TSC. Currently GECKO-A is tuned to match experimentally observed precursor decay, ozone, NOx, and particulate SOA time series which serves to constrains the mechanism output. However, concentrations of TSC in the chamber and GECKO-A datasets are often different because of differing vapor deposition losses. Constraining those losses should serve to increase GECKO-A's fidelity to observed reality.

The first results in Chapter 3 demonstrated how GECKO-A can be used to reduce ambiguity in chamber data by suggesting structures and identities for ions detected in CIMS. Future work can focus on determining if other functional groups may decompose and the extent to which we may expect them to decompose. Future work should also be performed to understand differences in observed decomposition in each CIMS since the decomposition analysis in Chapter 3 focused primarily on decomposition upon detection with a PTR-MS. Chamber dataset also often contain species/ions whose time series suggest that they are real oxidation products but whose m/z's do not allow for a reasonable formula or chemical structure. Future work may elucidate from whence these ions arise and whether they represent organic species which may be unmeasured or undermeasured if they are fragments of an identified species. This work may be performed empirically and via quantum chemical simulations of ion fragmentation to create a CIMS fragmentation SAR, so to speak. This may allow researchers to predict how unidentified species

may fragment upon detection in any given CIMS. All of this future work will help decrease uncertainty in chamber measurements.

Chapter 4 provided an example by which we edited GECKO-A SARs to attempt to yield improved agreement with chamber data. The examples presented in that chapter are not meant to suggest that GECKO-A's SARs can not be improved, but rather to illustrate the process by which we can understand the effects of editing SARs on overall chamber-GECKO agreement. We performed our edits manually in a sweeping fashion, multiplying every SARs-predicted reaction by the same factor. It is unlikely that every SARs-predicted rate is inaccurate by the same amount, and the ideal magnitude of the SARs edits are also uncertain. We propose that future work be conducted in a Monte Carlo style to map out the error metric agreement landscape arising from editing multiple SARs at once. Subsets of each SARs may also be edited independently of one another which is not something we performed in this thesis. Running this type of Monte-Carlo analysis with GECKO-A will be laborious and time consuming because a new mechanism must be generated each time a new SARs edit is made. However, we believe that this proposed work is important to fully characterize which SARs edits or combination of SARs edits yield the best improvement in agreement between GECKO-A and chamber datasets. These edits may then, in turn, direct future empirical studies to more accurately measure rates for reactions which the improved GECKO-chamber agreements suggest are particularly important.

We also used the error metric to analyze how well GECKO-A and MCM are each able to encapsulate chamber observations. In each case (except for the end of the isoprene experiments) GECKO-A performed equally well or slightly better than MCM. However, GECKO-A performed significantly better than MCM for the 1,2,4-TMB oxidation system. It is worth noting again that the α-pinene and isoprene systems have been extensively scrutinized by our field over the past several years while the 1,2,4-TMB system has been relatively understudied. The MCM-GECKO comparisons suggest that increased a priori knowledge of the chemical system of interest decreases the significance or prevalence of the GECKO-

predicted reactions and rates in the final GECKO-A mechanisms. The comparisons also suggest that for systems for which empirical studies are lacking, GECKO-A provides significant benefits to the final mechanism in terms of agreement with chamber observations. Therefore, other systems which have not been studied as thoroughly as isoprene or pinene, for example, may benefit from using GECKO-A simulations to direct empirical studies to measure key reactions and their corresponding rates.

The studies presented in this thesis point to future technical advances which would be beneficial for advancing the field of atmospheric chemistry as a whole. Developing new methods to predict how chemical species behave in different CIMS's ionization regions will allow for more accurate TotalC accounting by determining whether each ion (including those for which a reasonable corresponding structure does not exist) is derived from a whole stable species or is formed from the fragmentation of another species. Similarly, developing methods to elucidate the structure for each species detected via CIMS would allow for much closer mechanism-measurement comparisons. The methods discussed in this thesis relied upon binning species by Cnum and OSc, in part, because structural characteristics for most species were unable to be empirically determined. Knowing the structure of each species in the chamber will also allow for the creation of more accurate mechanisms and more accurate SARs. Empirically derived mechanisms will benefit because more detailed structural information allows one to more closely and confidently relate specific species as parent and child in each reaction pathway. SARs will be improved because they rely on, in part, accurate empirical rate constant data for a wide variety of species with different chemical constituents, and the locations of those constituents is highly relevant for an SAR. Additionally, SARs are currently less accurate for highly functionalized species, so empirical structural information would be helpful for increasing the accuracy of rate-constant predictions for these species. All of these aspirational advances in instrumentation will broadly benefit the field and help increase clarity on whether measurement-mechanism discrepancies are arising because of uncertainties in measurements.

The implications of this work extend past decreasing uncertainties in chamber measurements and improving GECKO-A's mechanism generation capabilities. By improving our understanding of atmospherically relevant chemistry, we can better understand how VOC's contribute to the production of pollutants including tropospheric ozone, CO_2, and SOA particulate matter (Heald & Kroll, 2020). Ozone and particulate matter at ground level negatively impact respiratory health, and all three pollutants influence Earth's climate either as greenhouse gases in the cases of CO_2 and ozone or by scattering light and influencing cloud formation in the case of SOA particulate matter. VOC's are also the dominant contributor to the overall OH reactivity of the atmosphere and therefore play an important role in controlling ambient concentration of the OH radical. OH concentrations strongly influence the oxidizing capacity of the atmosphere which, in turn, influence SOA formation and evolution. This feedback is just one example of how the atmosphere is a highly connected and complex chemical system, but the work in this thesis will hopefully increase our understanding of its behavior so we can better predict its behavior and its influences on Earth's climate and human health.

3. References

Bianchi, F., Kurtén, T., Riva, M., Mohr, C., Rissanen, M. P., Roldin, P., Berndt, T., Crounse, J. D., Wennberg, P. O., Mentel, T. F., Wildt, J., Junninen, H., Jokinen, T., Kulmala, M., Worsnop, D. R., Thornton, J. A., Donahue, N., Kjaergaard, H. G., & Ehn, M. (2019). Highly Oxygenated Organic Molecules (HOM) from Gas-Phase Autoxidation Involving Peroxy Radicals: A Key Contributor to Atmospheric Aerosol. *Chemical Reviews*, *119*(6), 3472–3509. https://doi.org/10.1021/ACS.CHEMREV.8B00395

Crounse, J. D., Nielsen, L. B., Jørgensen, S., Kjaergaard, H. G., & Wennberg, P. O. (2013). Autoxidation of organic compounds in the atmosphere. *Journal of Physical Chemistry Letters*, *4*(20), 3513–3520. https://doi.org/10.1021/JZ4019207/SUPPL_FILE/JZ4019207_SI_001.PDF

Heald, C. L., & Kroll, J. H. (2020). The fuel of atmospheric chemistry: Toward a complete description of reactive organic carbon. *Sci. Adv*, *6*. https://www.science.org